

Doctoral dissertation

Antitumor effects and predictive marker identification  
for a novel non-ATP-competitive MEK1/2 selective inhibitor,  
SMK-17

March 2015

Masaki Kiga

## Table of Contents

<b>1. Chapter 1; Introduction to this study</b> .....	<b>7</b>
1.1 Beginnings of chemotherapy agents .....	8
1.2 Kinase inhibitors .....	9
1.3 MAPK pathway and the molecular target drugs .....	12
1.4 Wnt/ $\beta$ -catenin pathway .....	15
1.5 Predictive biomarker for cancer therapy .....	17
1.6 Motivation for this study .....	19
<b>2. Chapter 2; Creation of potent MEK1/2 inhibitors</b> .....	<b>20</b>
2.1 Background of Chapter 2 .....	21
2.2 Results and discussion .....	22
2.2.1 Set up of a cell-free assay system .....	22
2.2.2 Set up of a cell-based assay system .....	27
2.2.3 Screening of our compounds .....	30
2.3 Materials and methods in Chapter 2 .....	33
2.3.1 Reagents and compounds .....	33
2.3.2 Cell-free kinase reaction and detection by HTRF .....	34
2.3.3 Cell lines .....	35
2.3.4 Cell ELISA .....	35
2.3.5 Western blot analysis .....	36
<b>3. Chapter 3; Analysis of a novel MEK1/2 inhibitor, SMK-17 (RCR-5886)</b> .....	<b>38</b>
3.1 Background of Chapter 3 .....	39
3.2 Results and discussion .....	39
3.2.1 Potency of diphenyl amine sulfonamide derivatives as a MEK1/2 inhibitor .....	39
3.2.2 Binding mode of SMK-17 with MEK1 .....	46
3.2.3 ATP dependency of kinase inhibition of SMK-17 .....	49
3.2.4 Kinase inhibitory selectivity of SMK-17 .....	52
3.2.5 Inhibition of intracellular MEK1/2 and cell growth by SMK-17 .....	56
3.2.6 In vivo antitumor activity in an allograft model .....	68
3.2.7 In vivo antitumor activity on a xenograft model .....	74
3.3 Conclusion of Chapter 3 .....	78
3.4 Materials and methods in Chapter 3 .....	79
3.4.1 Compounds .....	79
3.4.2 Kinase selectivity .....	79

3.4.3	Physicochemical study .....	79
3.4.4	Docking study of SMK-17 with human MEK1 .....	79
3.4.5	Cell culture .....	80
3.4.6	Western blot analysis.....	80
3.4.7	Cell cycle measurement .....	81
3.4.8	In vivo antitumor study .....	82
3.4.9	Pharmacokinetic studies (drug concentration measurement in vivo) .....	82
<b>4.</b>	<b>Chapter 4; Predictive biomarker identification for a MEK1/2 inhibitor .....</b>	<b>84</b>
4.1	Background of Chapter 4 .....	85
4.2	Results and discussion .....	86
4.2.1	SMK-17 inhibited cell proliferation in K-Ras or BRAF mutated tumor cell lines.....	86
4.2.2	SMK-17 induced apoptosis in active $\beta$ -catenin mutated cell lines .....	91
4.2.3	Active mutation of $\beta$ -catenin is associated with SMK-17 induced apoptosis .....	98
4.2.4	TCF4 activity is related to MEK inhibitor induced apoptosis in $\beta$ -catenin mutant cell lines.....	101
4.2.5	Involvement of c-Myc-mediated apoptosis gene expression in SMK-17 induced apoptosis.....	107
4.2.6	Apoptosis induction of SMK-17 on $\beta$ -catenin mutated xenograft models .....	111
4.3	Conclusion of Chapter 4 .....	114
4.4	Materials and methods in Chapter 4 .....	116
4.4.1	Cell lines and cell culture.....	116
4.4.2	Cell growth inhibition assay .....	116
4.4.3	Western blot analysis.....	117
4.4.4	Cell cycle and apoptosis measurements .....	118
4.4.5	TCF4 reporter and expression vectors.....	118
4.4.6	RNA interference .....	119
4.4.7	In vivo antitumor experiments.....	119
<b>5.</b>	<b>Chapter 5; Beyond therapy for <math>\beta</math>-catenin mutated tumors with MEK1/2 inhibitors .....</b>	<b>121</b>
5.1	Background of Chapter 5 .....	122
5.2	Results and discussion .....	124
5.2.1	Manipulation of TCF4 transcription activity in an APC mutated cell line .....	124
5.2.2	Partial inhibition of TCF4 transcription activity in an APC mutated cell line maximized by SMK-17 induced apoptosis.....	127
5.3	Conclusion of Chapter 5 .....	130

5.4	Materials and methods in Chapter 5 .....	131
5.4.1	Gene-Switch system to manipulate TCF4 transcription activity .....	131
5.4.2	Other protocol except for the Gene-Switch system.....	131
<b>6.</b>	<b>Chapter 6; Conclusion of this study.....</b>	<b>132</b>
<b>7.</b>	<b>References .....</b>	<b>137</b>
7.1	References in Chapter 1 .....	137
7.2	References in Chapter 2 .....	142
7.3	References in Chapter 3 .....	143
7.4	References in Chapter 4 .....	144
7.5	References in Chapter 5 .....	147
7.6	References in Chapter 6 .....	147
<b>8.</b>	<b>Appendix data.....</b>	<b>149</b>
8.1	Complete potency data of our MEK inhibitors .....	150
<b>9.</b>	<b>The archive location of specimens and raw data.....</b>	<b>151</b>
<b>10.</b>	<b>Related our patents and publications .....</b>	<b>152</b>
<b>11.</b>	<b>COI disclosure information of the author.....</b>	<b>153</b>
<b>12.</b>	<b>Acknowledgments .....</b>	<b>154</b>

Figure 1	Development history of representative antitumor drugs .....	11
Figure 2	MAPK pathway and related oncogenic mutations .....	14
Figure 3	Wnt/ $\beta$ -catenin pathway with or without Wnt stimulation .....	16
Figure 4	Chemical structure of PD184352 as a reference compound .....	23
Figure 5	MEK1/2 induced ERK2 phosphorylation in the cell-free kinase reaction.....	23
Figure 6	Diagrams of the detection and reaction systems for MEK1/2 kinase reactions using HTRF method.....	24
Figure 7	Confirmation of detection for MEK1/2 activity by Western blot analysis and the HTRF method.....	25
Figure 8	Optimization of MEK1 amount for a kinase reaction .....	26
Figure 9	Optimization of substrate amount for a MEK1 kinase reaction.....	26
Figure 10	EGF-induced ERK1/2 phosphorylation in NIH 3T3 cells, and inhibitory effect of a MEK1/2 inhibitor.....	28
Figure 11	Optimization of detection conditions for phosphorylated ERK1/2 (Cell ELISA system) .....	28
Figure 12	Concentration-dependent inhibitory effect against ERK1/2 phosphorylation by a MEK1/2 inhibitor in NIH3T3 cells.....	29

Figure 13	Chemical structure of RCR-5523 as a lead compound of the derivatization..	31
Figure 14	Chemical structures of our representative potent MEK inhibitors.....	32
Figure 15	Binding mode of SMK-17 with MEK1 .....	47
Figure 16	Diagrams explaining the binding mode of SMK-17 with MEK1 .....	48
Figure 17	MEK1 kinase inhibition by SMK-17 in various ATP concentrations .....	50
Figure 18	Dixon plot demonstrating the non ATP-competitive manner of SMK-17 to a MEK1 kinase reaction.....	51
Figure 19	Kinase inhibitory profiling of SMK-17 .....	53
Figure 20	Growth inhibition profile of SMK-17 against tumor cell lines.....	57
Figure 21	Effects of SMK-17 on cell cycle, MEK/ERK, and cyclin D1 proteins in HT-29 cells.....	60
Figure 22	Effects of SMK-17 on cell cycle, MEK/ERK, and cyclin D1 proteins in colon 26 cells.....	61
Figure 23	Effects of SMK-17 on cell cycle, phosphorylated ERK, and cyclin D1 proteins in Panc-1 cells .....	63
Figure 24	Effects of SMK-17 on cell cycle, phosphorylated ERK, and cyclin D1 proteins in LNCaP cells .....	64
Figure 25	Concentration-correlation between intracellular MEK1/2 inhibition and cell cycle arrest intensity on SMK-17 treated HT-29 cells .....	66
Figure 26	Western blot analysis for phosphorylated and total ERK5, ERK1/2, and AKT proteins .....	67
Figure 27	In vivo PD efficacy of SMK-17 on a colon 26 allograft model.....	69
Figure 28	Quantified in vivo PD efficacy of SMK-17 on a colon 26 allograft model....	70
Figure 29	In vivo antitumor activity of SMK-17 in a colon 26 allograft model .....	72
Figure 30	In vivo antitumor activity of SMK-17 on an HT-29 xenograft model .....	75
Figure 31	In vivo analysis of downstream and related proteins of MEK1/2 in the SMK-17 administered HT-29 xenograft mice .....	77
Figure 32	Relative IC <sub>50</sub> values for a panel of tumor cell lines harboring several oncogenic mutations .....	87
Figure 33	Scatter plot of IC <sub>50</sub> values of SMK-17 for a panel of tumor cell lines harboring several oncogenic mutations .....	89
Figure 34	Scatter plot of IC <sub>50</sub> values of U0126 for a panel of tumor cell lines harboring several oncogenic mutations .....	90
Figure 35	MEK inhibitor selectively induced apoptosis in $\beta$ -catenin mutated cell lines	92

Figure 36	SMK-17 selectively induced G1 arrest in $\beta$ -catenin wild type cells and apoptosis in $\beta$ -catenin mutant cells.....	93
Figure 37	Active mutation of $\beta$ -catenin is associated with SMK-17 induced apoptosis	96
Figure 38	Active mutation of $\beta$ -catenin is associated with PD184352 induced apoptosis	97
Figure 39	SMK-17-treated A375 cells with an expression vector encoding active $\beta$ -catenin.....	99
Figure 40	Accelerated SMK-17 induced apoptosis in A375 cells with an active $\beta$ -catenin expression vector.....	100
Figure 41	Activation of Wnt/ $\beta$ -catenin signaling by Wnt3a treatment in A375 cells ...	102
Figure 42	Activation of Wnt/ $\beta$ -catenin signaling by Wnt3a induced apoptosis in A375 cells.....	103
Figure 43	Expression of DN-TCF4 reduced the Wnt/ $\beta$ -catenin signal in HCT 116 cells	105
Figure 44	Expression of DN-TCF4 reduced SMK-17 induced apoptosis in HCT 116 cells.....	106
Figure 45	Involvement of c-Myc on SMK-17 induced apoptosis in HCT 116 cells.....	109
Figure 46	Involvement of c-Myc on SMK-17 induced apoptosis in Wnt3a stimulated A375 cells.....	110
Figure 47	Antitumor activities of SMK-17 in vivo.....	112
Figure 48	Apoptosis induction by SMK-17 administration in a $\beta$ -catenin mutated tumor model in vivo.....	113
Figure 49	Possible mechanism for SMK-17-induced apoptosis and crosstalk between Wnt/ $\beta$ -catenin and MAPK pathways .....	115
Figure 50	MFP-induced DN-TCF4 expression using a Gene-Switch system in DLD-1 cells.....	125
Figure 51	Attenuated TCF4 transcription activity by MFP treatment in DN-TCF4 expressing DLD1 cells.....	126
Figure 52	SMK-17 induced apoptosis was maximized by a low concentration treatment of MFP in DN-TCF4 expressing DLD-1 cells .....	128
Figure 53	SMK-17 induced apoptosis was not significantly accelerated by overexpression of active $\beta$ -catenin in DLD-1 cells .....	129
Figure 54	Diagram of this study showing the response of MEK1/2 inhibitors of tumors harboring oncogenic mutations.....	135
Figure 55	Proposed machinery of the response of tumor cells with various TCF4 activities to MEK1/2 inhibitors.....	136

Table 1	Representative predictive biomarkers available in clinical use .....	18
Table 2	Identification of a sulfamide compound as a MEK1/2 inhibitor.....	41
Table 3	Structure-activity relationship of piperidine sulfamide scaffold for MEK inhibition and solubility screening.....	44
Table 4	All kinase inhibitory activity data concerning inhibition% of each human kinase by 1000 nM of SMK-17 .....	54
Table 5	Plasma drug concentration in CDF1 mice.....	73
Table 6	Plasma drug concentration in Balb/c-nu/nu (nude) mice.....	76

**1. Chapter 1; Introduction to this study**



## 1.1 Beginnings of chemotherapy agents

Cancers represent one of the leading causes of pathological death in developed countries and have the potential to become the number one killer in the first quarter of this century<sup>1)</sup>. Therefore, cancer chemotherapy continues to play an increasingly important role in the direct management of malignancies or as an adjuvant drug to surgery and radiotherapy. A variety of agents for cancer chemotherapy have been clinically approved. Although the mode of action (MoA) of many of these agents has only recently been understood, the history of cancer chemotherapies dates back into the nineteenth century.

The history of systematic clinical chemotherapy dates back to the period following World War I. This involved the poison gases known as mustard gases. The research conducted at the US Chemical Warfare Service provided evidence on the effects of mustard gases. In this study, rabbits injected at the maximum tolerated dose (MTD) showed a significant decrease in leucocyte numbers after injection, and damage to bone marrow was also observed. This study served to focus on the effect of leucopenia regarding the principal constituent of mustard gas, dichloroethyl sulphide. The observed leucopenia was largely a result of the dichloroethyl sulphide causing damage to dividing cells, and its potential to control cancers was also investigated. ASTA Medica developed prodrug forms of dichloroethyl sulphide. This study led to the eventual success of nitrogen mustards in established chemotherapy regimens. To this day, the nitrogen mustard is the first clinical candidate, and one of the simplest members of this class. Mechlorethamine is still used for the control of non-Hodgkin lymphoma. There are some structural relative drugs available for clinical use, including cyclophosphamide

(employed against leukaemia, lymphoma, breast cancer, lung cancer, prostatic cancer and ovarian cancer) and melphalan (approved for multiple myeloma, ovarian cancer and as an adjuvant in primary breast cancer management)<sup>2)</sup>.

One of the most promising and publicized antitumor agents to be developed in recent years is the natural product, paclitaxel (Taxol)<sup>3)</sup>. This compound was isolated from the bark of the pacific yew *Taxus brevifolia* by NCI. The MoA of its cytotoxic efficacy was discovered in 1979, showing that paclitaxel interacts with intracellular microtubules, promoting microtubule assembly and inhibiting tubulin disassembly<sup>4)</sup>. The FDA approved paclitaxel for the treatment of ovarian cancer in 1992, and in 1994 it was approved for treatment against breast cancer, becoming one of the most promising anticancer agents to emerge in history<sup>1)</sup>. However, chemotherapy agents including paclitaxel have a bunch of very real problems about adverse effects based on the cytotoxicity to human normal cells.

## **1.2 Kinase inhibitors**

A small molecule kinase inhibitor, imatinib mesylate (Gleevec) had been developed by Novartis since 1998. Imatinib is a one of successful molecular targeted agents, commonly called as “Magic bullets” of cancer care based on high selectivity to tumor cells. The clinical success of imatinib in chronic myeloid leukaemia (CML) and gastrointestinal stromal tumors (GIST) has established a good exemplar for the treatment of tumors whose growth is acutely dependent on specific targets on behalf of cytotoxic chemotherapy<sup>5)</sup>. CML is driven by the mutant kinase fusion protein, Bcr/Abl, which leads constitutive activation of the Abl kinase, whereas GIST is caused by activating

point mutations in the c-Kit or platelet derived growth factor receptor (PDGFR)-kinases. Imatinib selectively blocks the activity of all the above-described kinases and induces significant clinical responses in all three situations in a manner that correlates with the presence of these mutations in the tumor<sup>6)</sup>. The development history of representative antitumor drugs including paclitaxel and imatinib is summarized in Figure 1.

In lung cancer, clinical responses to epidermal growth factor receptor (EGFR) inhibitors are associated with point mutations in the EGFR kinase domain<sup>7),8)</sup>. A clear prediction from this experience is that clinical responses to kinase inhibitors occur in tumors bearing activating mutations that drive tumor progression. Extending this paradigm to larger numbers of cancer patients required the establishment of kinase mutation frequency in human cancer on a much broader scale such as the human genome project<sup>9)</sup>. Indeed, initial efforts from several groups at the Sanger Institute, the Eli & Edythe L. Broad Institute, and Johns Hopkins University have found previously unsuspected kinase mutations in human tumors<sup>10),11),12),13),14)</sup>.

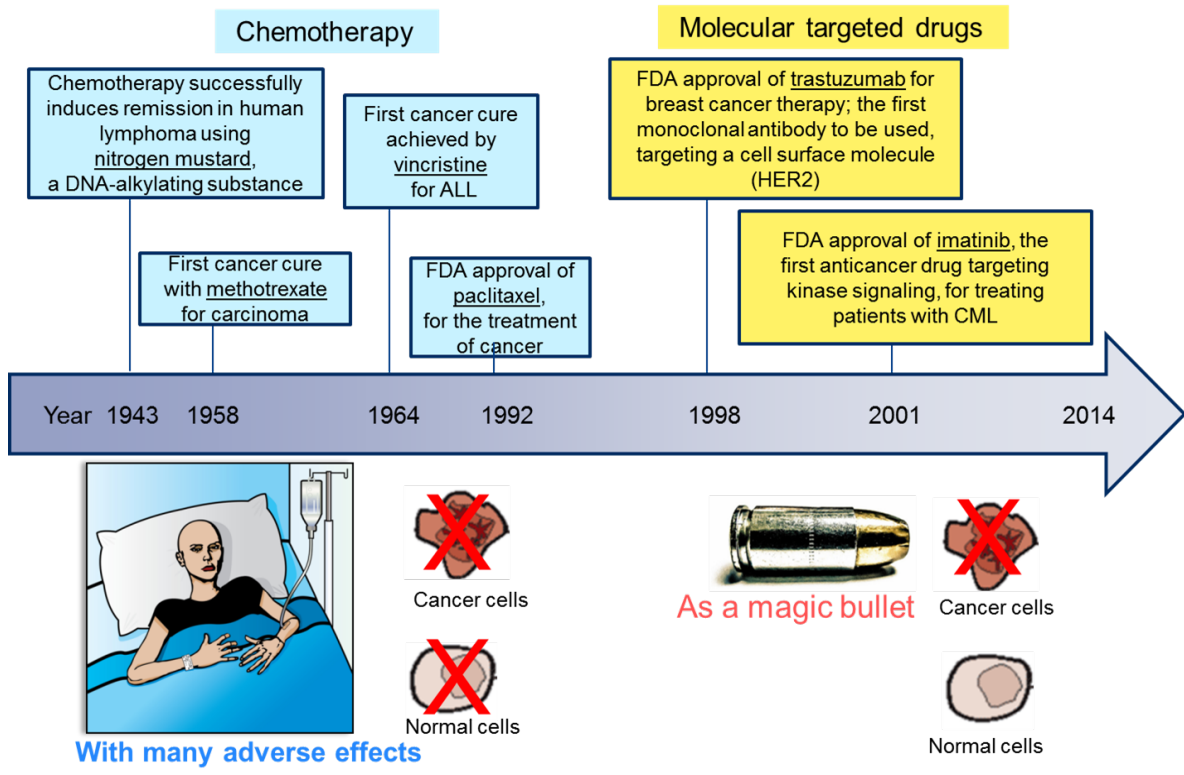


Figure 1 Development history of representative antitumor drugs

### 1.3 MAPK pathway and the molecular target drugs

Mitogen-Activated Protein Kinases (MAPKs) are a well-known family of serine/threonine protein kinases that play an important role in many intracellular responses such as cell proliferation, survival, differentiation, migration, and apoptosis<sup>15)</sup>. The Extracellular-signal Regulated Kinase 1 and 2 (ERK1/2) are the first characterized members of the MAPKs family. ERK1/2 are activated by a phosphorylation cascade, mainly downstream from the receptor tyrosine kinases, the ras protooncogene, raf family including BRAF, and MEK1/2. Activated MEK1/2 catalyzes the phosphorylation of ERK1/2. These MAPKs phosphorylate a variety of substrates, including p90RSK and the transcription factor Elk-1, which mainly promote cell growth<sup>16), 17)</sup> as shown in the diagrams in Figure 2. MEK1/2, also known as MAP2K1 or MKK1/2, are members of a large family of dual-specificity kinases (MKK1 - MKK7) that phosphorylate threonine and tyrosine residues of various MAPKs<sup>18)</sup>. The only identified substrates of MEK1/2 are ERK1/2 thus far. This tight selectivity suggests that MEK1/2 are essential regulators for the MAPK pathway.

Constant activation of the MAPK pathway, because of aberrant receptor tyrosine kinase activation and ras or BRAF mutations, is frequently found in human cancers and represents a major factor in determining abnormal cell growth<sup>19)</sup>. Approximately 30% of all human cancers contain an activating ras mutation. The incidence of k-ras mutations is particularly high in pancreatic and colon cancers (90% and 44%, respectively)<sup>20)</sup>. Oncogenic V600E mutations in BRAF have been found in 66% of melanomas and 69% of papillary thyroid cancers<sup>21), 22)</sup>. Furthermore, aberrant activation of the MAPK pathway correlates with tumor progression and poor prognosis in patients

with various cancers<sup>23)</sup>. Although active mutations of MEK1/2 have not been found in major human cancers, the constitutive expression of MEK1/2 is sufficient to induce transformation<sup>24), 25)</sup>. Targeting MEK1/2 with a small molecule inhibitor is a very attractive strategy because of the potential to prevent all upstream aberrant oncogenic signaling<sup>26), 27)</sup>. Although previously reported MEK inhibitors, PD184352/CI-1040 and PD0325901, have been evaluated in a clinical study, these clinical trials were discontinued due to insufficient efficacy and undesirable adverse events<sup>28), 29), 30), 31)</sup>. As it stands now, selumetinib (ARRY142886 / AZD6244) and trametinib (JTP-74057 / GSK-1120212) have been evaluated for clinical proof-of-concept (POC). These MEK1/2 inhibitors have shown clinical responses in some patients with malignant melanoma and thyroid carcinoma<sup>31), 32)</sup>. However, they have not showed significant efficacy in clinical use yet.

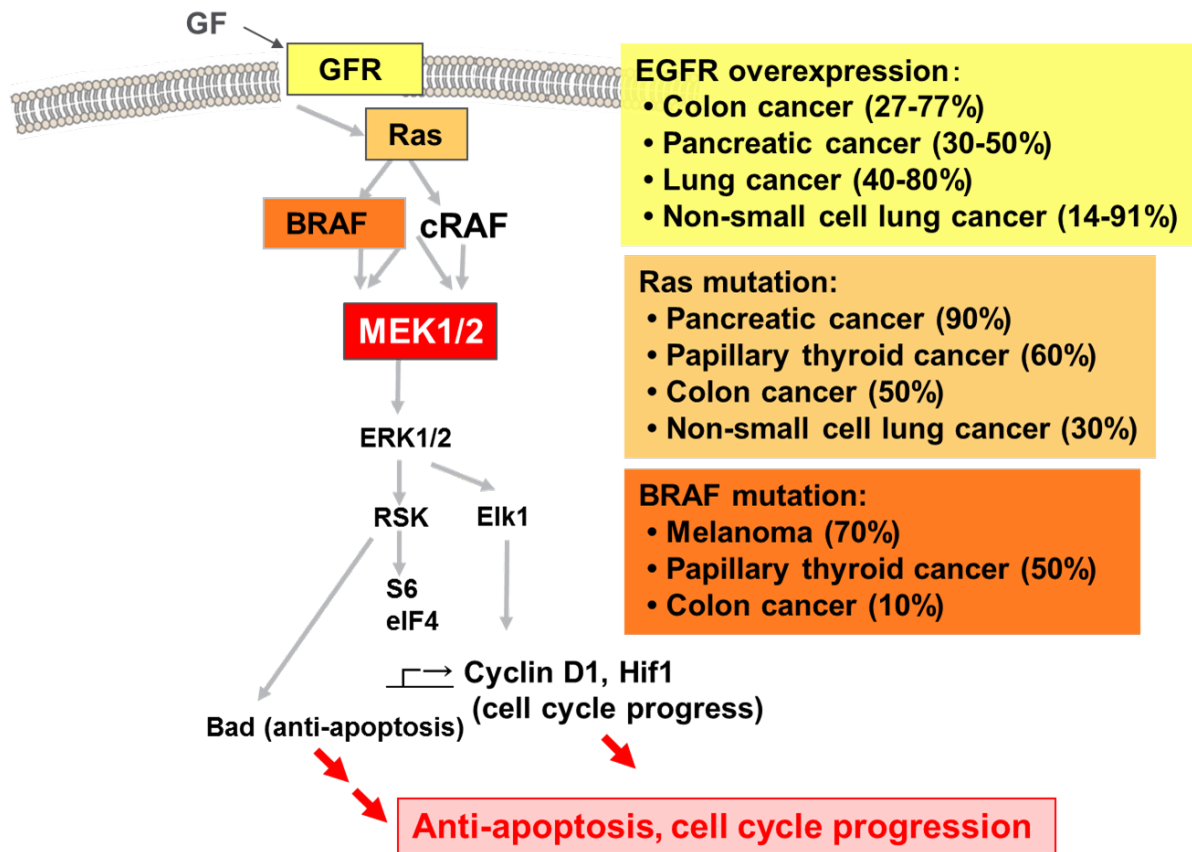


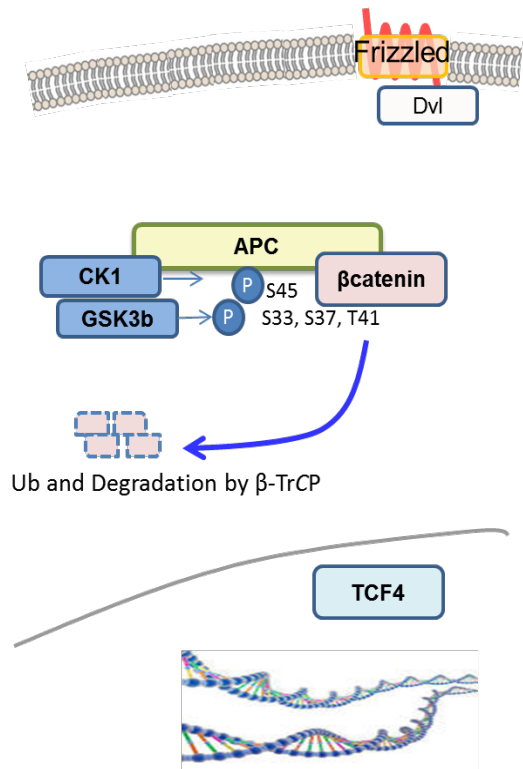
Figure 2 MAPK pathway and related oncogenic mutations

#### 1.4 Wnt/ $\beta$ -catenin pathway

Wnt signaling also plays a central role in cell proliferation and differentiation<sup>33</sup>). In the absence of a Wnt stimulus,  $\beta$ -catenin interacts with axin, glycogen synthase kinase-3 $\beta$  (GSK-3 $\beta$ , also called GSK3B as a HUGO gene name), and the adenomatous polyposis coli protein (APC). GSK-3 $\beta$  phosphorylates  $\beta$ -catenin and triggers its ubiquitination and degradation by  $\beta$ -Trcp<sup>34</sup>). Activation of the Wnt pathway inhibits GSK-3 $\beta$ -dependent phosphorylation of  $\beta$ -catenin, then stabilizes  $\beta$ -catenin, which results in the hypo-phosphorylated form, translocates to the nucleus and interacts with Transcription Factor 7-Like 2 (TCF7L2, also commonly called TCF4). Then TCF4 leads to the increased expression of c-Myc or Cyclin D1<sup>35), 36)</sup> as shown in the diagrams in Figure 3. Mutations of  $\beta$ -catenin enhance the stability of  $\beta$ -catenin and subsequent transactivation of TCF4, and such transactivation is found in a wide variety of human tumors<sup>37)</sup>. Although both MAPK and Wnt/ $\beta$ -catenin signals are very important intracellular signaling pathways, their crosstalk is not yet clear.



### Wnt OFF



### Wnt ON

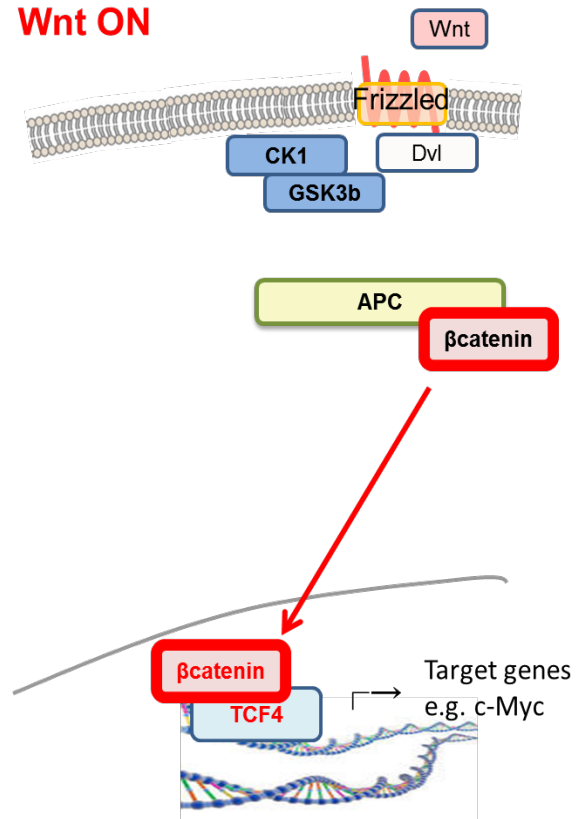


Figure 3 Wnt/ $\beta$ -catenin pathway with or without Wnt stimulation

## 1.5 Predictive biomarker for cancer therapy

Biomarkers are indispensable in determining the aggressiveness of each cancer and predicting the response to a treatment of molecular targeted drugs. This is because tumors exhibit particular biomarkers, which are responsive to the molecular targeted agents. The representative clinical biomarkers that predict responding tumors, called “predictive biomarkers” here, are summarized in Table 1.

For example, the HER2/neu amplification is a biomarker indicating a breast cancer responding to trastuzumab treatment<sup>38</sup>). A mutation of the proto-oncogene c-kit or fusion genes of bcr-abl are predictive biomarkers to find responder tumors to imatinib treatment<sup>39</sup>). Mutations in the tyrosine kinase domain of EGFR (e.g. T790M or L858R), a biomarker indicating a responder patient of Non-Small-Cell Lung Carcinoma (NSCLC) to EGFR kinase inhibitors such as gefitinib and erlotinib<sup>40</sup>).

All predictive biomarkers in clinical use described above are the “target-related” molecules. Other novel approaches unrelated directly to the drug target or drug metabolism may serve as potentially important therapeutic interventions in the treatment of cancer patients in the near future.

Table 1 Representative predictive biomarkers available in clinical use

Drug type	Drug name	Predictive biomarker
Chemotherapy	Irinotecan	UGT1A1
Hormonotherapy	Tamoxifen	CYP2D6
Molecular targeted drug	Trastuzumab	Her2/neu expression
	Imatinib and sunitinib	<i>c-kit</i> or <i>bcr-abl</i>
	Crizotinib	<i>EML4-ALK</i> fusion gene
	Gefitinib	<i>EGFR</i> T790M or L858R mutation
	MEK1/2 inhibitors	<i>BRAF</i> and <i>k-ras</i> mutation <u>so far</u>
	Vemurafenib	<i>BRAF</i> V600E mutation
	EGFR TKIs	<i>k-ras</i> mutation as a negative marker

## 1.6 Motivation for this study

For the reasons described above, more effective and highly selective MEK1/2 inhibitors and more suitable usage, including genotype-based patient selection, than the previously reported drugs and indication strategies, are needed for the battlefield of current cancer therapy. The motivation for this study was based on two aspects of my current studies. One is a responsibility for drug development as a researcher at a pharmaceutical company. The other is the mission to promote the development of biochemical science using a “good” compound without any off-target effects. At the same time, we definitely need to propose the best suited ways to use the molecular targeting drugs for each cancer patient and treatment.

Here I report the arrangement of the evaluation systems for the *in vitro* MEK1/2 inhibitor screening and representative potent compounds in Chapter 2. Next, I provide a detailed analysis of one of our MEK1/2 inhibitors, SMK-17 (RCR-5886) in Chapter 3. I reveal that SMK-17 is a hydrophilic, highly selective, and potent MEK1/2 inhibitor with a distinctively structured, piperidine sulfamide scaffold. Moreover, my collaborator, Ayako Nakayama and I focus on the predictive marker identification of this compound. We show an active  $\beta$ -catenin mutation (i.e. S37A or S45A activating point mutation) as a novel predictive biomarker of MEK1/2 inhibitors in Chapter 4. Finally, I propose a method of MEK1/2 inhibitor application to APC mutated tumors in Chapter 5.

**2. Chapter 2; Creation of potent MEK1/2 inhibitors**

## 2.1 Background of Chapter 2

The Ras/Raf/MEK/ERK pathway has been extensively studied in cancer biology and its relevance for tumorigenesis has been well established as described in Chapter 1.

Despite many efforts to clarify a cancer therapeutic agent specifically targeting this pathway (e.g., Ras, Raf, or MEK1/2 inhibitors), only three compounds, vemurafenib, trametinib, and selumetinib, have been improved even though they have issues such as rapidly acquired drug resistance for vemurafenib and insufficient antitumor efficacies of the MEK1/2 inhibitors in clinical. Thus, we currently need potent MEK1/2 inhibitors for further development of the possibility of pharmacological intervention to the aberrational MAPK pathway.

In this Chapter, I discuss the the MEK1/2 inhibitor creation process from the screening preparation to acquisition of potent MEK1/2 inhibitors. Firstly, I set up the in vitro assay systems for screening MEK1/2 inhibitors. At the same time, RCR-5523 was obtained as a novel compound with a piperidine sulfamide structure in former Sankyo's compound library. Then, we created and screened 1,004 derivatives of RCR-5523 as a lead compound. Finally, several compounds more potent than Pfizer's PD184352 in MEK1/2 inhibition were obtained.

## **2.2 Results and discussion**

### **2.2.1 Set up of a cell-free assay system**

For the purpose of screening for MEK1/2 inhibitors as antitumor agents, we established MEK1/2 inhibition assay systems in vitro. I set up the cell-free kinase assay system to evaluate inhibitory activities against MEK1 and 2 respectively. In this assay, I detected MEK1/2 induced ERK2 phosphorylation by the Homogenous Time Resolved Fluorescence (HTRF) method<sup>41</sup>.

I prepared full length human MEK1 and 2 for kinase reactions, and full length ERK2 as the substrate. For the kinase activities of MEK1/2 and inhibitory activity of PD184352 as a reference compound, the chemical structure is described in Figure 4, and they were evaluated by Western blot analysis (Figure 5). To improve screening throughput, I developed the detection system for ERK2 phosphorylation with HTRF as shown in the diagrams in Figure 6. I have confirmed detection of ERK2 phosphorylated by recombinant MEK1 by the HTRF method (Figure 7). Next, the amount of MEK1 between 0.1 and 30 ng and ERK2 between 1 and 300 ng were optimized for kinase reactions and detection (Figure 8 and Figure 9).

Finally, the optimal conditions used in the 384-well format were 30 ng of MEK1/2 as an enzyme source and 100 ng of ERK2 as a phosphorylated substance for my routine screening.

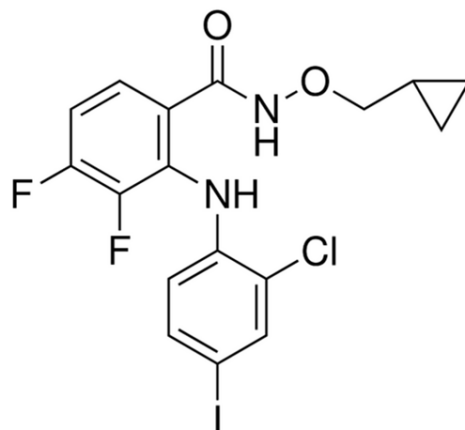


Figure 4 Chemical structure of PD184352 as a reference compound

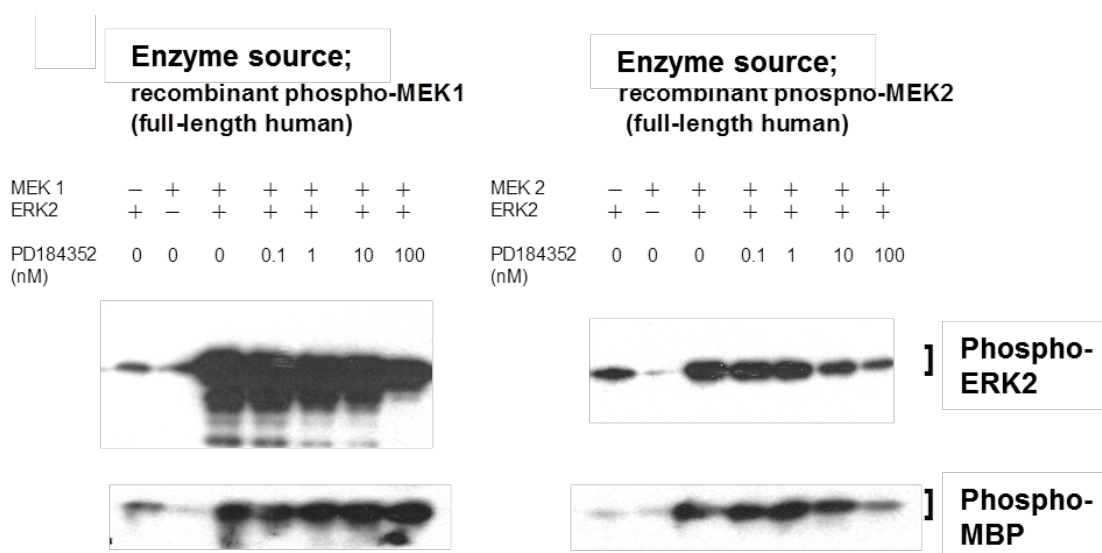


Figure 5 MEK1/2 induced ERK2 phosphorylation in the cell-free kinase reaction

I confirmed kinase reactions of recombinant human MEK1 and MEK2 proteins that induce phosphorylation of ERK2 and MBP as substrates of MEK1 and 2.

Phosphorylated substrates were detected by Western blot analysis.



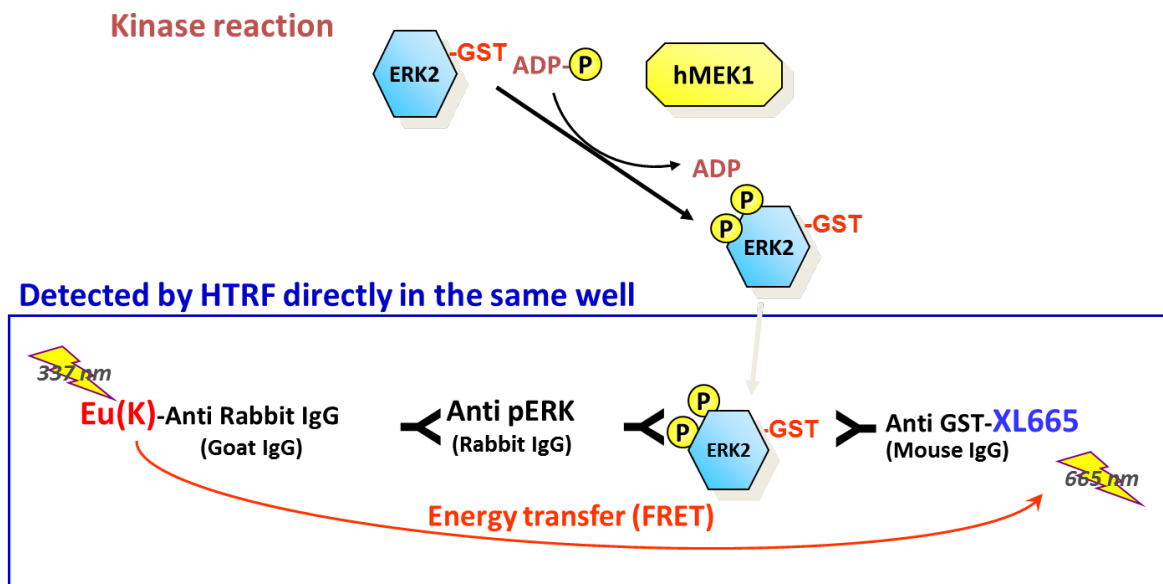


Figure 6 Diagrams of the detection and reaction systems for MEK1/2 kinase reactions using HTRF method

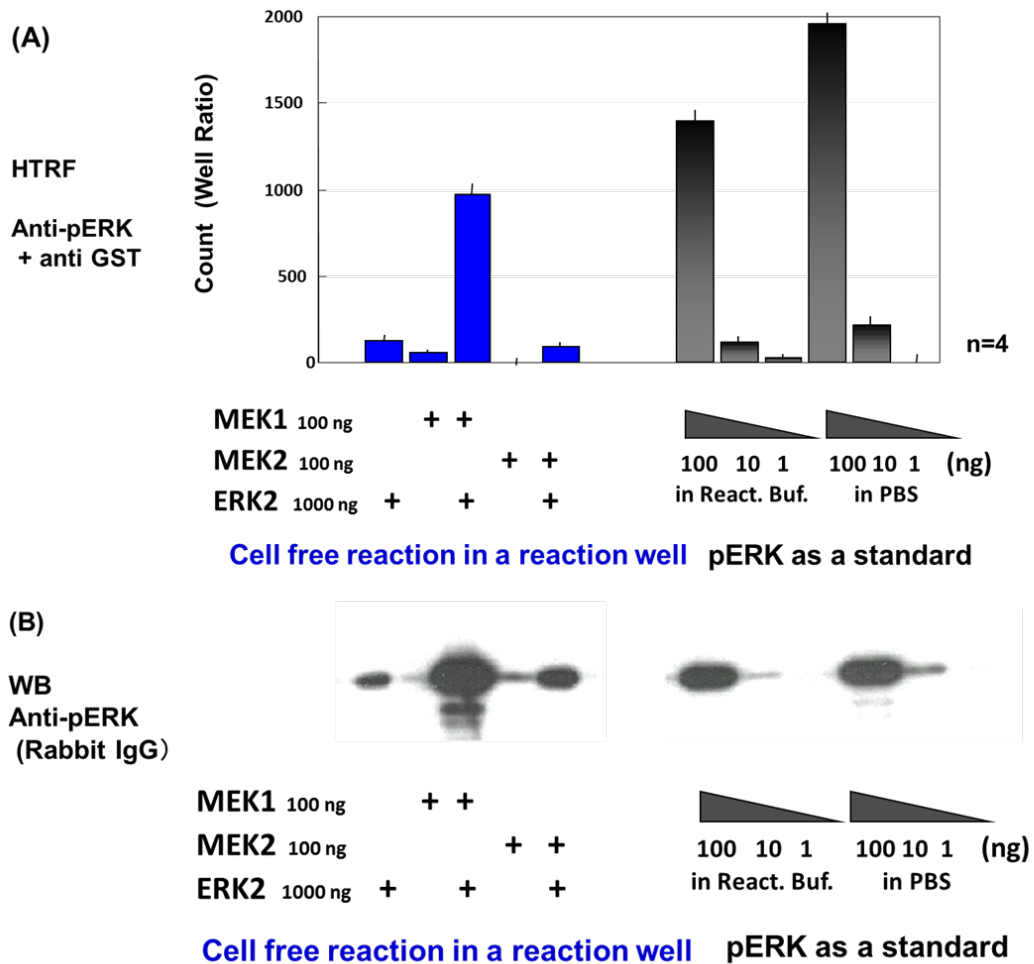


Figure 7 Confirmation of detection for MEK1/2 activity by Western blot analysis and the HTRF method

Detection of phosphorylated ERK2 induced by MEK1 or MEK2 was confirmed by the HTRF method (A) and Western blot (B) both.

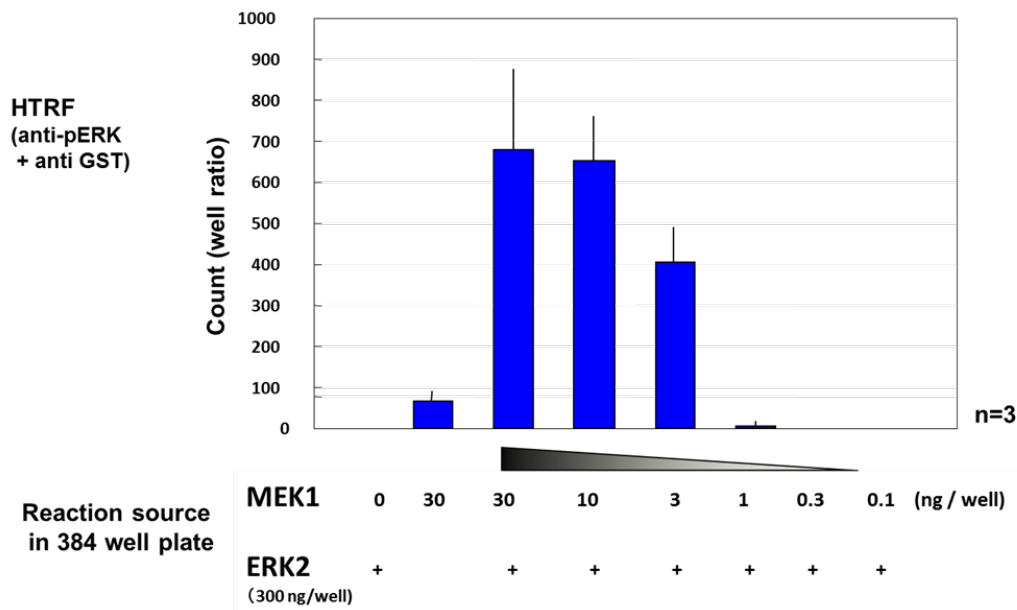


Figure 8 Optimization of MEK1 amount for a kinase reaction

The suitable MEK1 amount in the kinase reaction was confirmed by the HTRF method.

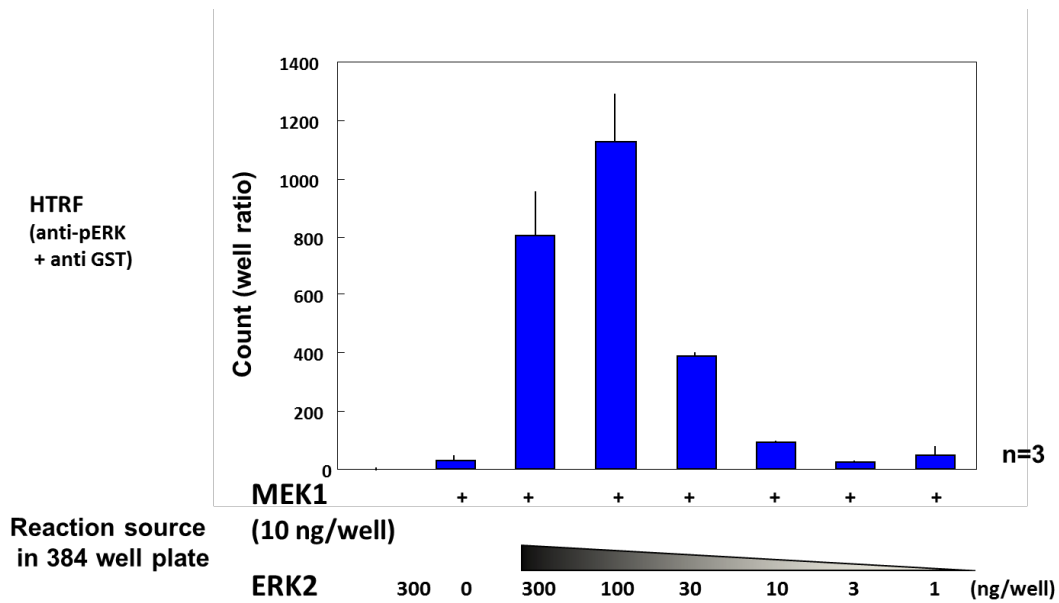


Figure 9 Optimization of substrate amount for a MEK1 kinase reaction

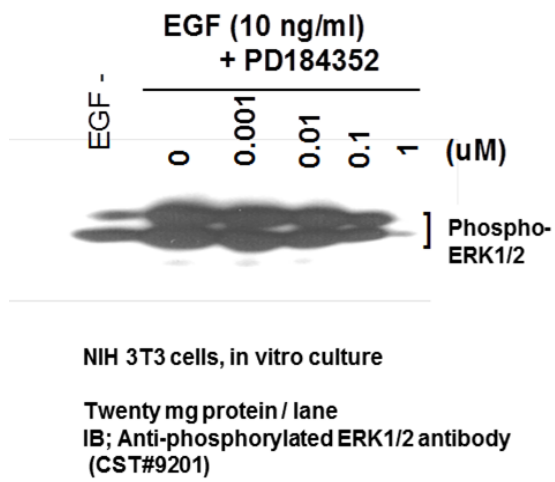
I also confirmed the suitable ERK2 amount as a substrate in the kinase reaction by the HTRF method.

### **2.2.2 Set up of a cell-based assay system**

I also developed a cell-based assay system to detect the phosphorylation of ERK1/2, which is transiently induced by Epidermal Growth Factor (EGF) stimulation in NIH 3T3 cells. Because the previous study demonstrated that NIH 3T3 cells express EGF receptors<sup>42)</sup>, I used this cell system. Inhibition of ERK1/2 phosphorylation by each compound was regarded as MEK1/2 inhibitory activities in cells. EGF stimulation induced transient ERK1/2 phosphorylation through the GFR-Ras-RAF- MEK-ERK pathway in NIH 3T3 cells. PD184352 inhibited the intracellular ERK1/2 phosphorylation (Figure 10). I set up the cell-ELISA detection system to improve assay throughput. In this assay, I tried to prepare for the protocol briefly summarized below; 1) The cells were directly immobilized and permeabilized using ice-chilled methanol. 2) The immobilized cells were incubated with antibodies to detect intracellular phosphorylated ERK1/2. 3) The cells captured by antibodies were collared by the reaction of HRP and OPD. Optimization of the conditions of cell-ELISA detection for phosphorylation of intracellular ERK1/2 is shown in Figure 11. These results demonstrated the optimal conditions for the cell-ELISA method, i.e., detection using antibody CST #9106 and bovine serum albumin (BSA) -based blocking buffer. Next, I checked for a good correlation between the results of the Western blot analysis and the results of cell-ELISA (Figure 12).



## Western blot



## Cell ELISA

Inhibition of EGF-induced Erk phosphorylation by PD184352

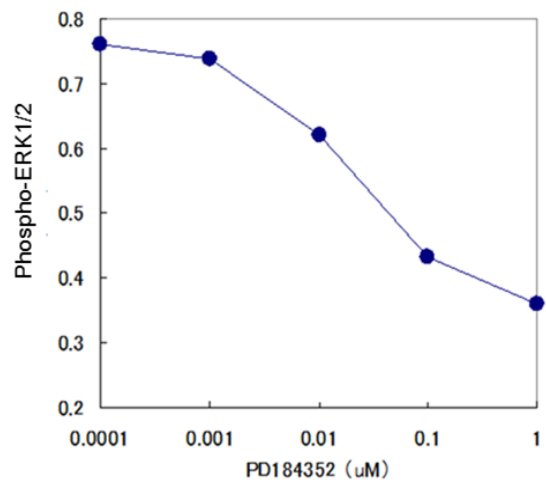


Figure 12 Concentration-dependent inhibitory effect against ERK1/2 phosphorylation by a MEK1/2 inhibitor in NIH3T3 cells

### 2.2.3 Screening of our compounds

We found a patentable, 3-4-difluoro-phenyl-methanesulfoamide compound, RCR-5523 (the chemical structure is shown in Figure 13) in former Sankyo's chemical library. I screened 1002 derivatives of RCR-5523 in the screening systems described above. Finally, 250 compounds were obtained, which showed  $IC_{50}$  values lower than 100 nM (shown in the Appendix data). In the in vitro screening, we measured the intra-cellular MEK1/2 inhibition activity of our compound with a cell-ELISA  $IC_{50}$  value using PD184352 as a reference compound for MEK1/2 inhibition. During the initial stage of this approach, we obtained three patentable and potent compounds, RCR-5789, -5885, and, -5886 (later referred as SMK-17). The chemical structures of the compounds are shown in Figure 14. All screening results of our compounds are shown in Appendix. We obtained 56 compounds that showed better activity than PD184352.

I will describe the detailed relationships between potency and chemical structure for representative and selected compounds in the next chapter.

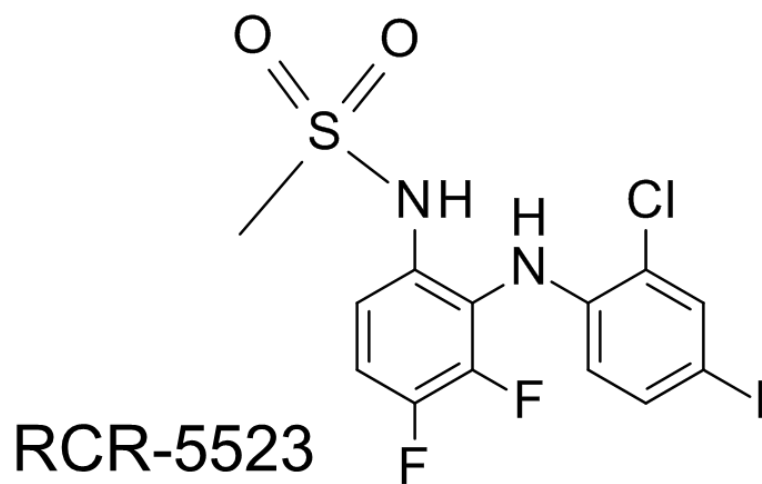


Figure 13 Chemical structure of RCR-5523 as a lead compound of the derivatization



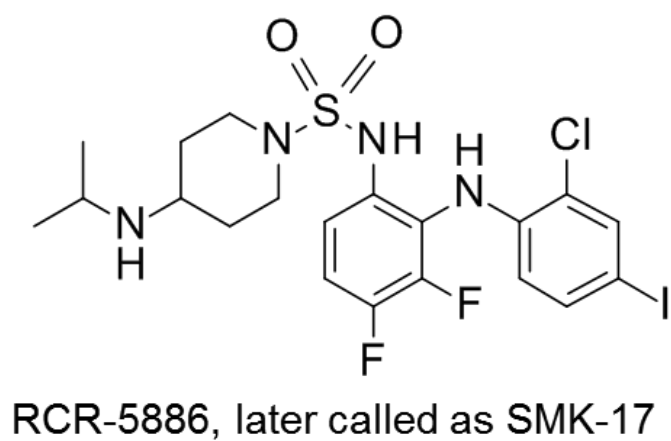
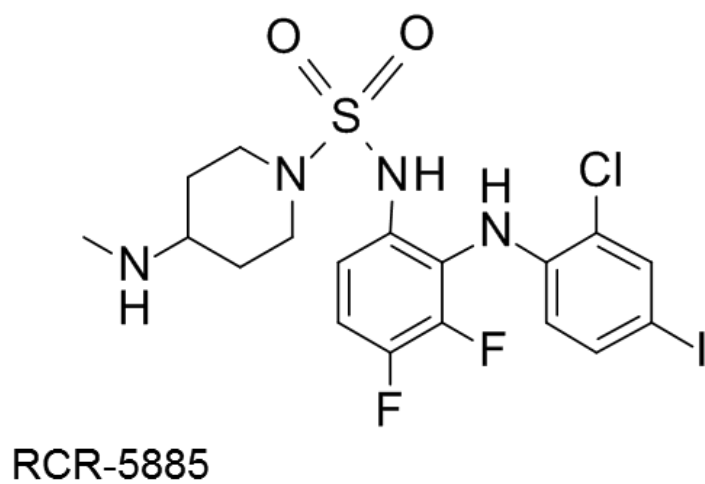
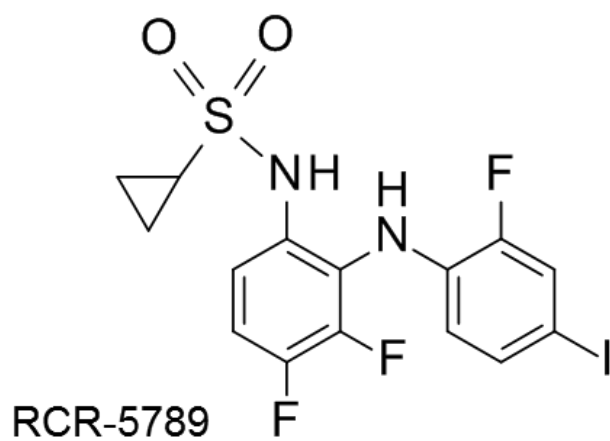


Figure 14 Chemical structures of our representative potent MEK inhibitors

## 2.3 Materials and methods in Chapter 2

### 2.3.1 Reagents and compounds

The reagents used in this study are described below.

Tris-HCl (Nacalai Tesque, Inc.), ethyleneglycol-bis (beta-aminoethylether)- N,N,N',N'-tetraacetic acid (EGTA) (Sigma- Aldrich Japan K. K.), bovine serum albumin (BSA) Fraction V (Sigma-Aldrich Japan K. K.), Na<sub>3</sub>VO<sub>4</sub> (Sigma-Aldrich Japan K. K.), MgCl<sub>2</sub> (Sigma-Aldrich Japan K. K.), KF (Sigma-Aldrich Japan K. K.), phosphate buffered saline (PBS) (Nissui Pharmaceutical Co., Ltd.), ethylenediamine- N,N,N',N'-tetraacetic acid, disodium salt, dihydrate (EDTA-2Na), active MEK1 and MEK2 made by ourselves according to the previous study<sup>43</sup>), unphosphorylated ERK2 (recombinant protein fused with GST, Upstate Ltd.), adenosine 5'-triphosphate (ATP) (Sigma-Aldrich Japan K. K.), anti-phospho ERK1/2 polyclonal antibody #9101 (Cell Signaling Technology, Inc.), polyclonal goat anti-rabbit antibody labeled with europium cryptate (PAR-K) (CIS Bio International), monoclonal anti GST antibody labeled with XL665 (Mab GST-XL) (CIS Bio International). Dulbecco's modified eagle medium (DMEM, Sigma-Aldrich Japan K. K.), fetal bovine serum (FBS, Lot AHM9419, HyClone Laboratories, Inc.), dimethyl sulfoxide (DMSO, Dojindo Laboratories Co., Ltd.), epidermal growth factor (EGF, Calbiochem), methanol (Wako Pure Chemical Industries, Ltd), skim milk (DIFCO, Becton Dickinson), a coloring reaction kit with OPD for HRP (Sumitomo Bakelite Co.), anti phospho-ERK1/2 monoclonal antibody #9106 (Cell Signaling Technology, Inc. ), anti phospho-ERK1/2 polyclonal antibody #9101 (Cell

Signaling Technology, Inc.), anti ERK1/2 polyclonal antibody #9102 (Cell Signaling Technology, Inc.), anti-mouse IgG HRP-linked #7076 (Cell Signaling Technology, Inc.), anti-rabbit IgG HRP-linked #7074 (Cell Signaling Technology, Inc.), Tris-HCl (Nacalai Tesque, Inc.), NaCl (high grade, Manac, Inc.), sodium dodecylsulfate (SDS, Wako Pure Chemical Industries, Ltd.), glycine (high grade, Nacalai Tesque, Inc.), methanol (high grade, Kanto Chemical Co., Inc.), IGEPAL CA-630 (corresponds to Nonidet P-40, Sigma-Aldrich Japan K. K.), phenylmethylsulfonyl fluoride (PMSF, Sigma-Aldrich Japan K. K.), deoxycholic acid (Sigma-Aldrich Japan K. K.), Tween 20 (Sigma-Aldrich Japan K. K.), glycerol (high grade, Wako Pure Chemical Industries, Ltd.), bromophenol blue (Nacalai Tesque, Inc.), acrylamide (Wako Pure Chemical Industries, Ltd.), N,N'-methylene-bis (acrylamide)-HG (Wako Pure Chemical Industries, Ltd.), BCA protein assay reagent (Pierce Chemical Co.), leupeptin (Sigma-Aldrich Japan K. K.) and pepstatin (Sigma-Aldrich Japan K. K.) .

All RCR-compounds and PD184352 were synthesized at Exploratory Chemistry Laboratories, of the former Sankyo Co., Ltd. Each compound was dissolved in DMSO and added to reaction systems (the final concentration of DMSO was 0.01% in each assay).

### **2.3.2 Cell-free kinase reaction and detection by HTRF**

Kinase reactions were conducted in 50  $\mu$ l of reaction buffer (50 mM Tris, pH 7.4 - 10 mM MgCl<sub>2</sub> - 2 mM EGTA - 1 mM Na<sub>3</sub>VO<sub>4</sub> -1 mg/ml BSA) containing 100  $\mu$ M ATP, 24 ng of active MEK1 or 2, 100 ng of GST fused ERK2 on a 1/2 area-96 well-EIA/RIA plate (Corning International K.K.) After incubation with each compound at 30°C for 30 minutes, the reactions were stopped by the addition of 25  $\mu$ l of detection buffer (1M KF-

50 mM EDTA- 0.1% PBS) containing 1/500 diluted PAR-K, 1/1000 diluted anti-phospho ERK1/2 polyclonal antibody and 1/250 diluted MAb GST-XL.

After overnight incubation with detection buffer, phosphorylated ERK2 was measured by HTRF. Each sample was irradiated by induction light at 337 nm and the excitation light was measured at both 620 nm and 665 nm after a 50  $\mu$ second delay with the Discovery HTRF microplate analyzer (PerkinElmer, Inc). The ratio of the 665 nm signal to the 620 nm signal was regarded a quantum phosphorylation of ERK2. Values of MEK absent from the negative control wells were taken as the baseline levels in each plate.

In this experiment, IC<sub>50</sub> (50% inhibitory concentration) of MEK inhibition were calculated using the linear regression method. Two concentrations of each compound, which gave MEK1/2 inhibitions above and below closest to 50%, were chosen to calculate the IC<sub>50</sub> values.

### **2.3.3 Cell lines**

Mouse fibroblast NIH 3T3 cells were purchased from the American Type Tissue Culture Collection, and were cultured in DMEM supplemented with 10% FBS at 37°C and 5% CO<sub>2</sub> atmosphere.

### **2.3.4 Cell ELISA**

NIH 3T3 cells ( $1.2 \times 10^4$  cells in each well) were seeded in a 24-well flat-bottomed plate (Nunc, Thermo Fisher Scientific Inc.) and cultured for 3 days. Culture medium was changed with 0.2% FBS-DMEM. After 24 hours of incubation, each compound solution in DMSO was added. After 1 hour of incubation with each compound, EGF (final

concentration was 10 ng/ml) was added. Five minutes later, medium was removed and washed with cold PBS containing 1 mM Na<sub>3</sub>VO<sub>4</sub>, fixed with -20°C methanol for 5 minutes. Fixed cells were blocked with blocking buffer (1% BSA -0.05% Tween20 -PBS or 5% skim milk - 0.05% Tween20 -PBS) for 1 hour, and incubated with primary antibodies in 1/1000 dilution for 2 hours at 4°C. The cells were washed with 0.05%-Tween20 -PBS twice, and then incubated with HRP-linked secondary antibodies in 1/1000 dilution at 4°C. After 1 hour of incubation, the cells were washed 3 times, and a color reaction was started with an OPD coloring reaction kit. Then, the absorbance at 490 nm was measured with a micro plate reader (Model 3550, Bio Rad).

In this experiment, IC<sub>50</sub> (50% inhibitory concentration) of MEK inhibition was calculated using the linear regression method, the same way as with the cell-free assay.

### **2.3.5 Western blot analysis**

NIH 3T3 cells were washed once with PBS containing 1 mM Na<sub>3</sub>VO<sub>4</sub> and lysed with RIPA buffer (50 mM Tris HCl (pH 7.5) - 150 mM NaCl - 1 mM Na<sub>3</sub>VO<sub>4</sub> - 0.1% SDS - 0.5% deoxycholic acid - 1% IGEPAL CA-630 - 1 µg/ml leupeptin -1 µg/ml pepstatin - 1 mM PMSF) for 1 hour at 4°C. After incubation at 4°C, soluble supernatants of lysates were obtained by centrifuging them for 10 minutes with 12,000 x g. Protein concentrations of lysates were determined by BCA protein assay reagent.

SDS-polyacrylamide gels were prepared in a mini-slab gel (Nihon Eido Co., Ltd.). The gels and buffer were composed of the following: Stacking gel: 125 mM Tris-HCl (pH 6.8) - 0.1% SDS in 3% acrylamide solution (acrylamide: N,N'-methylene-bis acrylamide=29 : 1) Separating gel: 375 mM Tris-HCl (pH 8.8) - 0.1% SDS in 10% acrylamide solution (acrylamide: N,N'-methylene-bis acrylamide=29 : 1) Electrophoresis

buffer: 25 mM Tris (pH 8.3) - 250 mM glycine - 0.1% SDS. Before electrophoresis, lysates containing 20 µg of proteins were added with x3 SDS sample buffer (150 mM Tris-HCl (pH 6.8) - 6% SDS - 0.3% bromophenol blue - 30% glycerol) and boiled for 3 minutes at 100°C. All of the samples were separated by electrophoresis at 60 V for 3 hours.

After electrophoresis, the gels were soaked in Tris-glycine buffer (25 mM Tris - 250 mM glycine) with 10% methanol and all of the proteins were transferred to polyvinylidene difluoride (PVDF) membranes electrically using Mini Trans-Blot Cell (Bio-Rad Laboratories). Blotting was performed at 60 V for 2 hours in Tris-glycine buffer with 10% methanol. After transferring the proteins, the membranes were subjected to blocking for 30 minutes (blocking solution: 5% skim milk - 10 mM Tris HCl (pH 7.5) - 150 mM NaCl - 0.05% (v/v) Tween 20), and then reacted with either anti-ERK1/2 rabbit polyclonal or anti-phospho-ERK1/2 mouse monoclonal antibodies overnight at 4°C. Both antibodies were used in 1/1000 dilution. After washing the membranes 3 times for 5 minutes at room temperature with TBST buffer (10 mM Tris-HCl (pH 7.5) - 150 mM NaCl - 0.05% (v/v) Tween 20), they were reacted with horseradish peroxidase-conjugated anti-mouse IgG antibody (Cell Signaling Technology) or anti-rabbit IgG antibody (Cell Signaling Technology) in 1/1000 dilution for 30 minutes at room temperature. After washing the membranes with TBST buffer 6 times, detection was performed by chemiluminescence using LumiGlo reagent and X-ray films XAR-5 (Kodak).

**3. Chapter 3; Analysis of a novel MEK1/2 inhibitor, SMK-17 (RCR-5886)**

### **3.1 Background of Chapter 3**

The derivatives of N-[2-(2-Chloro-4-iodo-phenylamino)-3,4-difluorophenyl]-methanesulfonamide as novel MEK1/2 inhibitors were shown in the previous chapter.

In this chapter, I describe our discovery of RCR-5886, referred to as SMK-17, to be a representative potent MEK1/2 inhibitor with high aqueous solubility among our potent compounds. We evaluated the docking study with MEK1, kinetics study, and kinase profiler analysis to confirm the allosteric nature and high selectivity of SMK-17.

Moreover, in vivo antitumor activities of SMK-17 by oral administration in animal models are presented in this chapter.

### **3.2 Results and discussion**

#### **3.2.1 Potency of diphenyl amine sulfonamide derivatives as a MEK1/2 inhibitor**

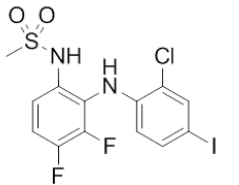
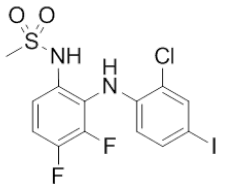
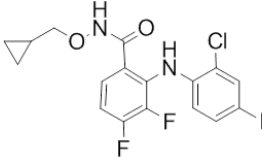
In this chapter, the discovery of the new derivative series of diphenyl amine sulfonamide as potent MEK inhibitors is discussed, with an optimization summary of the sulfonamide modification, which has culminated in the identification of the potent and highly water soluble MEK inhibitor, SMK-17 (referred to as RCR-5886 in Chapter 2, compound **17** in Table 2). The goal of this study was to identify a compound that possessed potent antitumor activity in vivo with high oral availability, which required high aqueous solubility for oral absorption as well as strong MEK inhibiting activity. An HTRF based kinase assay was employed as the primary screening described in the



previous chapter. Then, phospho-ERK detecting cell ELISA was used for measuring intracellular MEK activity. Oral absorption of each compound was predicted by calculated lipophilicity (cLogD) and aqueous solubility.

We identified a novel compound, N- [2-(2-Chloro-4-iodo-phenylamino) - 3,4-difluorophenyl]- methanesulfonamide (called RCR-5523, compound **1** in Table 2) as a MEK1/2 inhibitor in the above-described screening. It has sulfamide substituent different to previously reported MEK inhibitors such as U0126, PD98059, and PD184352. This compound showed weak activity in in vitro assays and poor water solubility, less than 0.5  $\mu$ M of solubility at pH 6.8 solution. We adopted compound **1** as a lead compound for derivatization and attempted to obtain derivatives with improved potency and aqueous solubility for the development of an oral absorbable potent MEK1/2 inhibitor.

Table 2 Identification of a sulfamide compound as a MEK1/2 inhibitor

Compound		MEK1 kinase IC <sub>50</sub> (nM)	pERK in cell EC <sub>50</sub> (nM)	clogD <sub>7.4</sub>	Solubilities JP-1 / JP-2 (μM)
1		670	180	5.35	1.0 / <0.5
PD184352		33	79	8.01	<0.5 / <0.5

MEK1 kinase inhibition, intra-cellular MEK inhibition, cLogD, and aqueous solubility assay results of compound 1 and PD184352 as a reference compound.

As the first step of modification of the starting compound, we added the sulfonamide of compound **1** to the hydroxy-piperidine-group. As a result, compound **2** and **9** in Table 3 showed 17- and 3-fold increases in MEK1 kinase inhibition compared to compound **1**. As the second step, the terminal piperidine-sulfamide was added to various polar substituents to demonstrate the structure–activity relationship of this substructure. The structure-activity relationship was established with two varying positions (R1 and R2 in Table 3). The activities of the piperidine-sulfamide series indicated that a substituent of the chlorine group was desired at the R2 position in cell-based potency rather than the fluorine or methyl group, as evidenced by compounds **7-9**, **11-13**, **16**, and SMK-17. The cell-free activities of compounds including fluorine at the R2 (**12** and **16**) were more potent than activities of the chlorine groups (**13** and SMK-17). This reversal of potency order between cell-free and cell-based activity is considered to be due to the cell membrane permeability of these compounds. Additionally, an alkyl-amine substituent at the 4 (para) position of R1, which was adopted in compounds **11-19**, was the favorable structure for MEK inhibition of both cell-free and cell-based activity. In contrast, hydroxy- terminal substituents such as compounds **2**, **7-10**, and **20** were unfavorable. In particular an isopropyl-amine at the 4 position (SMK-17) was the optimal structure for both intra-cellular and cell-free MEK1 kinase inhibition.

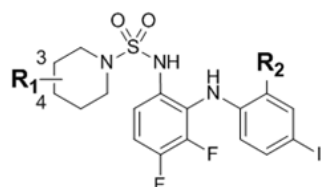
Low cLogD, which predicts the property of high water solubility, is required for in vivo exposure of orally-administered drugs. The cLogD of compound **1** is 3.95 and the solubility in JP-2 (pH 6.8) buffer is less than 0.5  $\mu\text{M}$ . Alkyl-amine adopted derivatives (compounds **3-6**, **11-19**) achieved lower cLogD and higher water solubility, of which the range was 61 to 88  $\mu\text{M}$  in JP-2 solution, compared with the piperidinol series

(compounds **2**, **7-10**) in addition to improvement of in vitro activities. Adoption of basic residue such as alkyl-amine in the R1 position is considered to contribute to the improvement of the polar character and high aqueous solubility.

Summarizing the above, we observed two significant structure-activity relationships in the compound optimization. First, substitution of alkyl-amine, especially an isopropyl-amine, at the R1 position provides better profiles of both aqueous solubility and in vitro activities. A comparison between the cell-based MEK inhibitory potencies of compound **9** and its isopropyl-amine analog (SMK-17) revealed an 8-fold improvement. The second critical finding was that the substituent of chlorine was desired at the R2 position rather than fluorine or methyl. Substitution of chlorine for fluorine at the R2 position of compound **16** gives SMK-17 a 4-fold increase in intra-cellular MEK inhibition. The same substitution in the piperidinol pair (analogs **8** and **9**) provides about a 3-fold improvement in cell potency.

The two structure-activity relationships provide the benefit of improved aqueous solubility and in vitro activity. We finally obtained SMK-17, which has more than 100-fold aqueous solubility in JP-2 and 11-fold strengthened MEK kinase inhibition.

Table 3 Structure-activity relationship of piperidine sulfamide scaffold for MEK inhibition and solubility screening

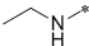
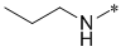
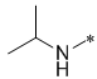
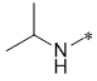
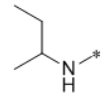
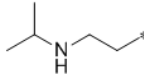
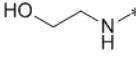
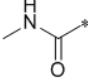


Template structure for this table

Compound	Substitution position	R1	R2	MEK1 kinase IC <sub>50</sub> (nM)	pERK in cell EC <sub>50</sub> (nM)	clogD <sub>7.4</sub>	Solubilities JP-1 / JP-2 (μM)
2	3-	HO*	Cl	40	360	4.65	- / -
3			F	42	770	3.41	100 / 86
4			F	270	1500	4.29	87 / 77
5			F	50	530	3.79	91 / 88
6			F	34	110	2.93	91 / 86
-----							
7	4-	HO*	Me	260	900	4.79	- / -
8		HO*	F	210	1500	5.07	12 / 21
9		HO*	Cl	210	400	4.78	- / -
10		HOCH <sub>2</sub> *	Cl	180	300	5.06	1 / 2
11			Me	290	1800	2.92	87 / 80
12			F	60	150	3.23	92 / 84
13			Cl	92	52	2.92	88 / 74

All tests were conducted with the same methods as Table 2. The table is continued on the next page.

(Table 3 contd.)

Compound	Substitution position	R1	R2	MEK1 kinase IC <sub>50</sub> (nM)	pERK in cell EC <sub>50</sub> (nM)	clogD <sub>7.4</sub>	Solubilities JP-1 / JP-2 (μM)
14	4-		Cl	74	800	3.41	89 / 61
15			Cl	72	190	3.93	- / -
16			F	33	220	4.11	74 / 90
17 (SMK-17)			Cl	62	50	3.80	91 / 77
18			Cl	20	210	4.22	- / -
19			F	14	130	3.95	86 / 78
20			F	41	430	3.42	- / -
21			Cl	210	46	4.44	3 / 1

### 3.2.2 Binding mode of SMK-17 with MEK1

To understand the characteristics of these derivatives, we built a docking model of SMK-17 and MEK1 (Figure 15). The predicted binding model showed that SMK-17 binds to an allosteric pocket adjacent to the ATP binding site similarly to U0126 or PD325089<sup>44)</sup>, which indicates that SMK-17 is a non-ATP-competitive inhibitor. This model predicted a very unique binding mode of DFG-In and Helix $\alpha$ C-Out (a brief diagram is shown in Figure 16). In addition, the protonated amine of the alkyl-amine group at the R1 forms salt-bridges with the gamma phosphate of ATP. The aliphatic carbons of the alkyl-amine substituent have hydrophobic interactions with M219 and V224 (out-of-sight in this figure) in the activation segment. This predicted binding mode supports the structure-activity relationship that inhibitory activity is well correlated with the size of alkyl-amine as shown in Table 3.

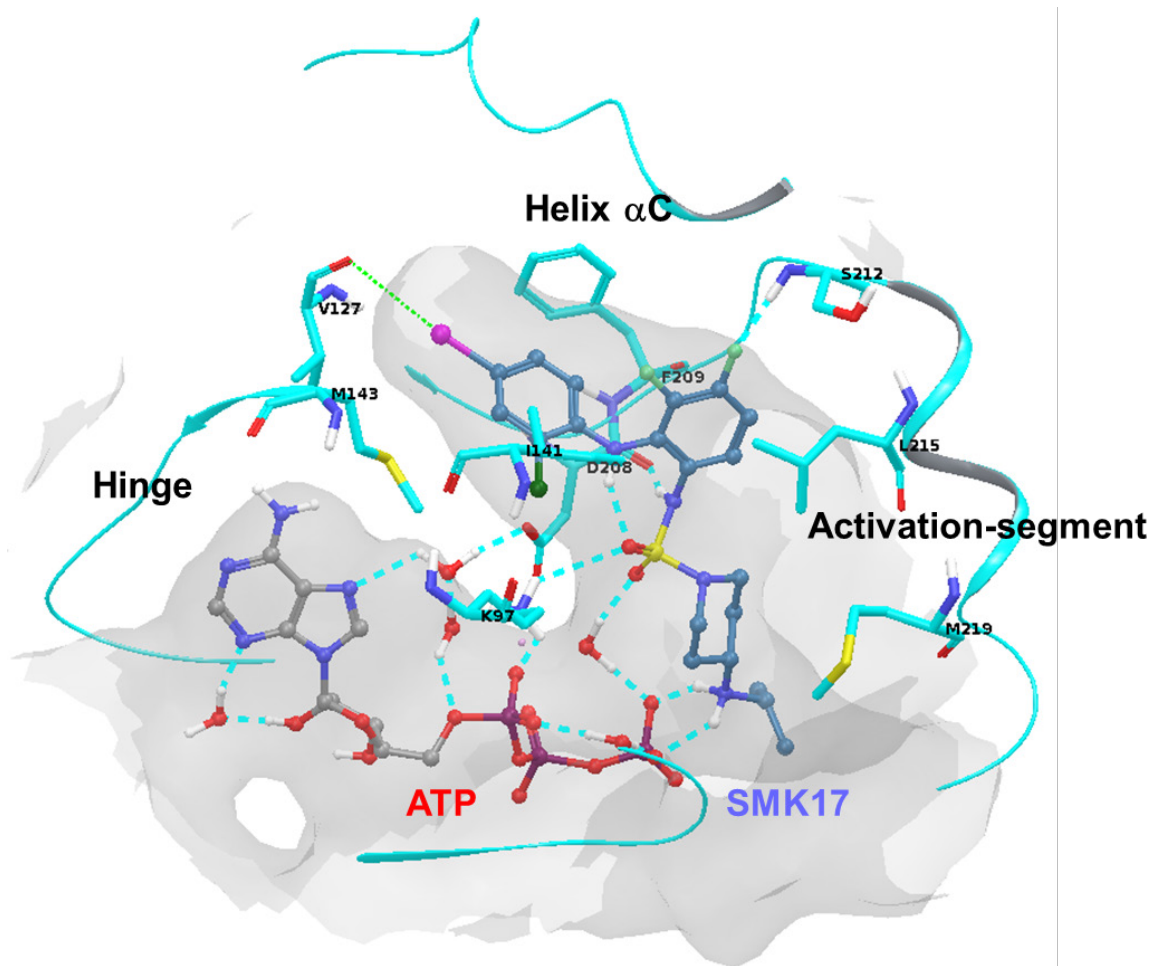


Figure 15 Binding mode of SMK-17 with MEK1

The predicted binding mode of SMK-17 with MEK1 viewed from the N-lobe. For simplicity, only important residues are shown. The hydrogen bonds and salt-bridges are represented by cyan dotted lines. The MEK1 pocket surface is shown as a transparent gray surface. The figure was generated using Maestro version 9.0.



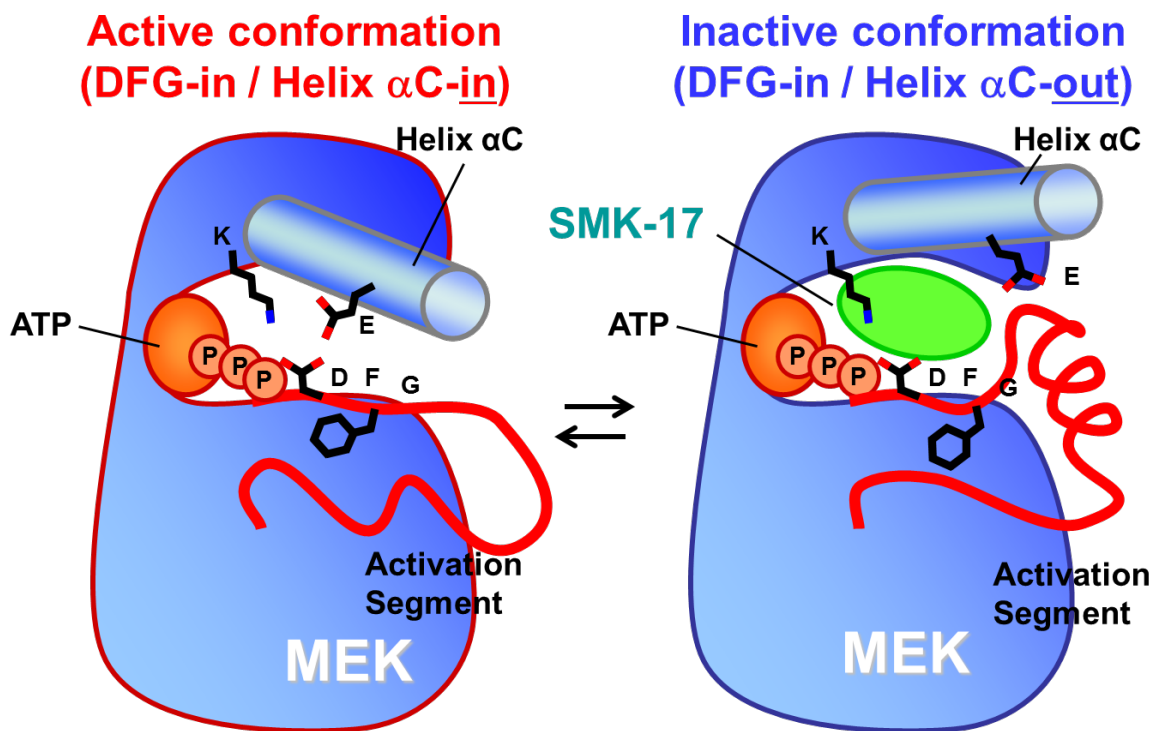


Figure 16 Diagrams explaining the binding mode of SMK-17 with MEK1

### **3.2.3 ATP dependency of kinase inhibition of SMK-17**

To confirm the allosteric binding character of SMK-17 predicted in Figure 15, I examined the ATP dependence of MEK1 inhibition by SMK-17. I tested MEK1 kinase inhibition at various concentrations of ATP from 10 to 1000  $\mu\text{M}$  (the concentration curves in Figure 17 and the Dixon plot in Figure 18 ). As a result, ATP concentration had minimal effect on the MEK1 inhibition of SMK-17. The  $\text{IC}_{50}$  values of SMK-17 for MEK1 kinase were 31.4 (ATP 10  $\mu\text{M}$ ), 36.6 (100  $\mu\text{M}$ ), and 36.5 nM (1000  $\mu\text{M}$ ) respectively. Thus, SMK-17 was regarded as a completely non-ATP-competitive inhibitor of MEK1. These results coincide with the prediction by the *in silico* binding model that SMK-17 does not exclude ATP from MEK1.

**SMK-17 inhibitory activity in 100  $\mu$ M ATP**  
hMEK1  $IC_{50}$  = 57 nM (average, n=5)  
hMEK2  $IC_{50}$  = 56 nM (average, n=2)

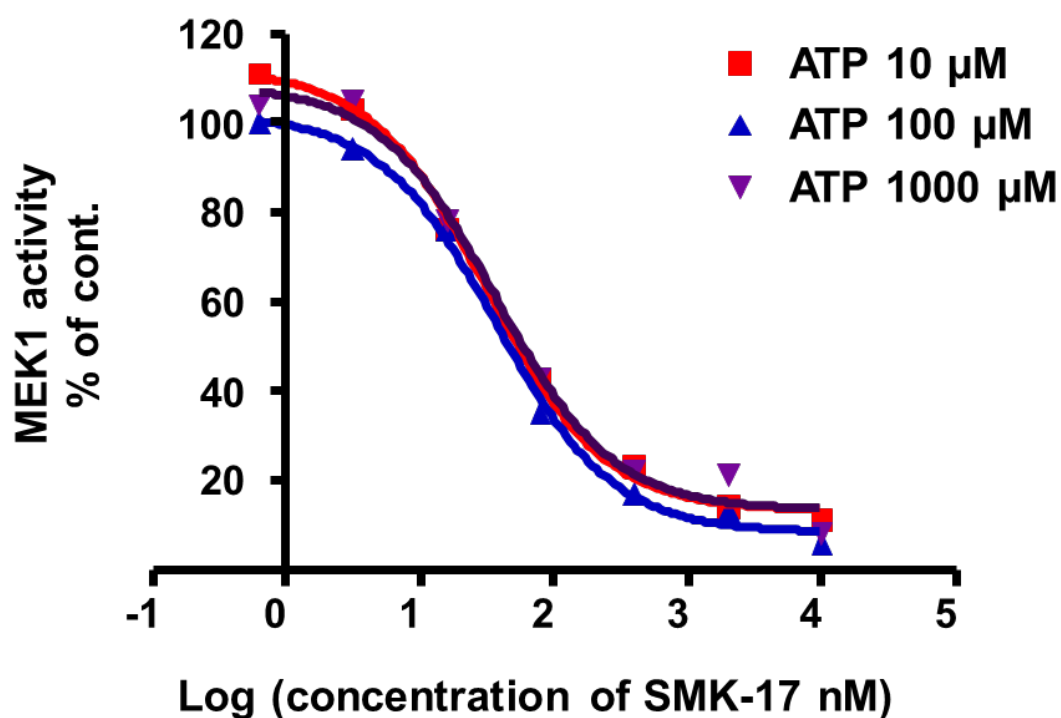


Figure 17 MEK1 kinase inhibition by SMK-17 in various ATP concentrations  
Phosphorylation of ERK2 induced by MEK1 was detected with the HTRF method.  
The  $IC_{50}$  value for MEK1 inhibition in this assay with 100  $\mu$ M of ATP represented 37 nM. The mean value of several independent experiments was 57 nM for MEK1 kinase inhibition (n=5), and 56 nM for MEK2 (n=2).

## Dixon plot

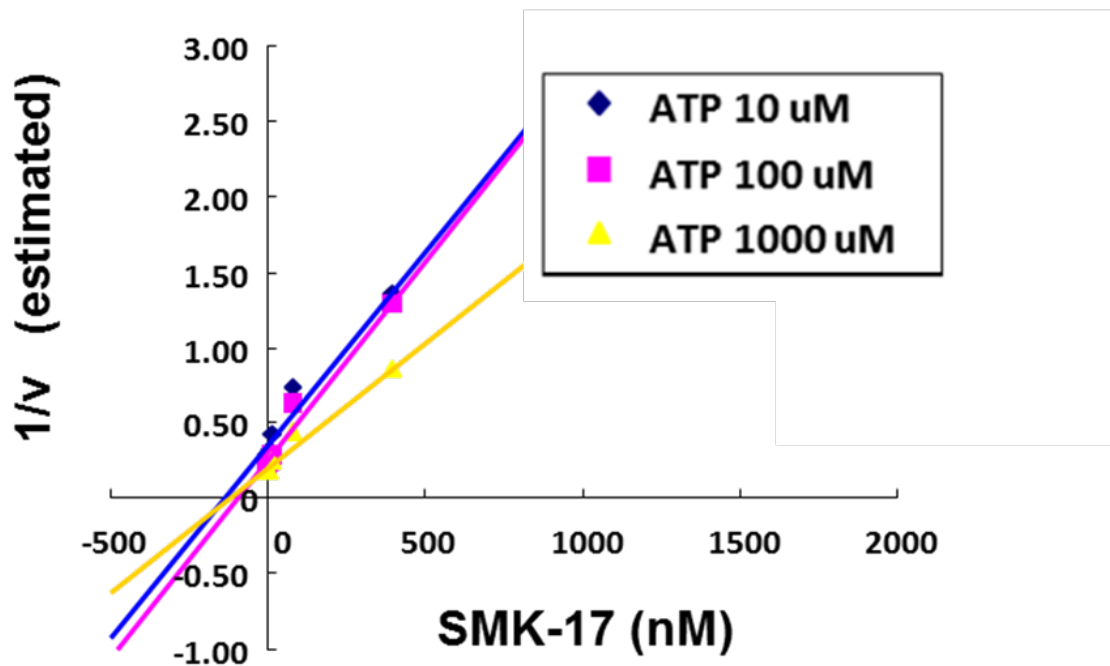


Figure 18 Dixon plot demonstrating the non ATP-competitive manner of SMK-17 to a MEK1 kinase reaction

The Dixon plot was created by the initial rates of kinase reactions ( $V$  as the initial velocity in this plot) of the recombinant MEK1 in various concentrations of ATP and SMK-17. Kinase reactions were performed using the same methods as the previous figure.

### 3.2.4 Kinase inhibitory selectivity of SMK-17

SMK-17 was further characterized for its kinase selectivity with Millipore's Kinase Profiler. The screen of 233 protein kinases incubated with 1000 nM of this compound, which was 18-fold concentration of IC<sub>50</sub> to MEK1 (Table 4). Figure 19 shows the Top 40 kinases, which were inhibited by SMK-17. MEK1 was the most sensitive kinase to SMK-17, and was inhibited by 74%. There was no significant (>50%) inhibition of any other protein kinases observed except for MEK1. Notably, SMK-17 had little effect on MEK1 isoforms, such as MKK4 (-29% inhibition), MKK6 (2%), and MKK7 (-32%). Non-ATP competitive but an allosteric binding mode of this compound probably contributes to the highly selectivity to MEK1/2.

Despite their allosteric inhibition mode, PD184352 and U0126 were previously reported to inhibit MKK5 as an off-target<sup>45</sup>). Conformation of the allosteric pocket of MEK1/2 is supposedly similar to that of MKK5. However, SMK-17 did not inhibit ERK5 phosphorylation, which is a substrate of MKK5 in both cell-based and in vivo studies. These results indicated that SMK-17 is a non-ATP-competitive and highly selective kinase inhibitor of MEK1/2.

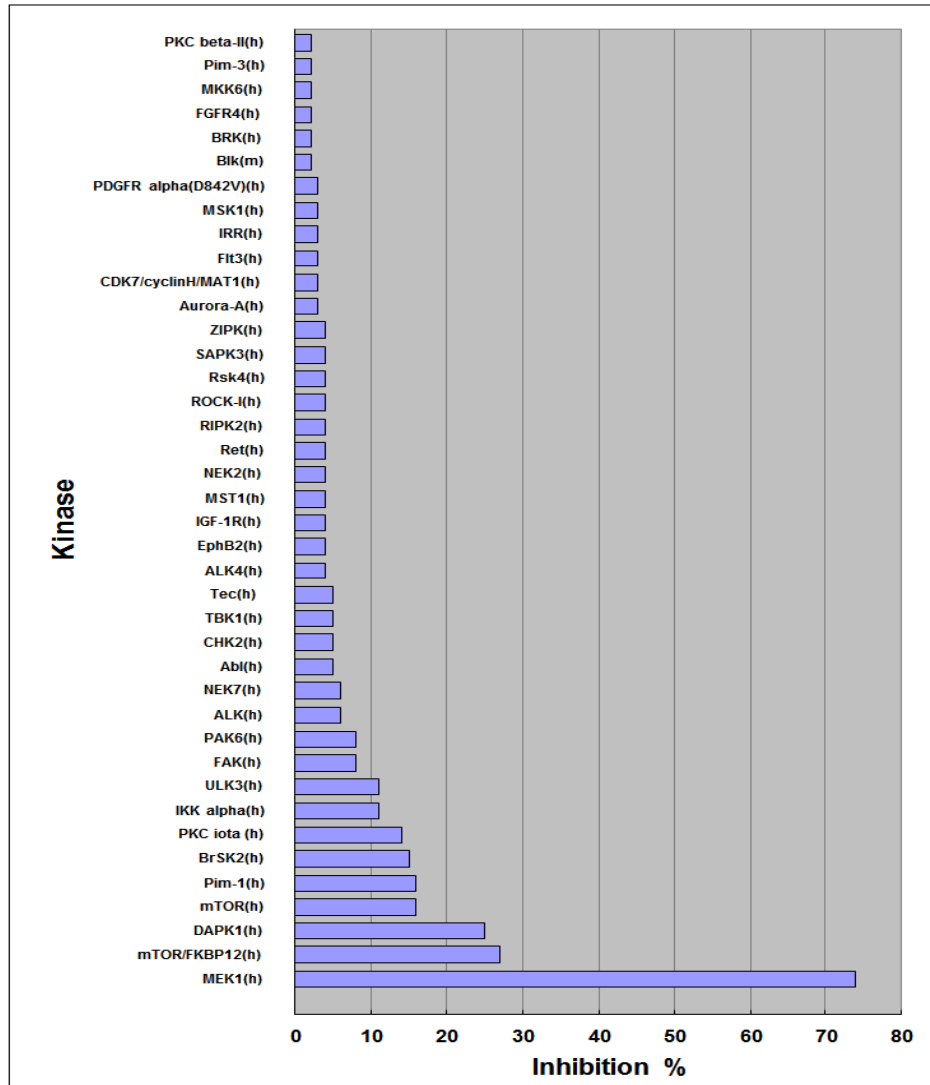


Figure 19 Kinase inhibitory profiling of SMK-17

The Millipore' Kinase Profiler data showing about 233 human kinases indicated that SMK-17 is a selective inhibitor against hMEK1 (1000 nM about 18 fold higher than  $IC_{50}$  for MEK1). The x-axis shows the percentage of inhibition against a specific kinase (y-axis). The top 40 kinases are shown in this figure.

Table 4 All kinase inhibitory activity data concerning inhibition% of each human kinase by 1000 nM of SMK-17

Kinase	Inhibition %	Kinase	Inhibition %
1 MEK1(h)	74	61 Lyn(h)	0
2 mTOR/FKBP12(h)	27	62 PKC $\mu$ (h)	0
3 DAPK1(h)	25	63 PKC $\zeta$ (h)	0
4 mTOR(h)	16	64 SGK3(h)	0
5 Pim-1(h)	16	65 TSSK2(h)	0
6 BrSK2(h)	15	66 Aurora-B(h)	-1
7 PKC $\iota$ (h)	14	67 Axl(h)	-1
8 IKK $\alpha$ (h)	11	68 CaMKIV(h)	-1
9 ULK3(h)	11	69 CK1 $\gamma$ 1(h)	-1
10 FAK(h)	8	70 CK2(h)	-1
11 PAK6(h)	8	71 Fgr(h)	-1
12 ALK(h)	6	72 GCK(h)	-1
13 NEK7(h)	6	73 Hck(h) activated	-1
14 Abl(h)	5	74 HIPK1(h)	-1
15 CHK2(h)	5	75 IRAK1(h)	-1
16 TBK1(h)	5	76 LOK(h)	-1
17 Tec(h) activated	5	77 MST2(h)	-1
18 ALK4(h)	4	78 PAK5(h)	-1
19 EphB2(h)	4	79 PDK1(h)	-1
20 IGF-1R(h)	4	80 PKA(h)	-1
21 MST1(h)	4	81 PKB $\gamma$ (h)	-1
22 NEK2(h)	4	82 PKC $\gamma$ (h)	-1
23 Ret(h)	4	83 PKC $\theta$ (h)	-1
24 RIPK2(h)	4	84 Syk(h)	-1
25 ROCK-1(h)	4	85 TAO1(h)	-1
26 Rsk4(h)	4	86 ARK5(h)	-2
27 SAPK3(h)	4	87 CaMKII $\beta$ (h)	-2
28 ZIPK(h)	4	88 CDK2/cyclinE(h)	-2
29 Aurora-A(h)	3	89 EphA2(h)	-2
30 CDK7/cyclinH/MAT1(h)	3	90 EphA4(h)	-2
31 Flt3(h)	3	91 MAPK2(h)	-2
32 IRR(h)	3	92 MELK(h)	-2
33 MSK1(h)	3	93 NEK6(h)	-2
34 PDGFR $\alpha$ (D842V)(h)	3	94 PKB $\alpha$ (h)	-2
35 Blk(m)	2	95 ROCK-II(h)	-2
36 BRK(h)	2	96 Ros(h)	-2
37 FGFR4(h)	2	97 Rsk2(h)	-2
38 MKK6(h)	2	98 SAPK2a(h)	-2
39 Pim-3(h)	2	99 SAPK2b(h)	-2
40 PKC $\beta$ II(h)	2	100 SAPK4(h)	-2
41 Rsk3(h)	2	101 TrkB(h)	-2
42 TLK2(h)	2	102 TSSK1(h)	-2
43 WNK3(h)	2	103 WNK2(h)	-2
44 AMPK( $\iota$ )	1	104 ASK1(h)	-3
45 CaMKI $\delta$ (h)	1	105 EGFR(h)	-3
46 CDK2/cyclinA(h)	1	106 IR(h)	-3
47 CK1 $\gamma$ 2(h)	1	107 JNK1 $\alpha$ 1(h)	-3
48 EphA3(h)	1	108 MAPKAP-K3(h)	-3
49 Mer(h)	1	109 MINK(h)	-3
50 MLCK(h)	1	110 MLK1(h)	-3
51 MuSK(h)	1	111 NLK(h)	-3
52 NEK11(h)	1	112 PASK(h)	-3
53 PRK2(h)	1	113 PrkX(h)	-3
54 TAO2(h)	1	114 PTK5(h)	-3
55 BrSK1(h)	0	115 Tie2(h)	-3
56 CaMKI $\delta$ (h)	0	116 ACK1(h)	-4
57 FGFR3(h)	0	117 CK2 $\alpha$ 2(h)	-4
58 Flt1(h)	0	118 GRK5(h)	-4
59 Fms(h)	0	119 JAK3(h)	-4
60 HIPK3(h)	0	120 Mnk2(h)	-4

The kinase tests were conducted using the same methods as the previous figure.

(Table 4 contd.)

121	Pik1(h)	-4
122	Pik3(h)	-4
123	ULK2(h)	-4
124	CDK5/p25(h)	-5
125	CDK5/p35(h)	-5
126	CLK3(h)	-5
127	EphA7(h)	-5
128	IRAK4(h)	-5
129	KDR(h)	-5
130	PKB $\beta$ (h)	-5
131	PRAK(h)	-5
132	SGK(h)	-5
133	SRPK1(h)	-5
134	STK33(h)	-5
135	CHK1(h)	-6
136	CK1(y)	-6
137	EphA1(h)	-6
138	FGFR1(h)	-6
139	Flt4(h)	-6
140	GRK6(h)	-6
141	GRK7(h)	-6
142	JNK2 $\alpha$ 2(h)	-6
143	Lck(h)	-6
144	MSSK1(h)	-6
145	BTK(h)	-7
146	CDK3/cyclinE(h)	-7
147	cKit(h)	-7
148	DDR2(h)	-7
149	DYRK2(h)	-7
150	EphB3(h)	-7
151	FGFR2(h)	-7
152	Fyn(h)	-7
153	Itk(h)	-7
154	PDGFR $\alpha$ (h)	-7
155	PKG1 $\alpha$ (h)	-7
156	Pyk2(h)	-7
157	SGK2(h)	-7
158	SIK(h)	-7
159	VRK2(h)	-7
160	CaMKI(h)	-8
161	c-RAF(h)	-8
162	DCAMKL2(h)	-8
163	DMPK(h)	-8
164	DRAK1(h)	-8
165	EphB4(h)	-8
166	IKK $\beta$ (h)	-8
167	LIMK1(h)	-8
168	MAPKAP-K2(h)	-8
169	PAK4(h)	-8
170	PKC $\eta$ (h)	-8
171	PKD2(h)	-8
172	PKG1 $\beta$ (h)	-8
173	CDK1/cyclinB(h)	-9
174	CSK(h)	-9
175	eEF-2K(h)	-9
176	EphA5(h)	-9
177	ErbB4(h)	-9
178	IR(h), activated	-9
179	PAR-1B $\alpha$ (h)	-9
180	Pim-2(h)	-9

181	PKC $\alpha$ (h)	-9
182	CDK9/cyclin T1(h)	-10
183	MRCK $\beta$ (h)	-10
184	PDGFR $\beta$ (h)	-10
185	Rsk1(h)	-10
186	TAO3(h)	-10
187	EphA8(h)	-11
188	Fes(h)	-11
189	PKC $\epsilon$ (h)	-11
190	Rse(h)	-11
191	TAK1(h)	-11
192	Yes(h)	-11
193	Bmx(h)	-12
194	CLK2(h)	-12
195	EphB1(h)	-12
196	HIPK2(h)	-12
197	JNK3(h)	-12
198	PKC $\delta$ (h)	-12
199	DAPK2(h)	-13
200	LKB1(h)	-13
201	MARK1(h)	-13
202	Ron(h)	-13
203	ZAP-70(h)	-13
204	Arg(h)	-14
205	cSRC(h)	-14
206	PAK2(h)	-14
207	PhkY2(h)	-14
208	SRPK2(h)	-14
209	IGF-1R(h), activated	-15
210	Met(h)	-15
211	PKC $\beta$ I(h)	-15
212	CaMKII $\gamma$ (h)	-16
213	MRCK $\alpha$ (h)	-16
214	p70S6K(h)	-16
215	JAK2(h)	-17
216	MSK2(h)	-17
217	Snk(h)	-17
218	CK1 $\gamma$ 3(h)	-18
219	Fer(h)	-18
220	NEK3(h)	-18
221	Txk(h)	-19
222	Hck(h)	-20
223	PAK3(h)	-20
224	Haspin(h)	-22
225	MST3(h)	-22
226	CK1 $\delta$ (h)	-24
227	TrkA(h)	-24
228	MAPK1(h)	-28
229	MKK4(m)	-29
230	GSK3 $\beta$ (h)	-32
231	MKK7 $\beta$ (h)	-32
232	EGFR(T790M)(h)	-34
233	GSK3 $\alpha$ (h)	-45



### **3.2.5 Inhibition of intracellular MEK1/2 and cell growth by SMK-17**

To further investigate the intra-cellular effects of SMK-17, the antiproliferative effect of SMK-17 was examined against murine colorectal cancer colon 26, human colorectal cancer HT-29, human pancreas cancer Panc-1, and human prostate cancer LNCaP. SMK-17 was active in suppressing cell growth in colon 26 and HT-29 cell lines, which harbors highly phosphorylated MEK1/2 and ERK1/2. The GI<sub>50</sub> values were 2.0 and 0.34  $\mu$ M, respectively (Figure 20). In contrast, SMK-17 was not effective on tumor cells, which do not have highly phosphorylated MEK1/2 and ERK1/2, such as Panc-1 and LNCaP cells. As previously reported with the other MEK inhibitor<sup>46)</sup>, SMK-17 is highly effective on the proliferation of tumor cells with aberrant activated MAPK pathway signaling, which is reflected by the phosphorylation levels of MEK1/2 and ERK1/2.

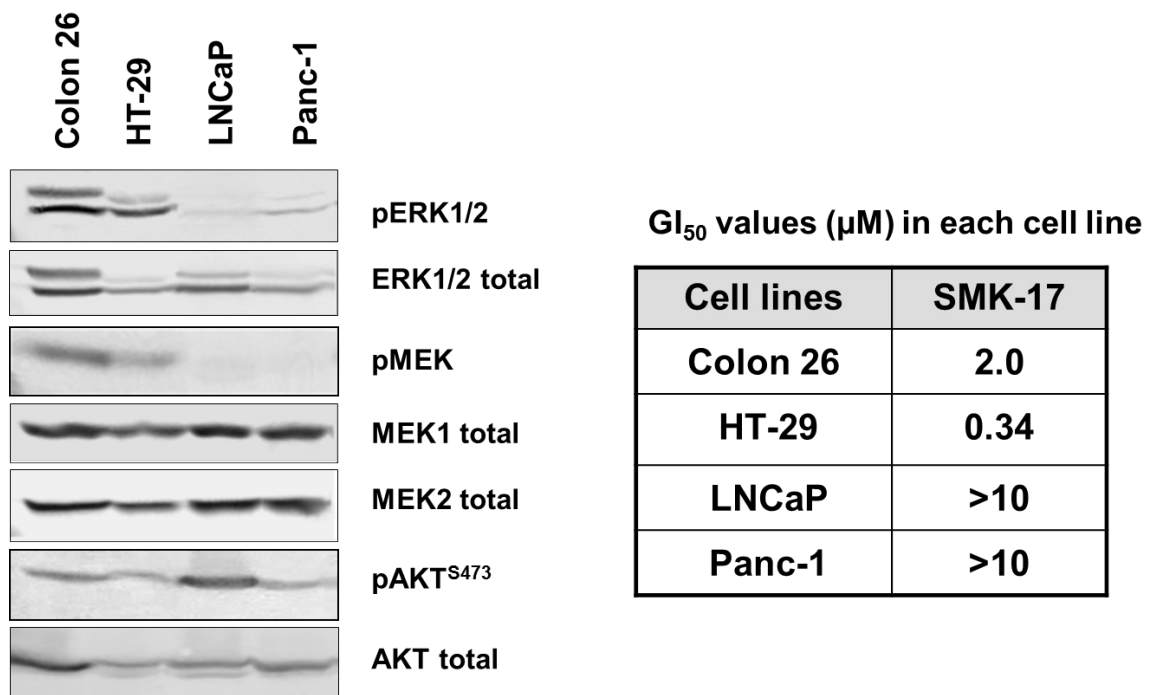


Figure 20 Growth inhibition profile of SMK-17 against tumor cell lines

Expression profiling was analyzed by Western blot analysis for pERK, ERK, pMEK, MEK1/2, pAKT S473, and AKT. The GI<sub>50</sub> values of SMK-17 in a 72 h ATP assay are shown.

To understand the underlying mechanism of SMK-17 on cancer cell proliferation, I analyzed its effect on the cell-cycle progression and cyclin D1 expression in tumor cells. In responsive cell lines, colon 26 and HT-29 colorectal cancer cells, inhibition of ERK1/2 phosphorylation by SMK-17 led to the G1 phase cell-cycle arrest at about 5-fold concentration of GI<sub>50</sub>, 10 μM in HT-29 and 1 μM in colon 26 (Figure 21 and Figure 22, which were similar to the effects of PD184352. Correspondingly, treatment with SMK-17 resulted in the down regulation of cyclin D1, a key cell-cycle regulator for G1-S phase progression, which is a typical physiological effect of MEK1/2 inhibitors<sup>47)</sup>.

It was reported that cyclin D1 is an unstable protein, of which the half-life is about 30 minutes<sup>48)</sup>. The amount of cyclin D1 protein decreased 8-16 hours after MEK was inhibited. The time-lagged response of cyclin D1 decrease can be explained by two independent regulatory mechanisms of cyclin D1. First, protein synthesis of cyclin D1 can be translated from the remaining mRNA. The translation of cyclin D1 does not stop although the MEK inhibitor suppresses MEK-ERK inducing cyclin D1 transcription activity. Second, phosphorylation of cyclin D1 at T286 by ERK enhances its ubiquitination and proteasomal degradation<sup>49)</sup>. Hence, inhibition of MEK-ERK attenuates phosphorylation of T286 and the degradation of cyclin D1 protein. Accordingly, inhibition of MEK-ERK results slows the decrease of cyclin D1. A negative feedback mechanism by ERK, which suppresses the upstream of the ras/raf signal pathway was reported in a previous study<sup>50)</sup>. In this study, we observed increased phosphorylation of MEK1/2 by SMK-17 in HT-29 cells. As the MEK inhibitor suppressed the activity of ERK including the negative feedback pathway, SMK-17 was

likely to cause increased MEK1/2 phosphorylation by inactivating the negative feedback mechanism.

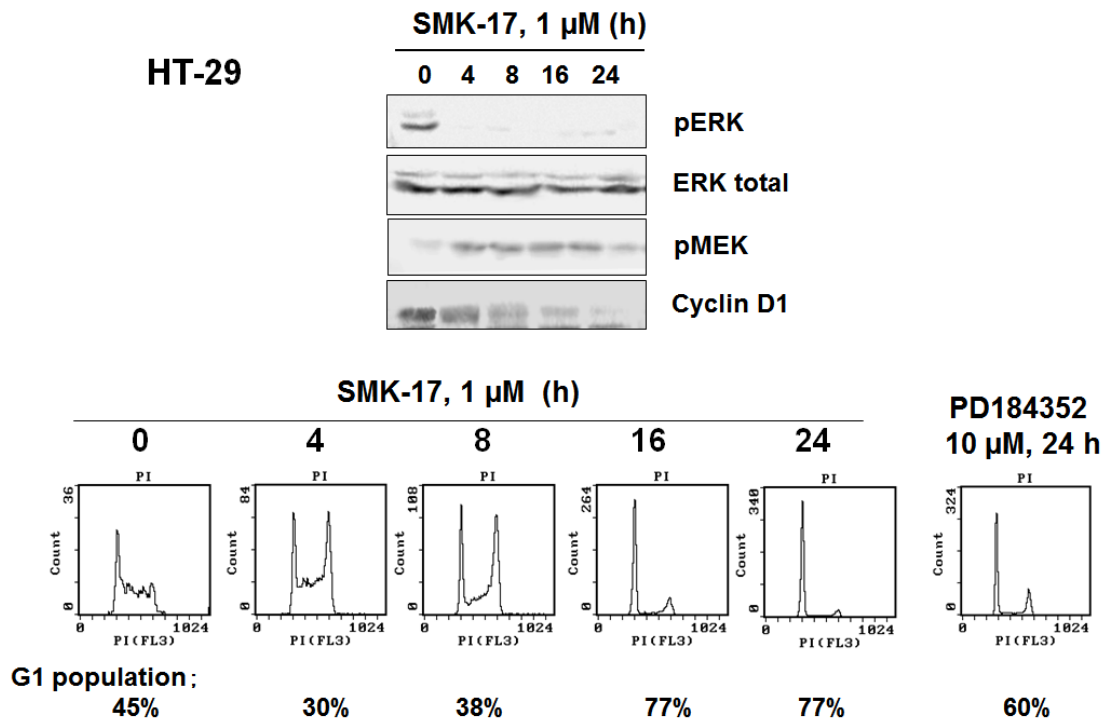


Figure 21 Effects of SMK-17 on cell cycle, MEK/ERK, and cyclin D1 proteins in HT-29 cells

HT-29 cells were treated with SMK-17 (1  $\mu$ M; 5 fold of  $GI_{50}$  for the cell line) or PD184352 for 24 h and cell cycle profiles were examined by FCM analysis. The values for cell cycle distribution were derived using MultiCycle software. SMK-17 affects the expressions of proteins that are critical to G1 phase transition in the cell cycle. Cells were treated with SMK-17 for 24 h, and the cell lysates were analyzed by Western blot analysis using antibodies as indicated.

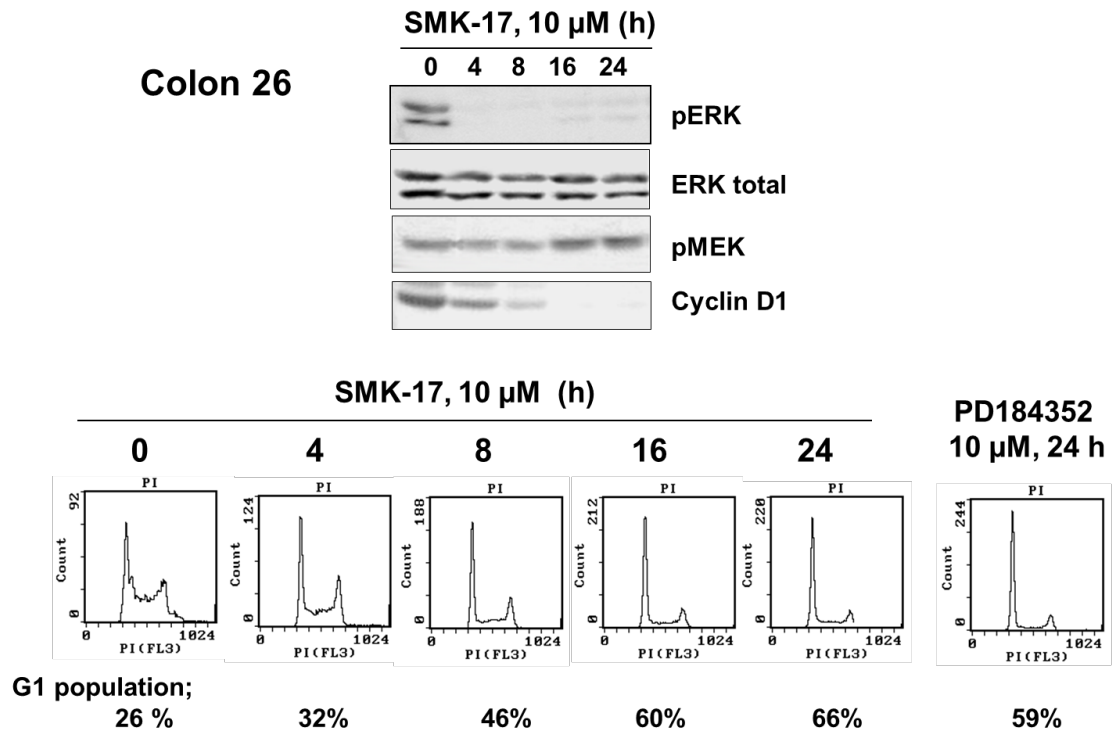


Figure 22 Effects of SMK-17 on cell cycle, MEK/ERK, and cyclin D1 proteins in colon 26 cells

Colon 26 cells were treated with SMK-17 (10  $\mu$ M, 5 fold of  $GI_{50}$  for the cell line) or PD184352 for 24 h and cell-cycle profiles were examined by FCM analysis. The other materials and methods are the same as the previous figure.

In contrast, in resistant Panc-1 and LNCaP cells, SMK-17 at the concentration of 30  $\mu$ M did not lead a marked G1 phase arrest and down-regulation of cyclin D1 (Figure 23 and Figure 24). It is possible that proliferation of resistant cell lines is independent of MEK/MAPK pathways because these cell lines have phosphorylated S473 of AKT, which represents PI3K/AKT pathway activation (Figure 20). PI3K dependent growth of Panc-1 cells are supported by several reports<sup>51),52),53)</sup>. Our results support the PI3K pathway-dependent growth of MEK inhibitor resistant cell lines. Furthermore, SMK-17 did not induce apoptosis as evident by sub G1 population on FCM analysis in all four cell lines, even at the conditions of fully MEK1/2 inhibited cells (e.g. 10  $\mu$ M of SMK-17 on HT-29 cells).

We also confirmed that SMK-17 did not induce apoptosis on these cell lines which was monitored with AnnexinV-APC and 7AAD double staining. These results indicated that inhibition of MEK/ERK signal pathways is not sufficient to induce apoptosis in all four cell lines.

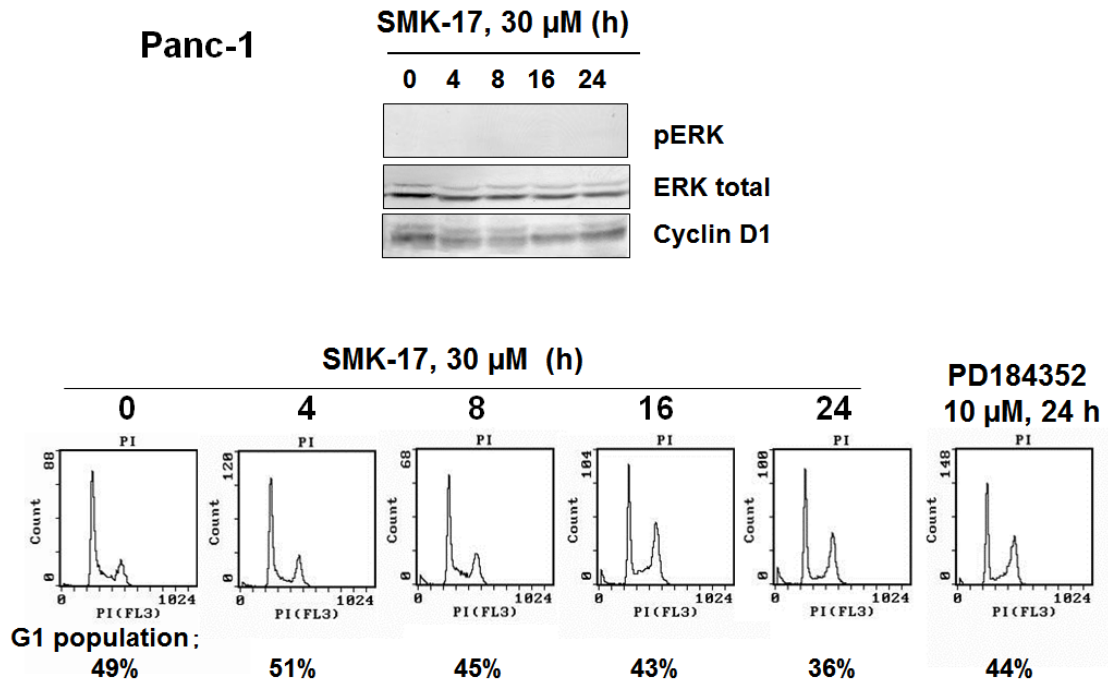


Figure 23 Effects of SMK-17 on cell cycle, phosphorylated ERK, and cyclin D1 proteins in Panc-1 cells

Panc-1 cells were treated with SMK-17 (30  $\mu$ M) or PD184352 for 24 h and cell cycle profiles were examined by FCM analysis. The values for cell cycle distribution were derived using MultiCycle software. SMK-17 did NOT affect the expressions of proteins that are critical to the G1 phase transition in the cell cycle in Panc-1 cells.



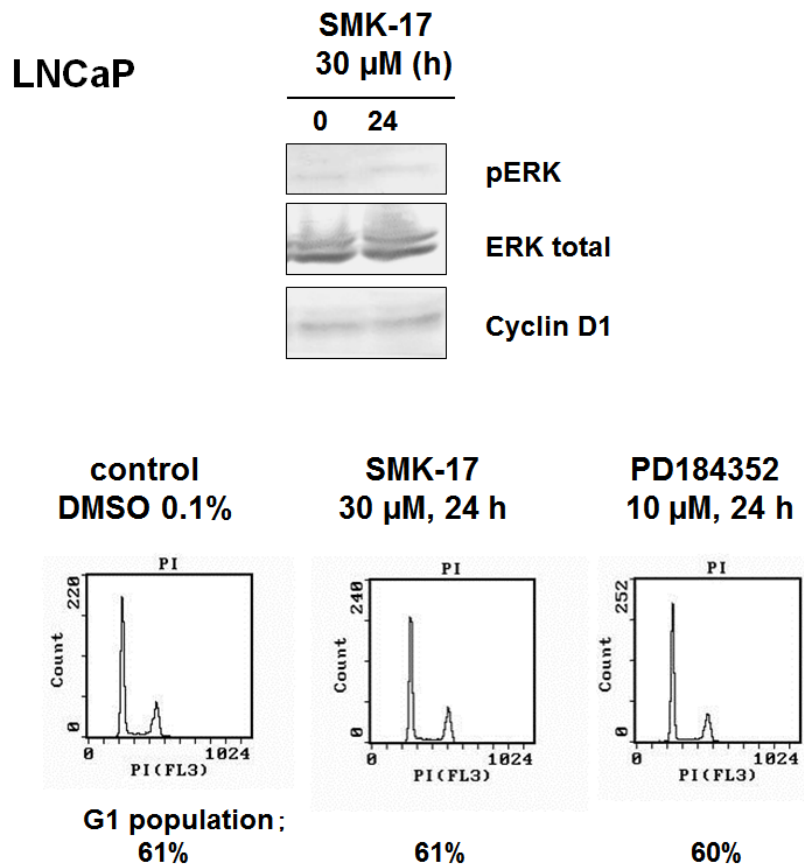


Figure 24 Effects of SMK-17 on cell cycle, phosphorylated ERK, and cyclin D1 proteins in LNCaP cells

LNCaP cells were treated with SMK-17 (30  $\mu$ M) or PD184352 for 24 h and cell cycle profiles were examined by FCM analysis. The other materials and methods are the same as the previous figure. SMK-17 did NOT affect the expressions of proteins that are critical to the G1 phase transition in the cell cycle in LNCaP cells.

To examine whether MEK1/2 inhibition of SMK-17 directly affects cell cycle arrest, we investigated the dose correlation between cell cycle arrest and intra-cellular MEK1/2 inhibition using HT-29 cells. As a result, an inverse correlation was seen between intensity of ERK phosphorylation and an increase of G1 population (Figure 25). Moreover, SMK-17 selectively inhibited Raf/MEK/ERK pathway activity in cells while having no effect on the activation status of other closely related intracellular signaling molecules such as ERK5, p38, JNK and AKT in the effective concentration (Figure 26). These results indicated that SMK-17 induced G1 arrest through intracellular MEK1/2 inhibition as an on-target effect.

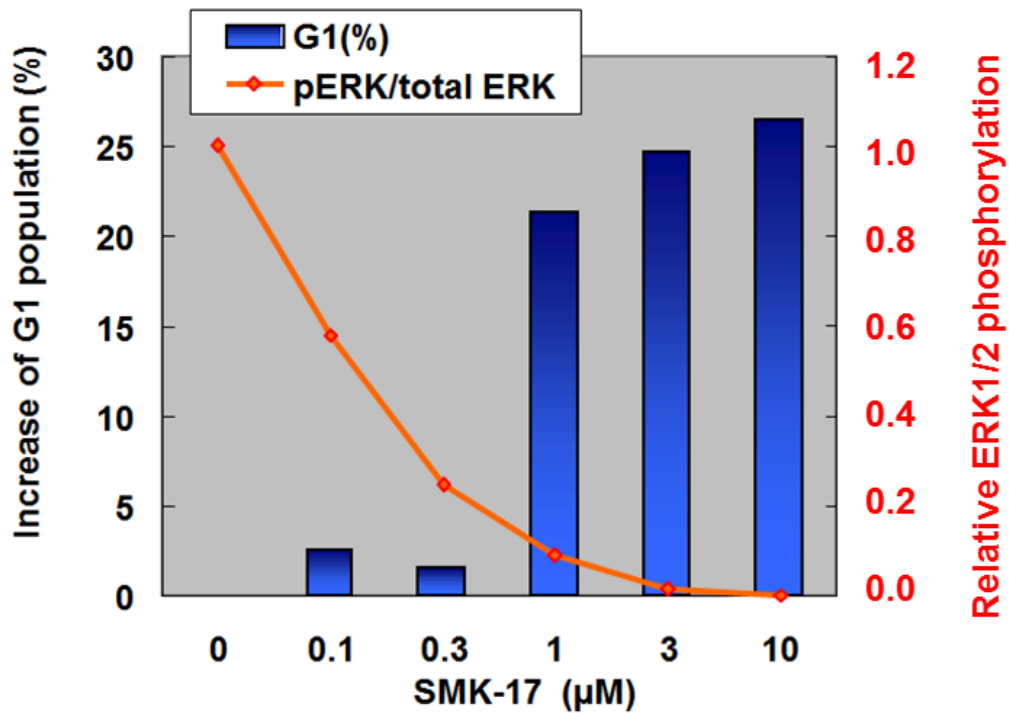


Figure 25 Concentration-correlation between intracellular MEK1/2 inhibition and cell cycle arrest intensity on SMK-17 treated HT-29 cells

Phosphorylation and total ERK expression after 24 h drug treatment were evaluated with Western blot analysis. The G1 phase population was examined by FCM analysis.

## HT-29 cells, in vitro culture

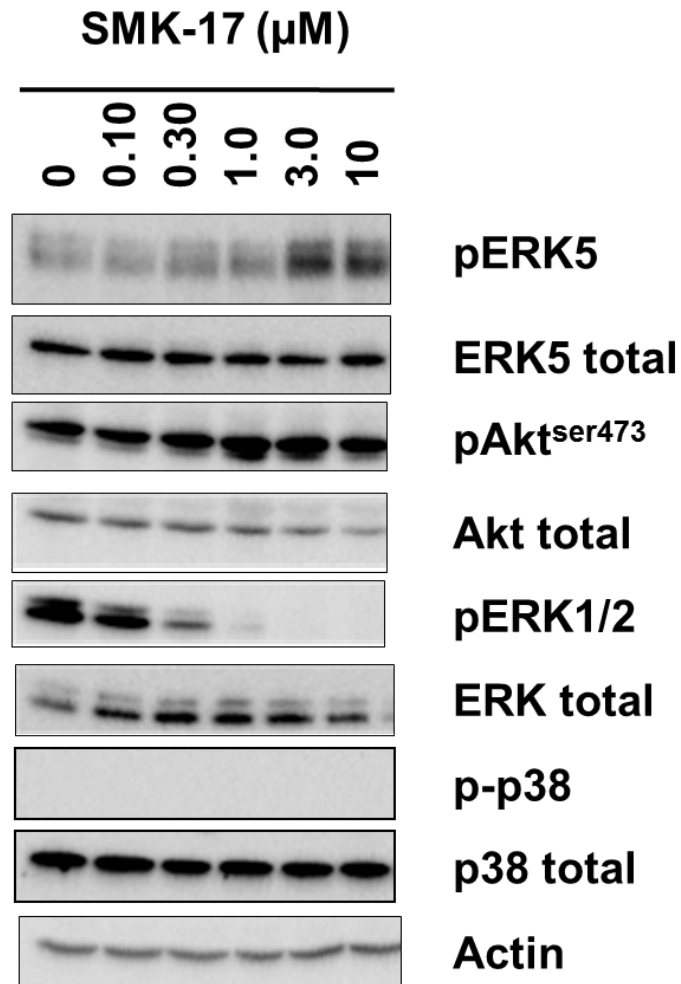


Figure 26 Western blot analysis for phosphorylated and total ERK5, ERK1/2, and AKT proteins

HT-29 cells treated with indicated concentrations of SMK-17 for 4 h. The cell lysates were analyzed by Western blot analysis using antibodies as indicated.

### **3.2.6 In vivo antitumor activity in an allograft model**

I evaluated the in vivo efficacy of SMK-17 using the murine colorectal colon 26 cells-implanted syngeneic model in CDF1 mice. Colon 26 cells have constitutively active k-ras mutation. After a single oral dose of SMK-17, the tumors were excised at various time points postdosing and the tumor lysates were analyzed for phospho-ERK1/2 and total ERK1/2 levels as a pharmacodynamic (PD) study. SMK-17 decreased the phospho-ERK1/2 level in tumor mass after 50 mg/kg administration for 6 h. Two hundred mg/kg treatment caused 24 h lasting phospho-ERK1/2 inhibition (Figure 27 and Figure 28 as quantification data).

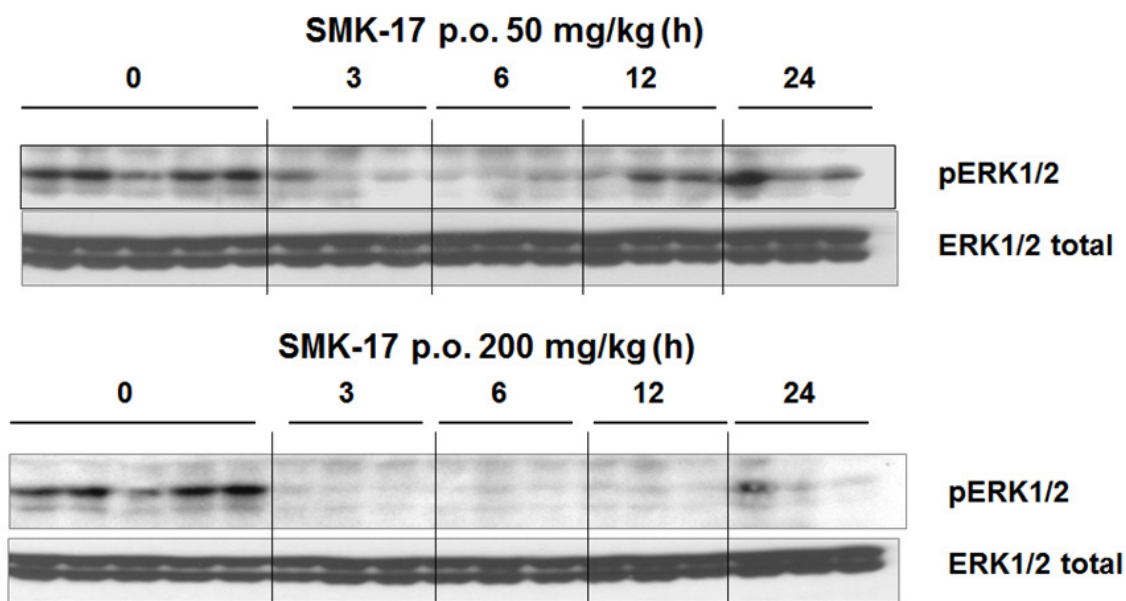


Figure 27 In vivo PD efficacy of SMK-17 on a colon 26 allograft model

After a single oral administration of SMK-17 to colon 26- CDF1 mice, the tumors were excised at various time points postdosing and tumor lysates were analyzed by Western blot analysis. Administration of SMK-17 at 50 mg/kg achieved phospho-ERK1/2 inhibition in tumors for 6 h. Significant phospho-ERK1/2 inhibition was observed up to 24 h postdosing from mice treated with 200 mg/kg compared to the untreated controls.

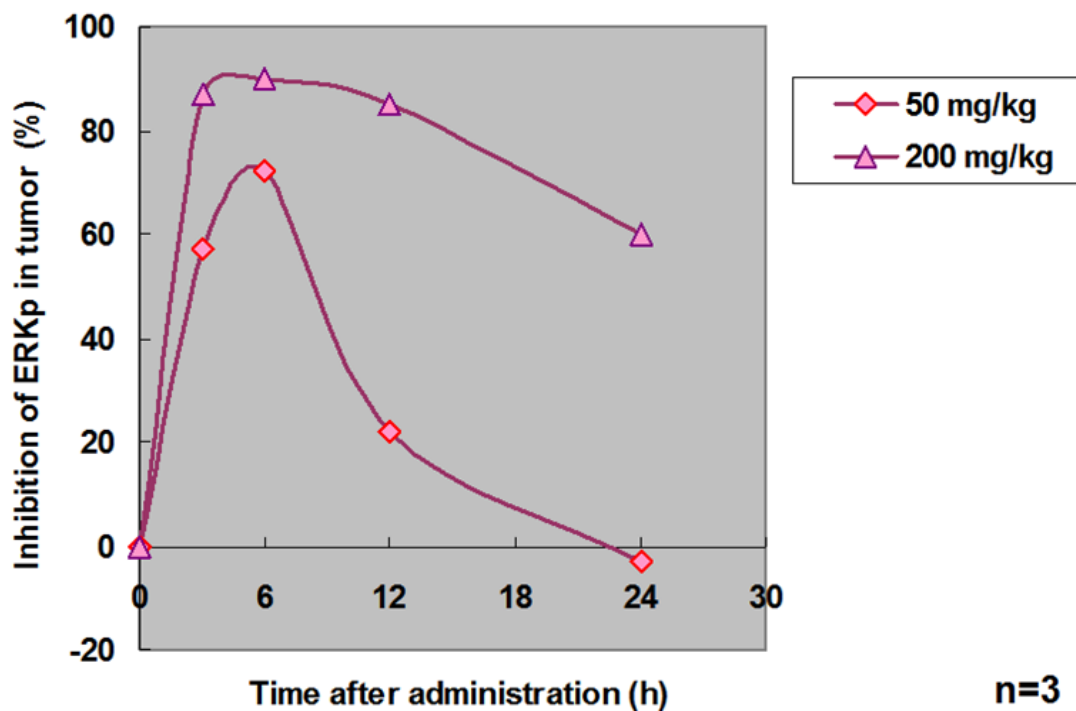


Figure 28 Quantified in vivo PD efficacy of SMK-17 on a colon 26 allograft model

A quantification result from the previous figure is shown. Inhibition of phospho-ERK1/2 in a tumor was calculated as described below. Phospho-ERK1/2 inhibition (%) =  $[1 - (\text{Mean of phospho-ERK intensity}) / (\text{Mean of total ERK intensity})] \times 100$ .

The antitumor activity of SMK-17 was evaluated in the same model in CDF1 mice. When SMK-17 was administered to mice once daily with doses at 50 and 200 mg/kg, antitumor activity was observed, from partial tumor growth inhibition at doses of 50 mg/kg to complete inhibition at 200 mg/kg (Figure 29) without significant body weight loss. In this experiment, PD184352 as a reference also showed tumor growth inhibition. In this syngeneic graft model, blood samples were collected from animals and the drug concentration in plasma was measured for pharmacokinetic and pharmacodynamic (PK/PD) analysis. SMK-17 concentrations in the plasma of mice are shown in Table 5. Complete inhibition of ERK phosphorylation in tumors was achieved when the plasma drug concentration was more than 0.83  $\mu\text{g/mL}$  (comparable to 1.4  $\mu\text{M}$ ,  $M_w=584.8$ ).

This minimum effective plasma concentration is similar to the  $GI_{50}$  value of colon 26 cells in vitro. For administration of 200 mg/kg of SMK-17, at which complete inhibition of intra-tumor MEK1/2 for 24 h per dosing occurs, tumor growth was completely inhibited. These results indicated that continuous exposure of SMK-17 was necessary for long lasting inhibition of intra-tumor MEK1/2 and complete tumor growth inhibition in an animal model.



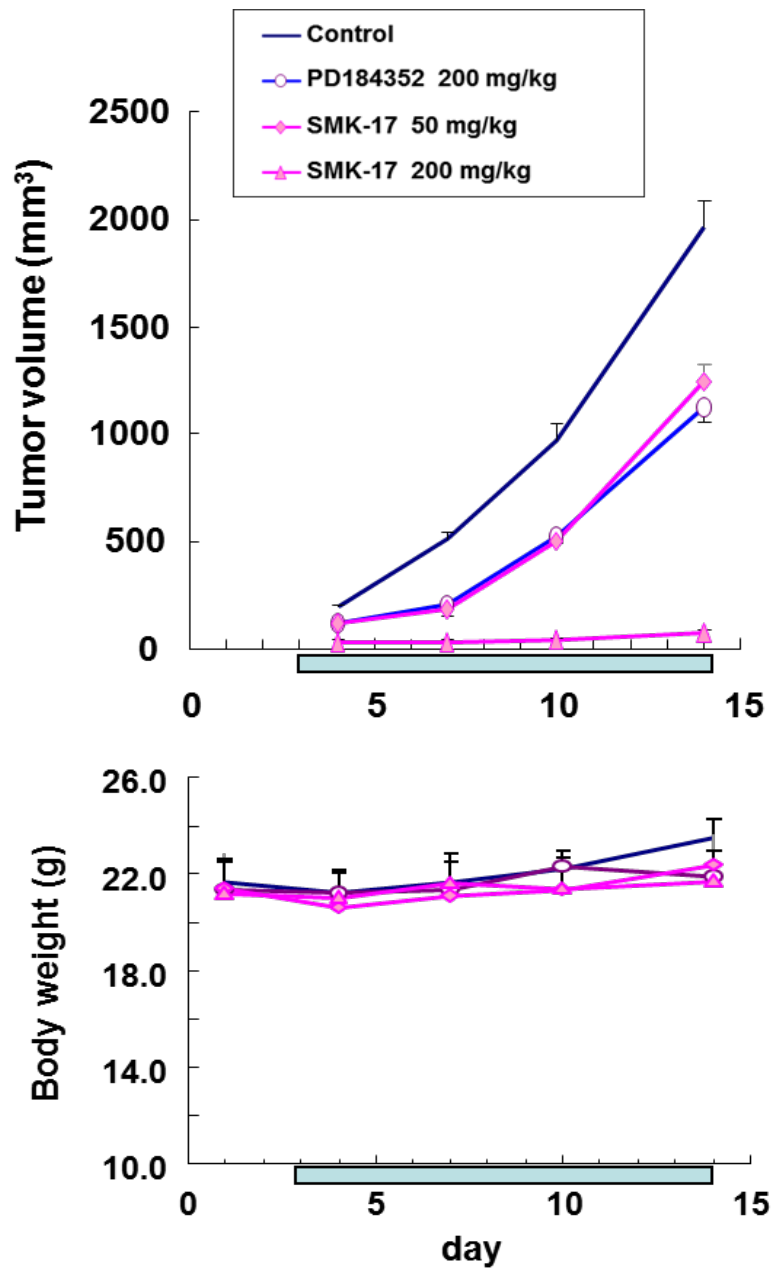


Figure 29 In vivo antitumor activity of SMK-17 in a colon 26 allograft model  
 SMK-17 exhibits significant in vivo antitumor efficacy that correlates with its inhibition of MAPK signaling in colon 26-CDF1 mice.

Table 5 Plasma drug concentration in CDF1 mice

<b>SMK-17 dose, time</b>	<b>50 mg/kg</b>		<b>200 mg/kg</b>	
	<b>6 h</b>	<b>24 h</b>	<b>6 h</b>	<b>24 h</b>
<b>Plasma</b>	<b>0.83</b>	<b>0.00</b>	<b>6.75</b>	<b>0.83</b>

SMK-17 concentration ( $\mu\text{g/mL}$ ) in plasma of drug-treated CDF1 mice after single oral administration is shown.

### **3.2.7 In vivo antitumor activity on a xenograft model**

We evaluated antitumor activity of SMK-17 against a xenograft model using HT-29 cells. SMK-17 was orally administered daily at doses ranging from 50-400 mg/kg in tumor bearing mice for 25 days and it showed statistically significant tumor growth inhibition with a dose-dependent manner (Figure 30). In the study, partial tumor growth inhibition was observed at doses between 50 and 200 mg/kg, and complete inhibition was observed at 400 mg/kg. Notable adverse effects were not observed in this study and the exposure was similar to the case with CDF1 mice (Table 6). SMK-17 exhibits significant in vivo antitumor efficacy that correlates with its inhibition of MAPK signaling (Figure 31).

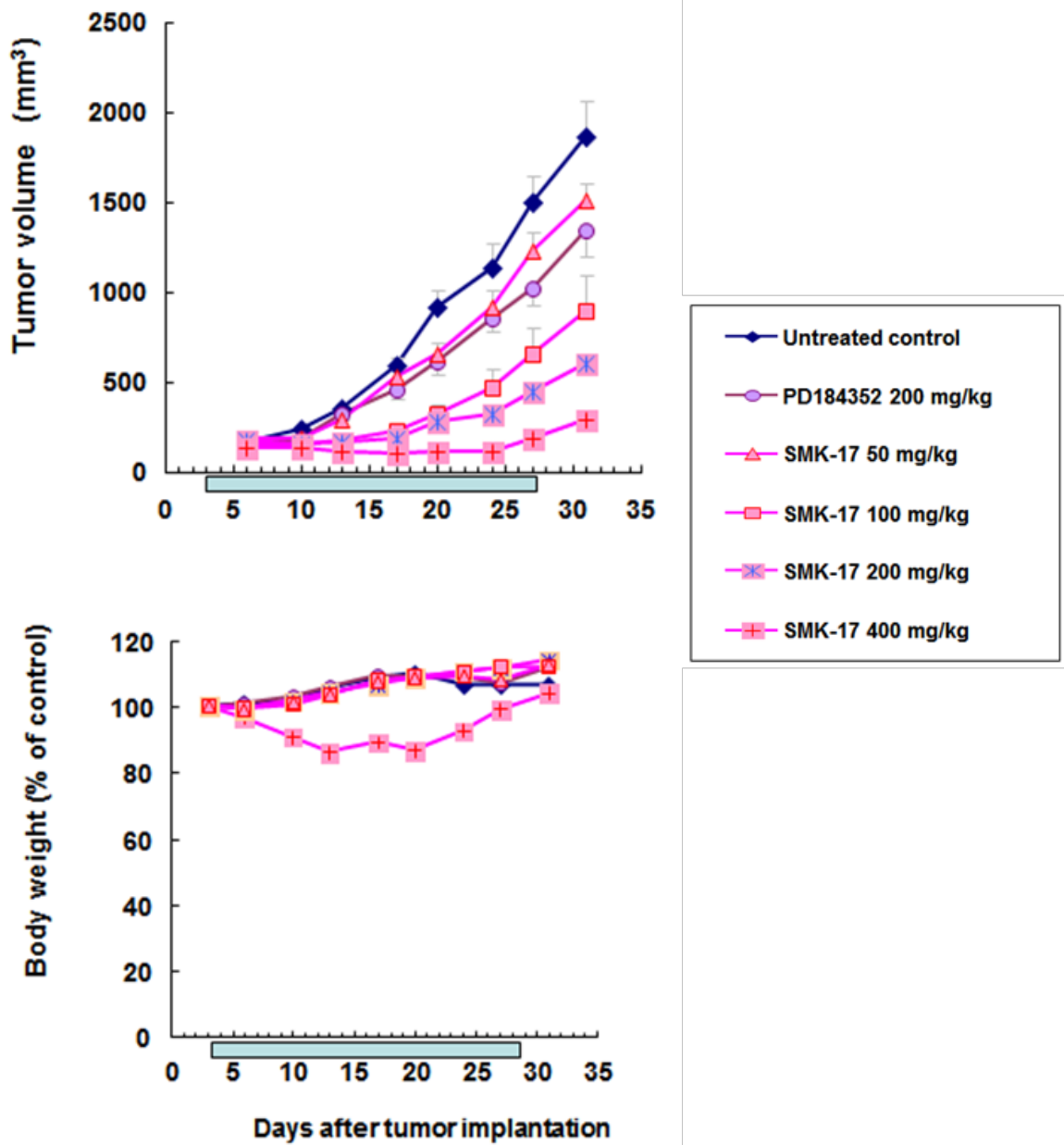


Figure 30 In vivo antitumor activity of SMK-17 on an HT-29 xenograft model  
 Oral administration of SMK-17 exhibits significant in vivo antitumor efficacy on an HT-29 tumor-bearing mice model.

Table 6 Plasma drug concentration in Balb/c-nu/nu (nude) mice

<b>SMK-17 dose</b>	<b>50 mg/kg</b>	<b>200 mg/kg</b>
<b>Plasma</b>	<b>1.17</b>	<b>8.08</b>

The SMK-17 concentration ( $\mu\text{g/mL}$ ) in plasma of drug-treated Balb/c-nu/nu mice 6 h after single oral administration is shown.

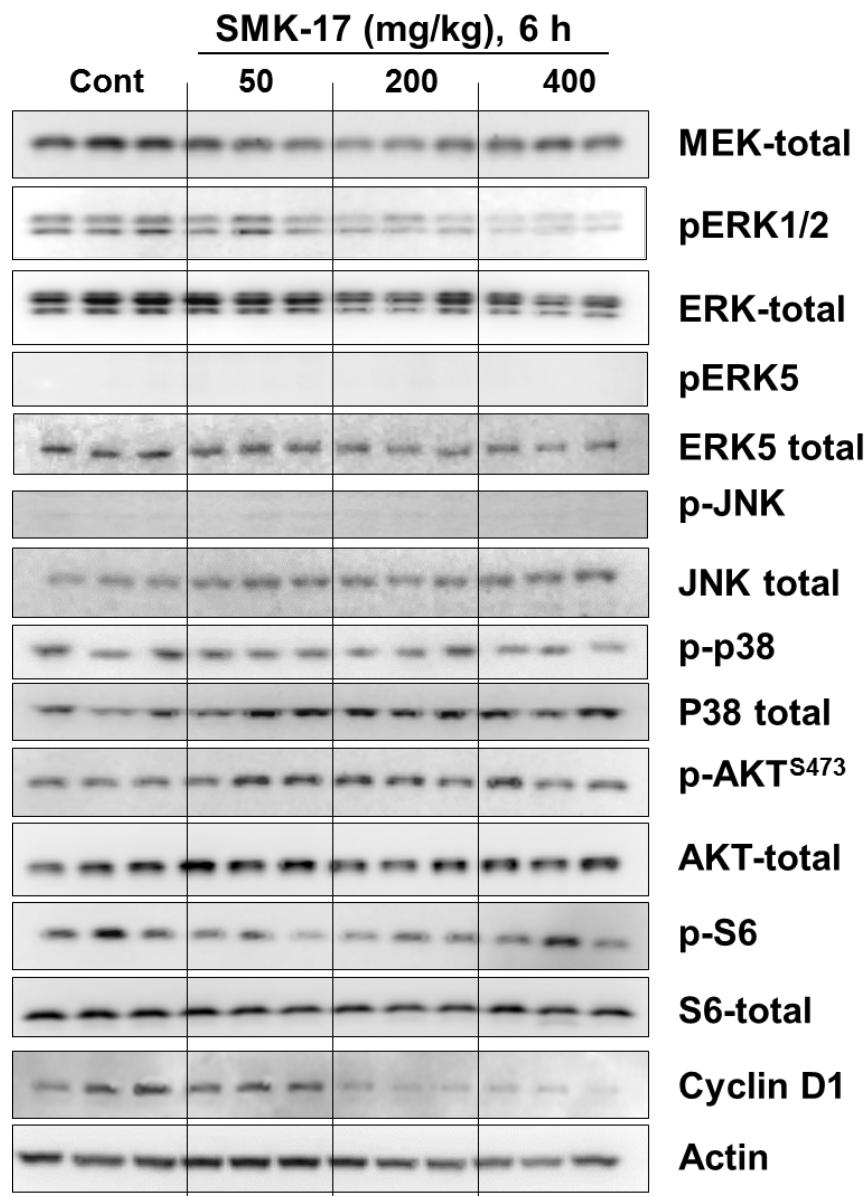


Figure 31 In vivo analysis of downstream and related proteins of MEK1/2 in the SMK-17 administered HT-29 xenograft mice

SMK-17 exhibits significant in vivo antitumor efficacy that correlates with its inhibition of MAPK signaling and its downstream proteins, especially decreasing cyclin D1.

### **3.3 Conclusion of Chapter 3**

We created very a potent MEK1/2 inhibitor, SMK-17, from our structure-activity correlation study of new derivative series of diphenyl amine sulfonamide. The kinase profiler and kinetics study revealed that SMK-17 is a completely non-ATP-competitive and highly selective MEK1/2 inhibitor.

Moreover, SMK-17 exhibited potent antitumor activity in animal models by oral administration. SMK-17 selectively blocked the MAPK pathway signaling without affecting any other signal pathways both in vitro and in vivo.

These findings suggest that SMK-17 is a useful chemical biology tool for characterizing the function of MEK/MAPK signaling both in vitro and in vivo.

### **3.4 Materials and methods in Chapter 3**

#### **3.4.1 Compounds**

All compounds shown in this chapter were synthesized in-house, according to the procedure described in the patent application (WO2004-083167).

#### **3.4.2 Kinase selectivity**

Kinase inhibitory selectivity of SMK-17 at 1000 nM was tested against 233 human kinases by Kinase Profiler<sup>TM</sup> (Millipore Inc.)

#### **3.4.3 Physicochemical study**

JP-1 (aqueous acidic solution, pH 1.2) and JP-2 (neutral pH solution, pH 6.8) were purchased from Kanto Chemical (Tokyo, Japan). The sample solution was assayed using HPLC methodologies. Two hundred fifty  $\mu$ M of the compound in aqueous CH<sub>3</sub>CN solution (1:1 (v/v)) was prepared to make a calibration curve. The solubility was determined by comparing the UV peak area of the standard solution. The cLogD values were calculated by CLOGP software version 4.8.2 (Daylight Chemical Information Systems, Laguna Niguel, California, USA).

#### **3.4.4 Docking study of SMK-17 with human MEK1**

The molecular docking study was performed using Glide version 5.5 (Schrödinger, New York, USA). The inhibitor was docked flexibly to an allosteric pocket adjacent to the ATP binding site of MEK1. The coordinates for the MEK1 were taken from the Protein



Data Bank (PDBID: 3E8N [17]). In this structure, an allosteric inhibitor was bound adjacent to the ATP. The inhibitor molecule and water molecules which are unlikely to be important for ligand binding were deleted. Four structural waters which were bound to the magnesium ion or the side chain of A208 in the catalytic site, or the phosphates of the ATP were preserved. After docking SMK-17 into the MEK1, energy minimization was performed on the complex with MacroModel version 9.7 (Schrödinger).

### **3.4.5 Cell culture**

Colon 26 cells were provided by the Institute of Development, Aging and Cancer, Tohoku University (Sendai, Japan). Other cell lines used in the experiments were purchased from American Type Culture Collection (ATCC), and they were maintained with the recommended media supplemented with 10% heat-inactivated fetal bovine serum (HyClone Laboratories, Thermo Fisher Scientific, Waltham, Massachusetts, USA).

### **3.4.6 Western blot analysis**

Anti-phospho-ERK (T202/Y204), anti-phospho-MEK (S217/221), anti-MEK1, anti-MEK2, anti-phospho-AKT (S473), anti-AKT, anti-cyclin D1, anti-phospho-S6 ribosomal protein (S235/236), anti-S6 ribosomal protein, anti-phospho-ERK5 (T218/Y220), anti-ERK5, anti-phospho-JNK (T183/Y185), anti-JNK, anti-phospho-p38 (T180/Y182), anti-p38 $\alpha$ , anti-mouse IgG HRP-linked (#7076), and anti-rabbit IgG HRP-linked (#7074) were obtained from Cell Signaling Technology. PhosphoSTOP; phosphatase inhibitor cocktail tablets and Complete Mini; protease inhibitor cocktail tablets were purchased from Roche Diagnostics (Indianapolis, Indiana, USA). Cells were seeded in 6-well plates (Corning) 1 day before compound treatment. Then, the cells

were treated with the compound for a specified period of time. Cells were harvested and lysed immediately with RIPA buffer (50 mM Tris HCl pH 7.5, 150 mM NaCl, 1 mM Na<sub>3</sub>VO<sub>4</sub>, 0.1% SDS, 0.5% deoxycholic acid, 1% IGEPAL CA-630, PhosphoSTOP tablet, and Complete Mini tablet). Tumor tissues were harvested from mice and stored at -80°C, and then disrupted by grinding for 30 sec at 2,500 rpm twice with a Multi-Beads Shocker (Yasui Kikai, Shizuoka, Japan) in the RIPA buffer. After incubation on ice for 30 min, the lysates were centrifuged at 14,000 G for 15 min to clear insoluble fragments. The supernatants were used for Western blot analysis. Equal amounts of total protein were resolved on SDS-PAGE gels and blotted with antibodies as indicated. The chemiluminescent signal was generated with Western Lightning Plus (PerkinElmer) and detected with an LAS-4000 imager (Fujifilm, Tokyo, Japan, maintained by GE Healthcare Japan, Tokyo, Japan). The densitometric quantitation of specific bands was determined using Multi Gauge Software (Fujifilm).

#### **3.4.7 Cell cycle measurement**

For growth inhibition experiments, cells were plated in black 96-well plates (Corning) at 1,000 cells / 100 µL/well. After 24-h culture, the compound was added and incubated for another 72 h. The cell number was measured using CellTiter-Glo (Promega, Fitchburg, Wisconsin, USA). Nonlinear curve fitting was performed using GraphPad Prism 4 from triplicate sets of data.

### **3.4.8 In vivo antitumor study**

Specific pathogen-free female nude mice (BALB/cA Jcl-nu) were purchased from CLEA Japan (Tokyo, Japan). Female CDF1 mice were obtained from Charles River Japan (Yokohama, Japan). SMK-17 and PD184352 were suspended in 0.5% methyl cellulose solution (Wako Pure Chemical Industries), and given daily to the animals by gavage (0.1 mL/10 g body weight). Control animals received 0.5% methyl cellulose solution for vehicle control. For the HT-29 study,  $2 \times 10^6$  tumor cell suspension was inoculated subcutaneously into the axillar region of the nude mice on Day 0.

Tumor-bearing nude mice were grouped, and started administration of SMK-17 or PD184352 on Day 6. For the colon 26 study,  $2 \times 10^5$  cells were inoculated subcutaneously into CDF1 mice on Day 0. Tumor-bearing mice were grouped, and drug treatment was started on Day 4. Tumor volumes were calculated using a microgauge (Mitsutoyo, Kawasaki, Japan) according to the following equations: Tumor volume (mm<sup>3</sup>) =  $1/2 \times (\text{tumor length}) \times (\text{tumor width})^2$ , T: mean tumor volume of the treated animal, C: mean tumor volume of the vehicle-treated animal.

### **3.4.9 Pharmacokinetic studies (drug concentration measurement in vivo)**

SMK-17 was dosed by oral gavage to tumor bearing mice. Three mice of each group were sacrificed after dosing, and plasma samples were collected and frozen at -25°C until analysis.

Acetonitrile deproteinized the plasma samples with a 2-fold volume of the sample. The supernatant was obtained after centrifugation at 15,000 G for 3 min at 4°C. Plasma concentrations of SMK-17 were determined using the high-performance liquid

chromatography (HPLC) analysis with UV detection at 280 nm. The mobile phase of HPLC was 0.5% phosphoric acid / acetonitrile (57/ 43, v/v) and the flow-rate was 1 mL/min through an YMC-Pack ODS-A column (A-312, 150 x 6.0 mm I.D., S-5  $\mu$ m, YMC, Kyoto, Japan).

#### **4. Chapter 4; Predictive biomarker identification for a MEK1/2 inhibitor**

#### **4.1 Background of Chapter 4**

Several MEK1/2 inhibitors (e.g., PD184352/CI-1040 and PD0325901) have been evaluated in clinical study. However, the clinical outcome as a single agent therapy of a MEK1/2 inhibitor has met with limited success. On the other hand, Wnt/ $\beta$ -catenin signaling also plays a central role in cell proliferation and differentiation. Although both MAPK signal and Wnt/ $\beta$ -catenin signal are very important intracellular signaling pathways, their crosstalk is not yet clear.

In this chapter, we classified human tumor cell lines as either sensitive or resistant to the MEK1/2 inhibitor, which was determined by apoptosis induction, not only by growth inhibition. We discuss the unexpected findings that mutated  $\beta$ -catenin in tumor cells promoted MEK1/2 inhibitor induced apoptosis. Our results suggest the possibility of the  $\beta$ -catenin mutation as a completely-novel predictive biomarker for the MEK1/2 inhibitor.

## 4.2 Results and discussion

### 4.2.1 SMK-17 inhibited cell proliferation in K-Ras or BRAF mutated tumor cell lines

SMK-17 was a potent and highly selective MEK1/2 inhibitor with IC<sub>50</sub> to MEK1 and 2 as 62 nM and 56 nM, respectively as described in Chapters 2 and 3. Several studies have reported a wide range of sensitivity to the anti-proliferative effects of MEK1/2 inhibitors. Because we have confirmed the remarkably highly selective MEK1/2 inhibition by SMK-17 without any off-targeting kinase, we examined the effect of SMK-17 on several types of human tumor cell lines. As shown in Figure 32, the cell lines with the BRAF V600E mutation such as colo-205, SK-MEL-1, HT-29, colo-201 and A375 cells were sensitive to SMK-17. Furthermore, the cell lines with the K-Ras (mostly G12V) mutation such as SW480, HCT 116, SW620, LS-174T and OVCAR-5 cells were moderately sensitive to SMK-17.

SMK-17 is found to be highly effective in proliferation of tumor cells with aberrant activated MAPK pathway signaling. Tumor cells harboring BRAF mutations were found to be more sensitive to SMK-17 than tumor cells with K-Ras mutations, as previously reported with the other MEK1/2 inhibitors<sup>46)</sup>. These observations can be explained by the fact that BRAF mutations could affect MEK1/2 activity directly, as it is an immediate upstream effector of MEK1/2, whereas Ras mutations are able to activate additional signaling pathways by bypassing MEK. Furthermore, a previous study showed that BRAF mutations predict sensitivity to MEK1/2 inhibition<sup>54)</sup>.

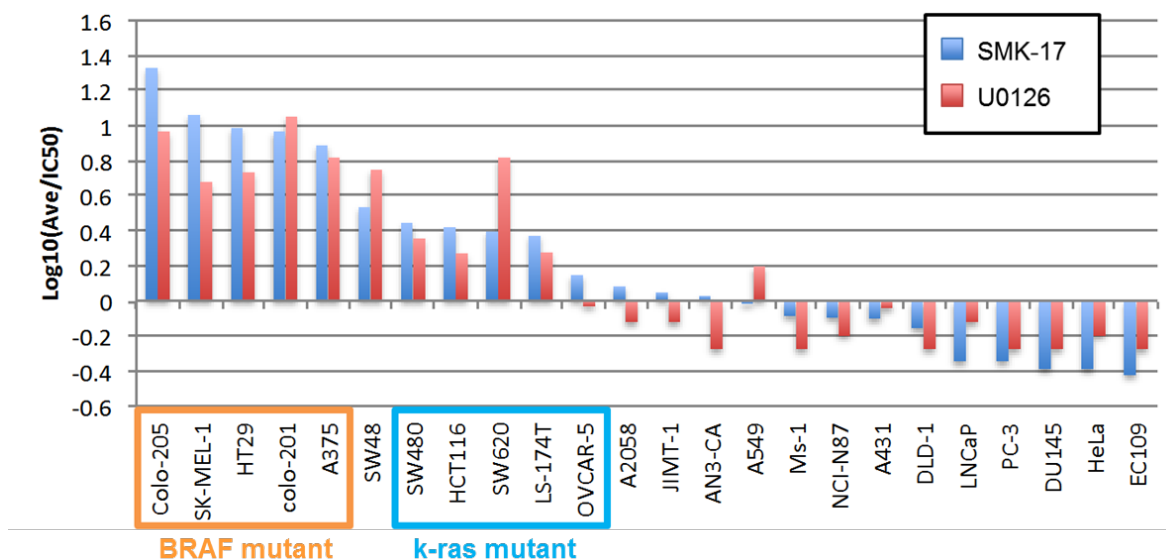


Figure 32 Relative IC<sub>50</sub> values for a panel of tumor cell lines harboring several oncogenic mutations

Cells were treated with the MEK1/2 inhibitors, SMK-17 and U0126. Each cell number was determined 72 h after compound treatment. The IC<sub>50</sub> value was calculated from dose-response curves as described in Materials and methods. The figure shows the differential growth inhibition pattern against 24 tumor cell lines. The Y-axis represents the difference in a logarithmic scale between the mean of Log IC<sub>50</sub> for 24 cell lines and the Log IC<sub>50</sub> for each cell line.



The scatter plots showing the Log IC<sub>50</sub> of cell lines mutated in the MAPK pathway including K-Ras or BRAF revealed that these cell lines show sensitivity to SMK-17 in a comprehensive manner (Figure 33). We used a similar analysis about the mutation in the PI3K pathway including PI3K or PTEN, p53, and Wnt/ $\beta$ -catenin pathway including APC or  $\beta$ -catenin. Significant differences were not observed in the cell lines harboring PI3K and *p53* gene mutations.

Interestingly, SMK-17-sensitive BRAF- and K-Ras-mutant cells can be classified into two groups based on the fate of cells following SMK-17 treatment. One contained tumor cells (BRAF mutant A375 and HT-29 cells, and K-Ras mutant SW620 cells) that caused cell cycle arrest by SMK-17 treatment, and another one contained tumor cells (BRAF mutant colo-201 cells, and K-Ras mutant HCT 116 and LS-174T cells) that undergo apoptosis under the condition where the phosphorylation of ERK1/2 was inhibited by SMK-17 (Figure 35, an explanation is provided later in this chapter). Therefore, it is difficult to predict the precise efficacy of SMK-17 whether it induced just cell growth inhibition or apoptosis from the status of mutation of BRAF or K-Ras.

On the other hand, we found significant differences in the sensitivities between cell lines harboring the Wnt/ $\beta$ -catenin pathway mutant and the rest of cell lines. Similar results were obtained when the other MEK1/2 inhibitor, U0126 was used instead of SMK-17 (Figure 34).

## SMK-17

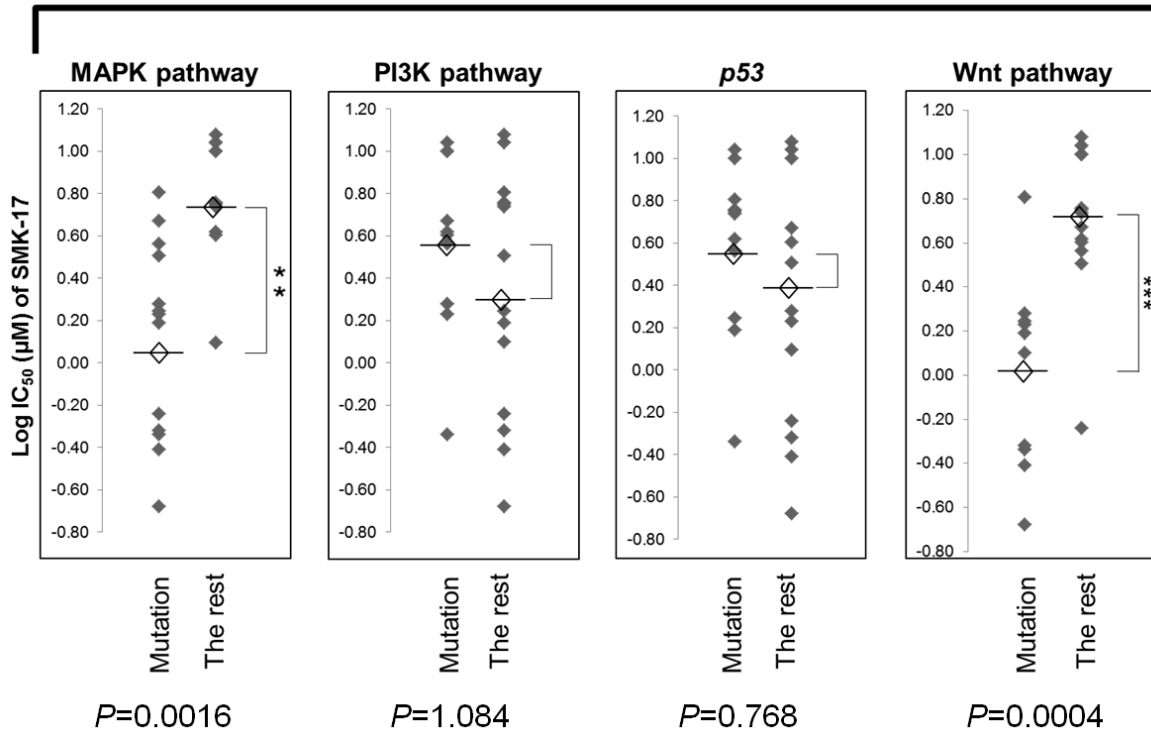


Figure 33 Scatter plot of IC<sub>50</sub> values of SMK-17 for a panel of tumor cell lines harboring several oncogenic mutations

SMK-17 selectively inhibits the proliferation of MAPK mutated tumor cell lines.

Scatter plots showing the Log IC<sub>50</sub> of mutated cell lines and the remaining cell lines in the MAPK, PI3K, p53, and Wnt/ $\beta$ -catenin pathways (in a left-to-right fashion). The *P* values were obtained using Student's *t* test for group comparisons with Bonferroni correction. \*\*\* in the plots represents *P* < 0.001. \*\* in the plots represents *P* < 0.005.

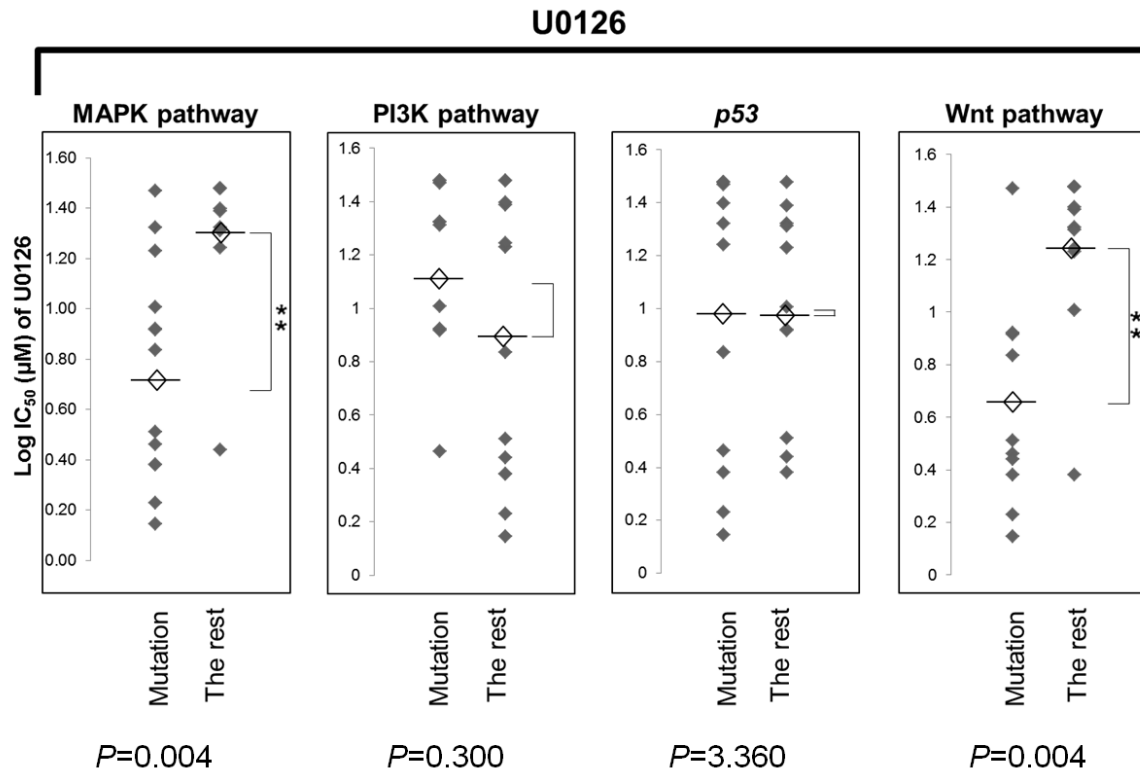


Figure 34 Scatter plot of IC<sub>50</sub> values of U0126 for a panel of tumor cell lines harboring several oncogenic mutations

Cells were treated with the classic MEK1/2 inhibitor, U0126. Scatter plots showing the Log IC<sub>50</sub> of mutated cell lines and the remaining cell lines in the MAPK, PI3K, p53, and Wnt/  $\beta$ -catenin pathways (in a left-to-right fashion). The *P* values were obtained using Student's *t* test for group comparisons with Bonferroni correction. \*\* in the plots represents *P* < 0.005.

#### **4.2.2 SMK-17 induced apoptosis in active $\beta$ -catenin mutated cell lines**

Amongst a representative subset of cell lines showing high sensitivity to SMK-17, less than 2.0  $\mu$ M of  $IC_{50}$ , A375, HT-29, HCT 116, colo-201 cells and SW48 cells were evaluated against the efficacy of SMK-17 to MAPK pathway, cell cycle, and apoptosis induction. SMK-17 inhibited ERK1/2 phosphorylation, which is reflected as intracellular MEK1/2 activity, in all cell lines in a dose-correlation manner (Figure 35). Treatment of SMK-17 at 1  $\mu$ M, which almost completely inhibited ERK1/2 phosphorylation, induced G1 cell cycle arrest in BRAF V600E mutant A375 and HT-29 cells (Figure 36). SMK-17 did not induce apoptosis in BRAF mutant A375 and HT-29 cells up to 10  $\mu$ M, as judged from the increase in sub G1 population by flow cytometry analysis. On the other hand, treatment of SMK-17 at the minimum effective concentrations for the inhibition of ERK1/2 phosphorylation, induced apoptosis in BRAF mutated colo-201 cells and K-Ras mutated HCT 116 cell lines, as observed from the detection of cleaved PARP by Western blot analysis. Apoptotic cell death by SMK-17 was further confirmed by the detection of sub G1 population in HCT 116 and colo-201 cells (Figure 36).

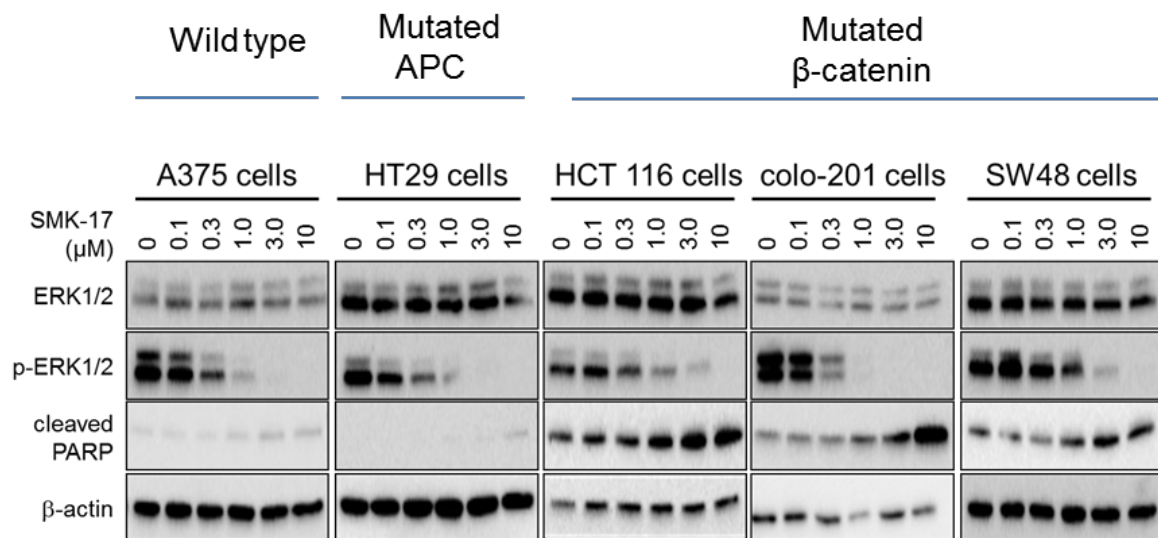


Figure 35 MEK inhibitor selectively induced apoptosis in  $\beta$ -catenin mutated cell lines

SMK-17 selectively induced apoptosis in  $\beta$ -catenin mutated cell lines such as HCT 116, colo-201, and SW48 at the lowest effective concentration. Cells were treated with the indicated concentrations of SMK-17. After 24 h treatment, cell lysates were immunoblotted for ERK1/2, phospho-ERK1/2 (p-ERK1/2), cleaved PARP and  $\beta$ -actin by Western blot analysis.

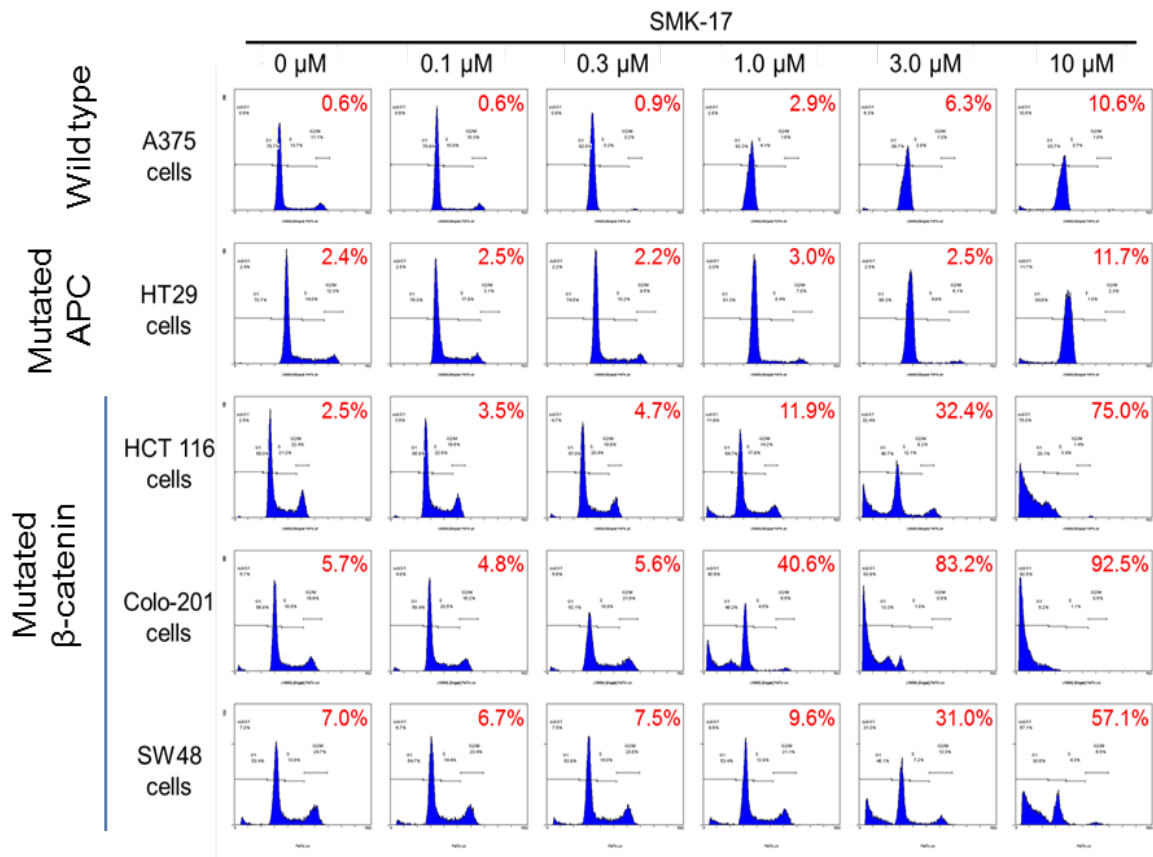


Figure 36 SMK-17 selectively induced G1 arrest in  $\beta$ -catenin wild type cells and apoptosis in  $\beta$ -catenin mutant cells

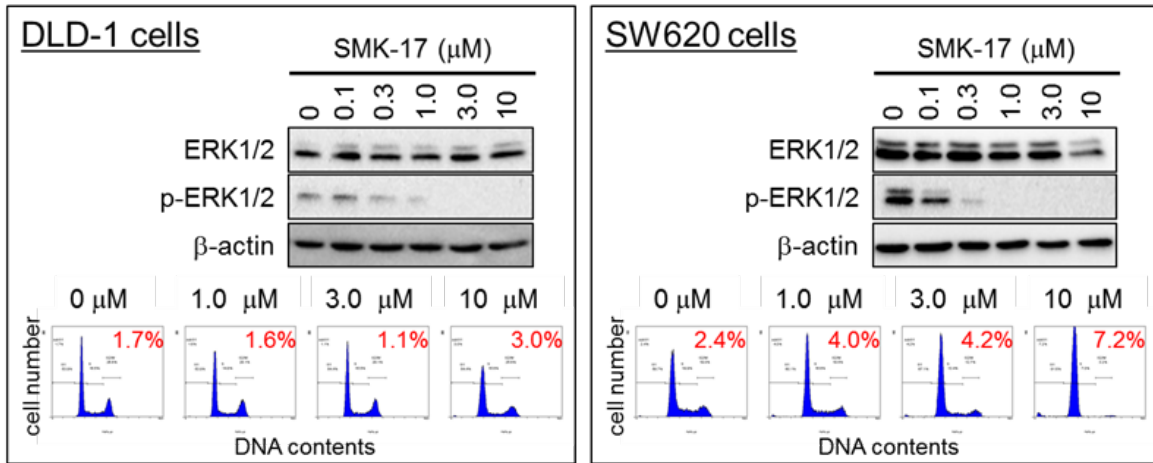
Cells were treated with the indicated concentrations of SMK-17. After 48 h treatment, sub G1 or G1 populations were analyzed by flow cytometry. A percentage of the sub G1 population (written in red) is indicated in each histogram.

Moreover, SW48 cell lines that do not carry mutations in either the K-Ras or BRAF gene underwent apoptosis under the condition where ERK1/2 phosphorylation is inhibited by SMK-17. These results indicated that the apoptosis-inducing ability of SMK-17 is not dependent on the status of the MAPK pathway of tumor cells. Therefore, we focused on the differences among the cell lines showing G1 arrest or apoptosis. An indication of this was the  $\beta$ -catenin status, because cell lines that underwent apoptosis by SMK-17 commonly harbored activating mutations of  $\beta$ -catenin. Dependence of SMK-17-induced apoptosis on  $\beta$ -catenin active mutations was further investigated. Other cell lines harboring  $\beta$ -catenin active mutations, SK-MEL-1 and LS-174T cells, also underwent apoptosis when cells were treated with SMK-17 cells, as judged from the increased population of the sub G1 peak (Figure 37), however, cell lines harboring K-Ras and APC mutations but not  $\beta$ -catenin active mutations, DLD-1 and SW620 cells, did not undergo apoptosis under the condition where ERK1/2 phosphorylation was completely inhibited by SMK-17. Next, we examined whether another MEK inhibitor also selectively induced apoptosis in cell lines harboring active mutation of  $\beta$ -catenin. As shown in Figure 38, 1.0  $\mu$ M of PD184352 completely inhibited ERK1/2 phosphorylation and induced cell cycle arrest at the G1 phase in HT29 cells. Similarly, in DLD-1 cells, PD184352 also inhibited ERK1/2 phosphorylation without a significant increase in the sub G1 population. On the other hand, PD184352 inhibited ERK1/2 phosphorylation at 0.3  $\mu$ M and over concentrations in HCT 116 cells, and induced an increase in the sub G1 population gradually in a dose dependent manner. Similar results were obtained in SW48 cells, indicating that MEK inhibitors selectively induced apoptosis in cell lines harboring active mutations of  $\beta$ -catenin.

Analyzing both, we discovered that a common feature of tumor cells that undergo apoptosis following SMK-17 treatment is that they harbor active mutations in  $\beta$ -catenin. Mutations in  $\beta$ -catenin of these cells involve the deletion or the exchange of serine and threonine residues at the positions 45 and 33; interfering with its efficient ubiquitination and degradation in the proteasome<sup>55</sup>): HCT 116 cells (S45 deletion), SW48 cells (S33Y), LS-174T cells (S45F), SK-MEL-1 cells (S33C). In addition, the cell lines colo-201/colo-205 showed a homozygous A-to-G missense transition mutation in codon 287 in exon 6, resulting in substitution of serine for asparagine (N287S). Thus, among the tumor cells we tested, only  $\beta$ -catenin active mutants, irrespective of the status of BRAF or K-Ras mutations, underwent apoptosis by treatment with MEK1/2 inhibitors at the minimum effective concentrations for the inhibition of ERK1/2 phosphorylation. The requirement of the  $\beta$ -catenin active mutation for SMK-17 induced apoptosis is discussed in the following paragraphs.



### Mutated APC



### Mutated β-catenin

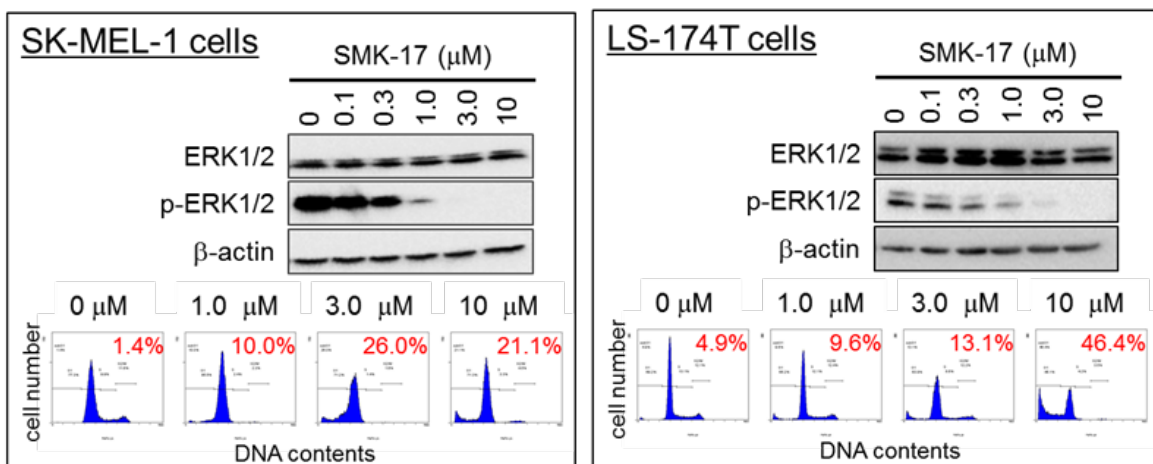
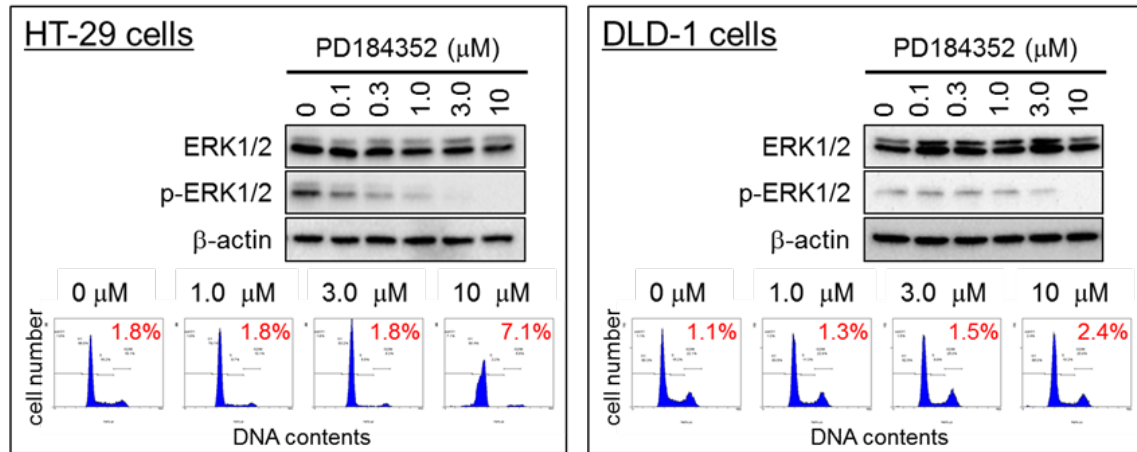


Figure 37 Active mutation of β-catenin is associated with SMK-17 induced apoptosis

Cells were treated with the indicated concentrations of SMK-17. After 24 h treatment, total ERK1/2, phosphorylated ERK 1/2 and actin were detected. After 48 h treatment, sub G1 or G1 populations were analyzed by flow cytometry. A percentage of the sub G1 population (written in red) is indicated in each histogram.

### Mutated APC



### Mutated $\beta$ -catenin

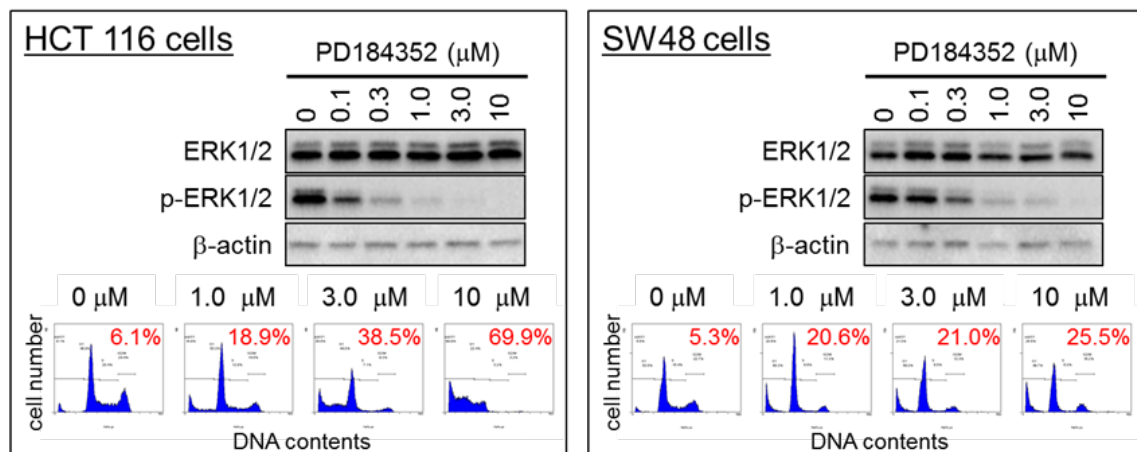


Figure 38 Active mutation of  $\beta$ -catenin is associated with PD184352 induced apoptosis

The cells were treated with the indicated concentrations of PD184352. After 24 h treatment, total ERK1/2, phosphorylated ERK1/2 and actin were detected. After 48 h treatment, sub G1 or G1 populations were analyzed by flow cytometry. A percentage of the sub G1 population (red) is indicated in each histogram.

### **4.2.3 Active mutation of $\beta$ -catenin is associated with SMK-17 induced apoptosis**

To test the hypothesis that active mutation of  $\beta$ -catenin might be responsible for MEK1/2 inhibitor mediated apoptosis, we transfected the active form of  $\beta$ -catenin (S37A, S45A) and EGFP expression plasmids in A375 cells harboring wild type  $\beta$ -catenin, and evaluated SMK-17 induced apoptotic cell death by the detection of cleaved PARP using Western blot analysis. As shown in Figure 39, forced expression of the active form of  $\beta$ -catenin by the expressing vector's transfection did not affect SMK-17-inhibited ERK1/2 phosphorylation but apoptosis was observed following SMK-17 treatment in A375 cells. Moreover, to quantitatively detect early apoptosis and late apoptosis induced by SMK-17, the active form of  $\beta$ -catenin/EGFP transfected A375 cells were stained with annexin V/APC and 7-AAD, and analyzed by flow cytometry gated on the GFP-positive cells. As shown in Figure 40, SMK-17 did not affect the population of annexin V<sup>+</sup>/7-AAD<sup>-</sup> cells (early apoptosis) and annexin V<sup>+</sup>/7-AAD<sup>+</sup> cells (late apoptosis) up to 10  $\mu$ M in control GFP expressing A375 cells. On the other hand, the percentages of not only early apoptosis but also late apoptosis were increased in a dose dependent manner in the active form of  $\beta$ -catenin expressing A375 cells (at 10  $\mu$ M SMK-17: 22.0% early apoptotic cells and 46.7% late apoptotic cells in the active form of  $\beta$ -catenin expressing A375 cells compared to 1.4% early apoptotic cells and 0.7% late apoptotic cells in the control GFP expressing A375 cells). These results indicated that expression of the active form of  $\beta$ -catenin would be responsible for SMK-17 induced apoptosis.

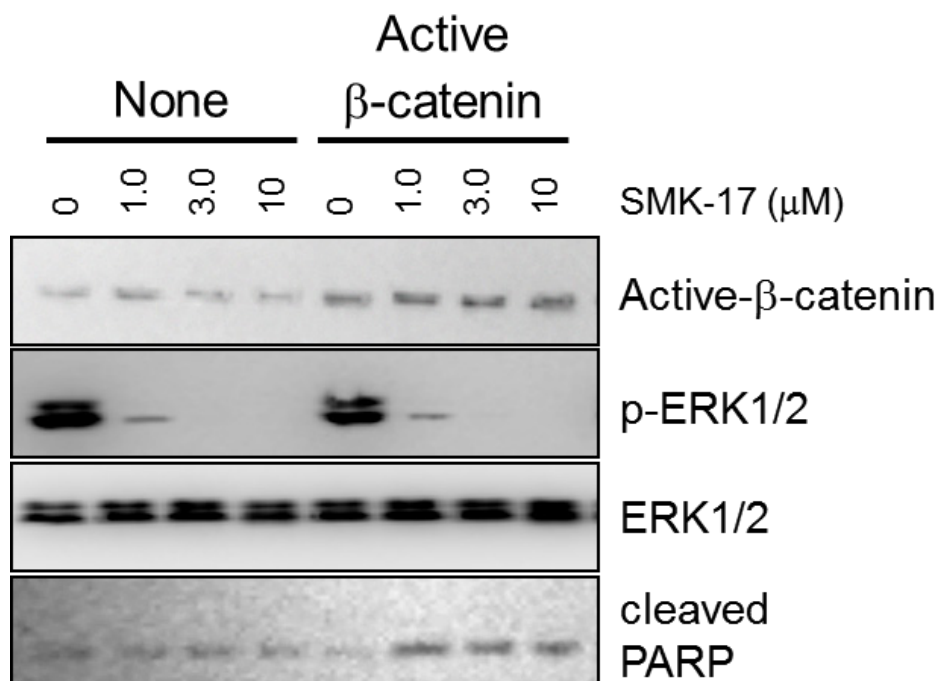


Figure 39 SMK-17-treated A375 cells with an expression vector encoding active  $\beta$ -catenin

A375 cells were transfected with the control vector or the active form of the  $\beta$ -catenin expressing vector. Transfected cells were treated with DMSO or SMK-17 (1.0, 3.0 and 10  $\mu$ M). After 48 h of the treatment, cell lysates were immunoblotted for ERK1/2, phospho-ERK1/2 (p-ERK1/2) and cleaved PARP by Western blot analysis.

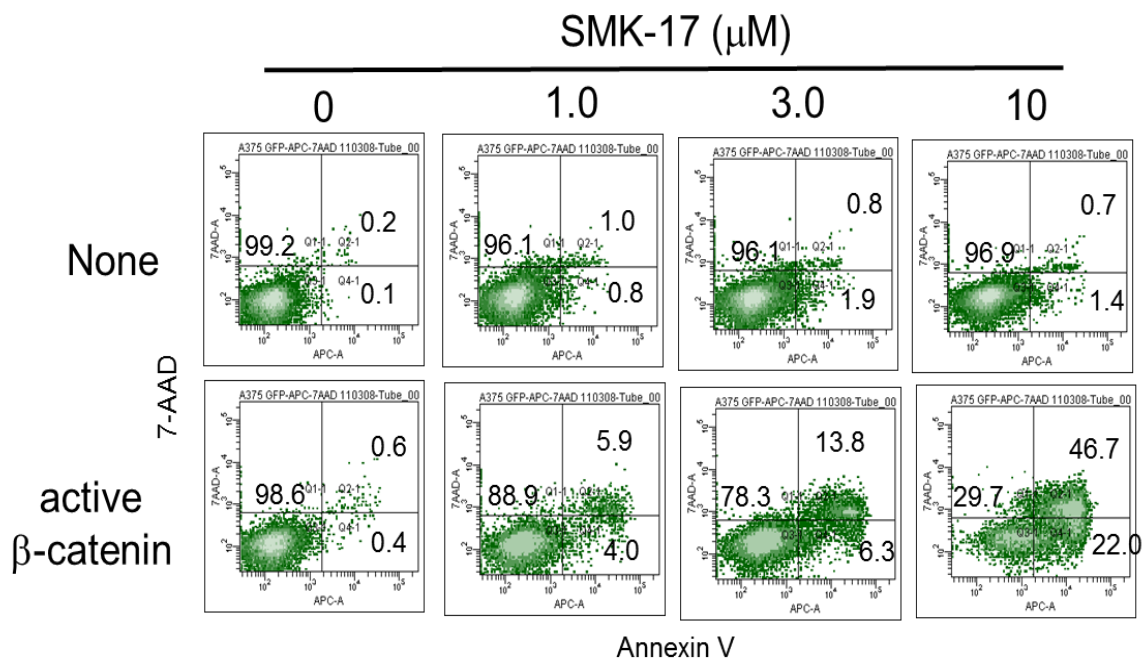


Figure 40 Accelerated SMK-17 induced apoptosis in A375 cells with an active  $\beta$ -catenin expression vector

A375 cells were transfected with the control vector or the active form of the  $\beta$ -catenin vector. Transfected cells were stained with annexin V/APC and 7AAD and analyzed by flow cytometry gated on GFP-positive cells. Annexin V positive cells were quantified as apoptotic cells.

#### **4.2.4 TCF4 activity is related to MEK inhibitor induced apoptosis in $\beta$ -catenin mutant cell lines**

To provide evidence that SMK-17 induced apoptosis could be regulated by the enhancement of  $\beta$ -catenin dependent transcriptional activation, A375 cells were co-transfected with the TOP FLASH<sup>56)</sup> and Renilla luciferase plasmids as an internal control for the luciferase reporter assay<sup>57)</sup>. The reporter vector- transfected cells were treated with recombinant Wnt3a (50 ng/mL), as a ligand for the Wnt/ $\beta$ -catenin pathway, for 24 h and luciferase activities were measured. We observed Wnt3a significantly accelerate TCF4 transcription activity in A375 cells (Figure 41). In these conditions with or without Wnt3a treatment in A375 cells, apoptosis induced by SMK-17 was determined by Western blot analysis. As a result, cleaved PARP, which is a representative apoptosis indicator, was significantly increased in the combination treatment with SMK-17 and Wnt3a compared to the treatment of a single-agent (Figure 42).

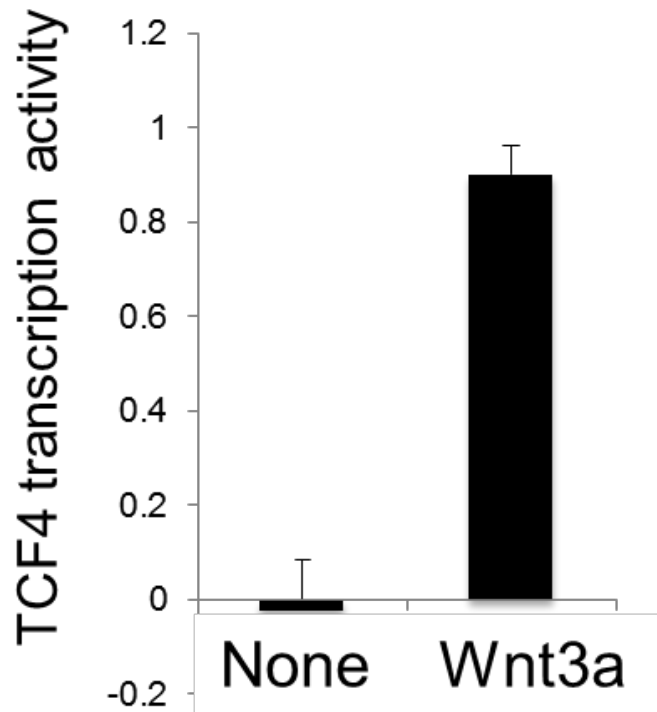


Figure 41      Activation of Wnt/ $\beta$ -catenin signaling by Wnt3a treatment in A375 cells

A375 cells were co-transfected with the TOP FLASH and Renilla luciferase plasmids as a control reporter. Transfected cells were treated with Wnt3a (50 ng/mL) for 24 h and luciferase activity was measured. TCF4 transcription activities were monitored as Wnt signal activities using TOP FLASH/ continuous Renilla luciferase assay (mean  $\pm$  SD, n=6). The ratio of the firefly luciferase intensity of TOP FLASH to one of the continuous Renilla luciferase was regarded as TCF4 transcription activity.

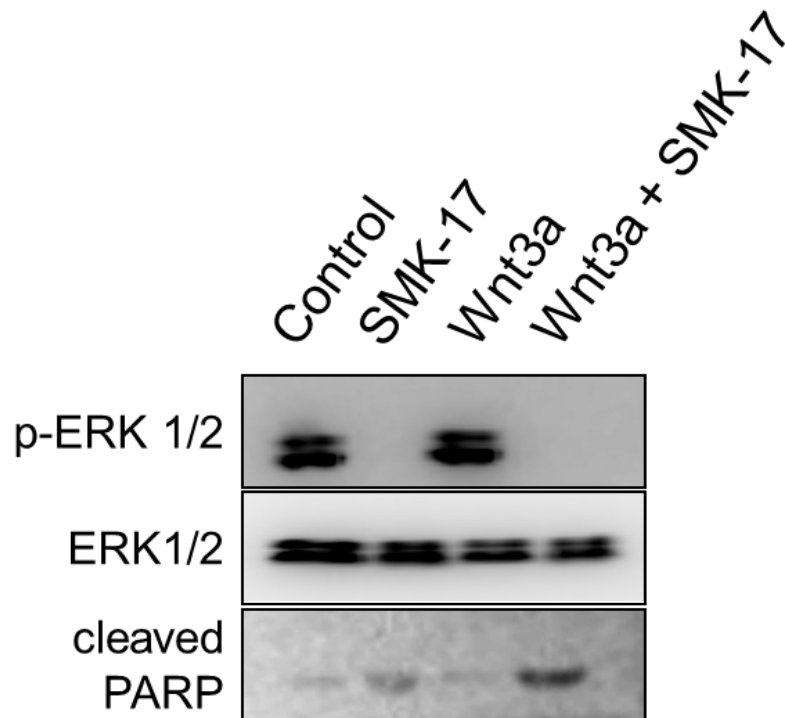


Figure 42 Activation of Wnt/ $\beta$ -catenin signaling by Wnt3a induced apoptosis in A375 cells

The cells were treated with DMSO or SMK-17 (10  $\mu$ M) with or without recombinant Wnt3a (50 ng/mL) for 48 h and cell lysates were immunoblotted for ERK1/2, phospho-ERK1/2 (p-ERK1/2) and cleaved PARP by Western blot analysis. Cleaved PARP was observed in combination treatment with SMK-17 and Wnt3a.



Furthermore, to confirm that the TCF4 transcriptional activity is involved in SMK-17-induced apoptosis, we next examined the effect of TCF4 down-regulation on SMK-17-induced cell death in HCT 116 cells harboring an active mutation of  $\beta$ -catenin. As shown in Figure 43, TCF4 transcription activity was successfully reduced by DN-TCF4 plasmid transfection (from 0.061 to 0.033 in the relative TOP FLASH intensity). Under this condition, transfected cells were treated with SMK-17, and cells were stained with annexin V/APC and 7AAD, followed by the analysis of apoptosis using flow cytometry (Figure 44). SMK-17 induced apoptosis in control EGFP expressing HCT 116 cells (at 10  $\mu$ M SMK-17: 23.2% annexin V<sup>+</sup>/7-AAD<sup>-</sup> and 17.1 % annexin V<sup>+</sup>/7-AAD<sup>+</sup>) was greatly diminished by the expression of DN-TCF4 (at 10  $\mu$ M SMK-17: 14.8% annexin V<sup>+</sup>/7-AAD<sup>+</sup> cells and 3.1% annexin V<sup>+</sup>/7-AAD<sup>+</sup> cells). Thus, SMK-17 induced apoptosis was observed in correlation to TCF4 transcription activity.

When taken together, we demonstrated the following; 1) Forced expression of the active form of  $\beta$ -catenin in A375 cells harboring wild type  $\beta$ -catenin induced apoptosis following SMK-17 treatment. 2) Stimulation of Wnt/ $\beta$ -catenin signaling with Wnt3a treatment enhanced the ability of SMK-17 to induce apoptosis in A375 cells. 3) Inhibition of  $\beta$ -catenin signaling by the expression of dominant negative TCF4 suppressed SMK-17 induced apoptosis in HCT 116 cells harboring active  $\beta$ -catenin mutations. Our results were consistent with the other findings that apoptosis mediated by targeted BRAF inhibition in melanoma is dependent upon  $\beta$ -catenin<sup>58</sup>).

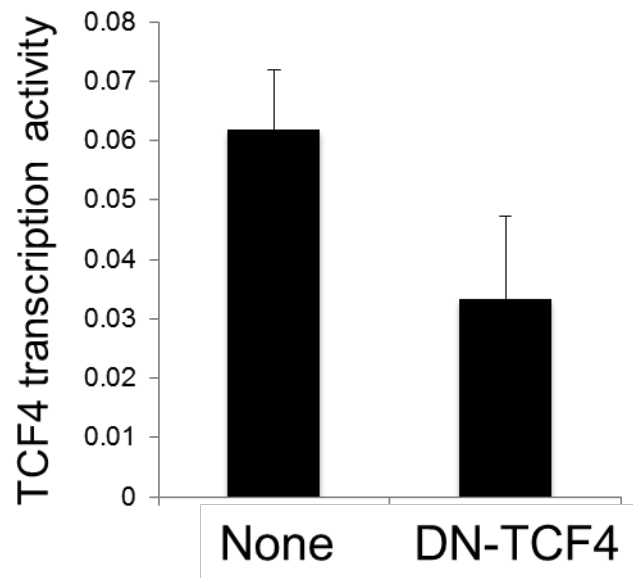


Figure 43 Expression of DN-TCF4 reduced the Wnt/ $\beta$ -catenin signal in HCT 116 cells

HCT 116 cells were transfected with DN-TCF4. The luciferase measurement was monitored through co-transfection with the TOP FLASH and Renilla luciferase plasmids.

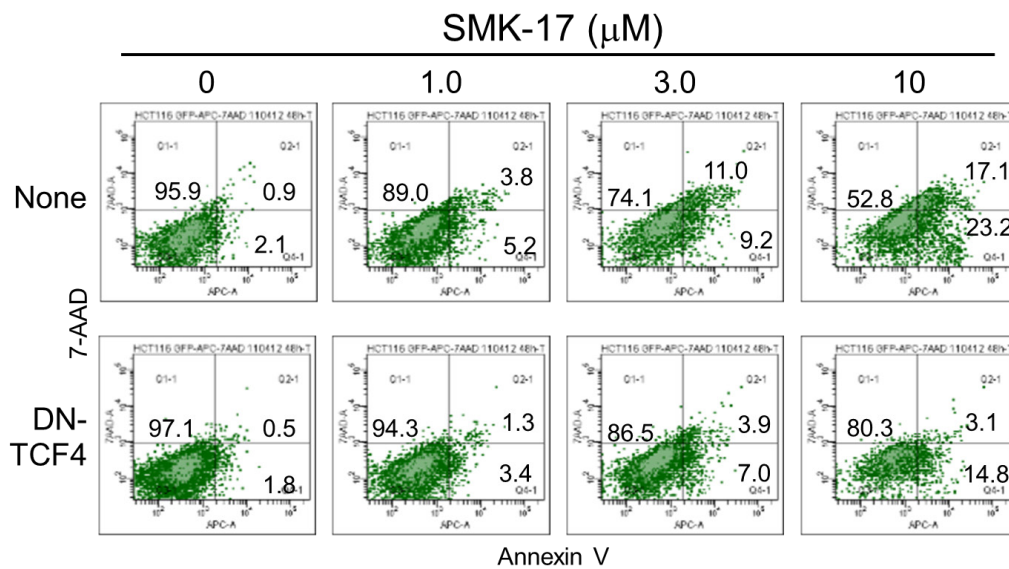


Figure 44 Expression of DN-TCF4 reduced SMK-17 induced apoptosis in HCT 116 cells

HCT 116 cells expressing DN-TCF4 were treated with the indicated concentrations of SMK-17 for 48 h and stained with annexin V/APC and 7-AAD. The cells were analyzed by flow cytometry gated on the GFP positive cells.

#### **4.2.5 Involvement of c-Myc-mediated apoptosis gene expression in SMK-17 induced apoptosis**

What remained unclear is the mechanism for SMK-17 induced apoptosis selectively in cell lines harboring active mutated  $\beta$ -catenin. Through the interaction with TCF4/LEF transcription factors,  $\beta$ -catenin promoted expression of Wnt target genes such as c-Myc, Cyclin D2 and CD44<sup>59)</sup>. There is now strong evidence that increased c-Myc expression is a key component of Wnt signaling that regulates the expression of target genes involved in diverse cellular processes such as apoptosis, cell cycle progression, cell growth and DNA replication<sup>60), 61)</sup>. Furthermore, c-Myc protein is known to be phosphorylated and stabilized by ERK1/2<sup>62)</sup>.

Then, we focused on the relationship of c-Myc because  $\beta$ -catenin-mediated increase in TCF4 transcription activity is involved in SMK-17 induced apoptosis. We examined the possibility of whether SMK-17 induced apoptosis in  $\beta$ -catenin mutant cells is mediated by c-Myc, whose promoters are directly activated by TCF4. For this, HCT 116 cells were transiently transfected with *c-myc* siRNA, and their cell viabilities following SMK-17 treatment were examined. As shown in Figure 45, the silencing of c-Myc expression consequently suppressed SMK-17 induced apoptosis, as judged from PARP cleavage. Furthermore, as shown in Figure 46, Wnt3a-induced PARP cleavage in SMK-17-treated A375 cells was also inhibited by the knockdown of c-Myc. These results indicated that c-Myc is a key regulator involved in MEK1/2 inhibitor induced apoptosis in the active condition of Wnt pathways such as  $\beta$ -catenin mutation or Wnt3a stimulation.

Nevertheless, c-Myc is confirmed to be responsible for the SMK-17 induced apoptosis

in tumor cells harboring  $\beta$ -catenin mutation, because c-Myc knockdown can inhibit SMK-17 induced apoptosis not only in  $\beta$ -catenin mutant HCT 116 cells but also in Wnt3a-stimulated A375 cells. The next question to be solved is which c-Myc-mediated apoptosis-related proteins contributed to SMK-17 induced apoptosis in tumor cells harboring  $\beta$ -catenin mutation. Several articles demonstrated the involvement of BIM in RAF- or MEK-inhibitor induced apoptosis<sup>(63),64),65),66),67)</sup>. BIM is a Bcl-2 homology domain 3-only (BH3-only) protein, and is known to bind and inhibit pro-survival Bcl-2 family members. Expression of BIM was regulated by c-Myc<sup>(68)</sup> and was inhibited by BRAF-MEK-ERK signaling in mouse and human melanocytes and in human melanoma cells<sup>(69)</sup>.

Therefore, inhibition of BRAF-MEK-ERK signaling seemed to increase the expression levels of BIM, thereby inducing apoptosis in cells. We also found that SMK-17 induced an increase in the expression levels of BIM under the condition where ERK phosphorylation was inhibited in  $\beta$ -catenin mutant HCT 116, SW48 and colo-205 cells. However, knockdown of BIM failed to suppress SMK-17 induced apoptosis in all cases we tested (data not shown, unpublished data by Y. Shikata). Therefore, c-Myc-mediated apoptosis-related proteins other than BIM might be responsible for active  $\beta$ -catenin-mediated apoptosis induced by SMK-17.

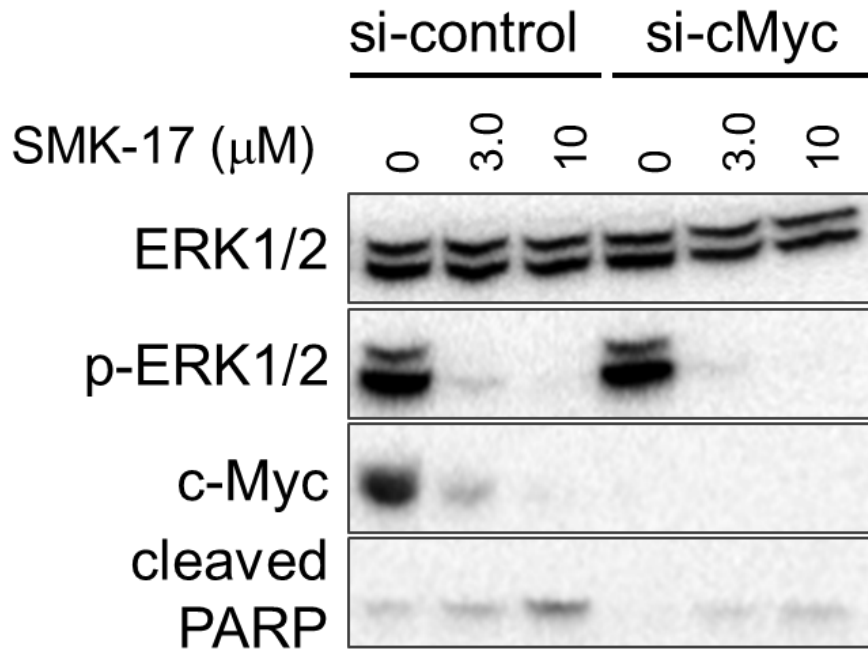


Figure 45 Involvement of c-Myc on SMK-17 induced apoptosis in HCT 116 cells  
HCT 116 cells were transfected with the control siRNA or *c-myc* siRNA.  
Transfected cells were treated with the indicated concentrations of SMK-17 for 24 h.  
Reduced expression of phospho-ERK1/2 (p-ERK1/2) and c-Myc protein, and  
increased expression of cleaved PARP were confirmed by Western blot analysis.

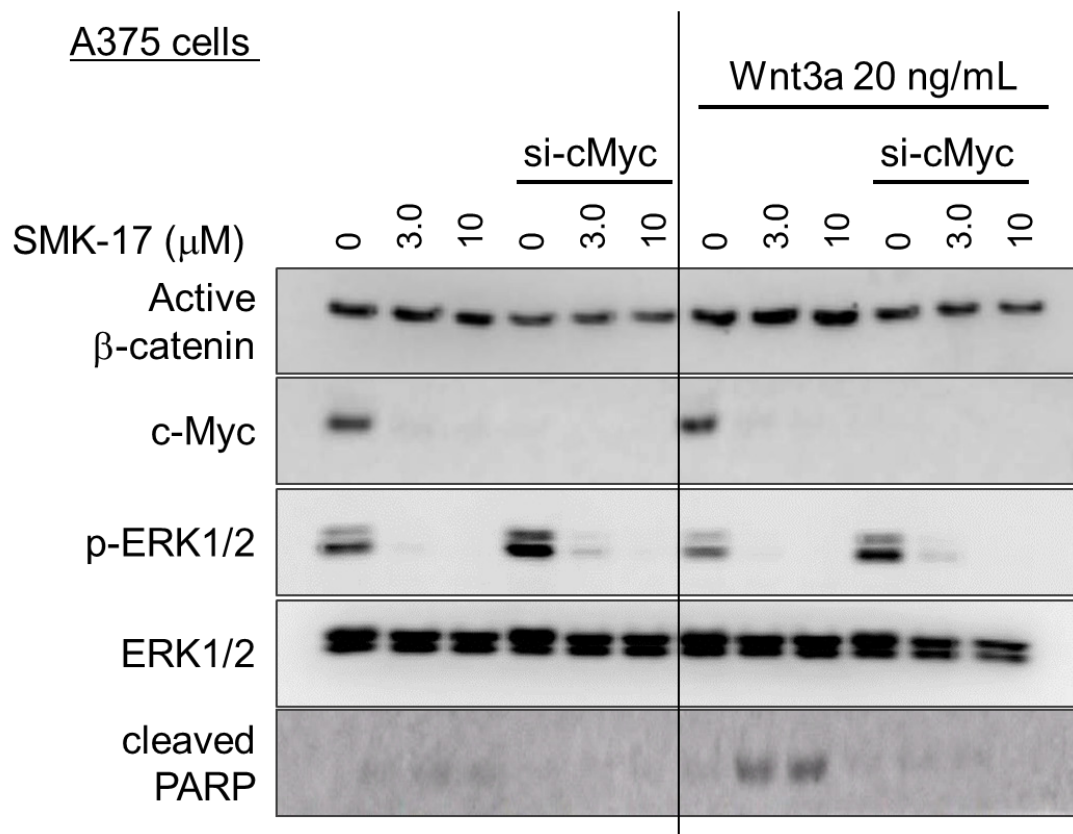


Figure 46 Involvement of c-Myc on SMK-17 induced apoptosis in Wnt3a stimulated A375 cells

A375 cells were transfected with the control siRNA or *c-myc* siRNA. Transfected cells were treated with the indicated concentrations of SMK-17 in the presence or absence of Wnt3a (20 ng/mL) for 24 h, and expression of ERK1/2, p-ERK1/2, c-myc, active  $\beta$ -catenin and cleaved PARP was detected by Western blot analysis.

#### **4.2.6 Apoptosis induction of SMK-17 on $\beta$ -catenin mutated xenograft models**

Because SMK-17 selectively induced apoptosis in cell lines harboring active mutation of  $\beta$ -catenin in vitro, we examined the ability for apoptosis induction of SMK-17 in vivo. Active  $\beta$ -catenin mutant tumor cells (SW48 and colo-205 cells) and wild type  $\beta$ -catenin tumor cells (A375 and HT-29 cells) were injected subcutaneously into NOD-SCID mice (for SW48 cells) or nude mice (for others) to establish xenograft models. Mice were then administered SMK-17 or the control vehicle by oral gavage. We confirmed inhibitory activities of SMK-17 to intratumor MEK monitored by phosphorylated ERK1/2 after a single shot of SMK-17 in SW48 and A375 cells in vivo (data not shown due to space limitations). As shown in Figure 47, tumor regression by daily oral multiple administration of half MTD (200 mg/kg) of SMK-17 was observed only in active  $\beta$ -catenin mutation xenograft models, SW48 and colo-205. On the other hand, the maximum effect of SMK-17 at MTD dosing (400 mg/kg) was just growth inhibition in A375 and HT-29 cells expressing wild type  $\beta$ -catenin without significant body weight loss. TUNEL staining revealed significant apoptosis induction in SW48 tumor tissues from the SMK-17-treated mice, but not the control mice (Figure 48). In contrast, apoptotic cells were not observed in A375 xenograft mice treated with SMK-17.



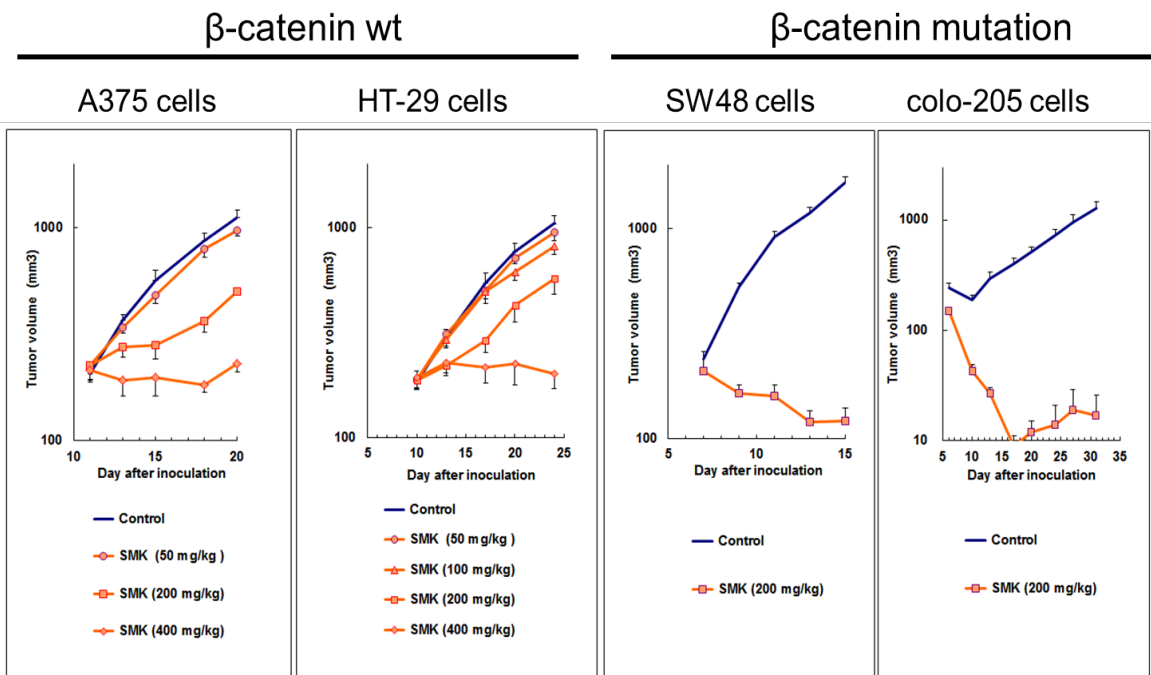


Figure 47 Antitumor activities of SMK-17 in vivo

SMK-17 induced tumor regression and apoptosis in β-catenin mutated cell lines in vivo. SMK-17 suspensions and control vehicle (0.5% MC) were given orally (po) once-daily.

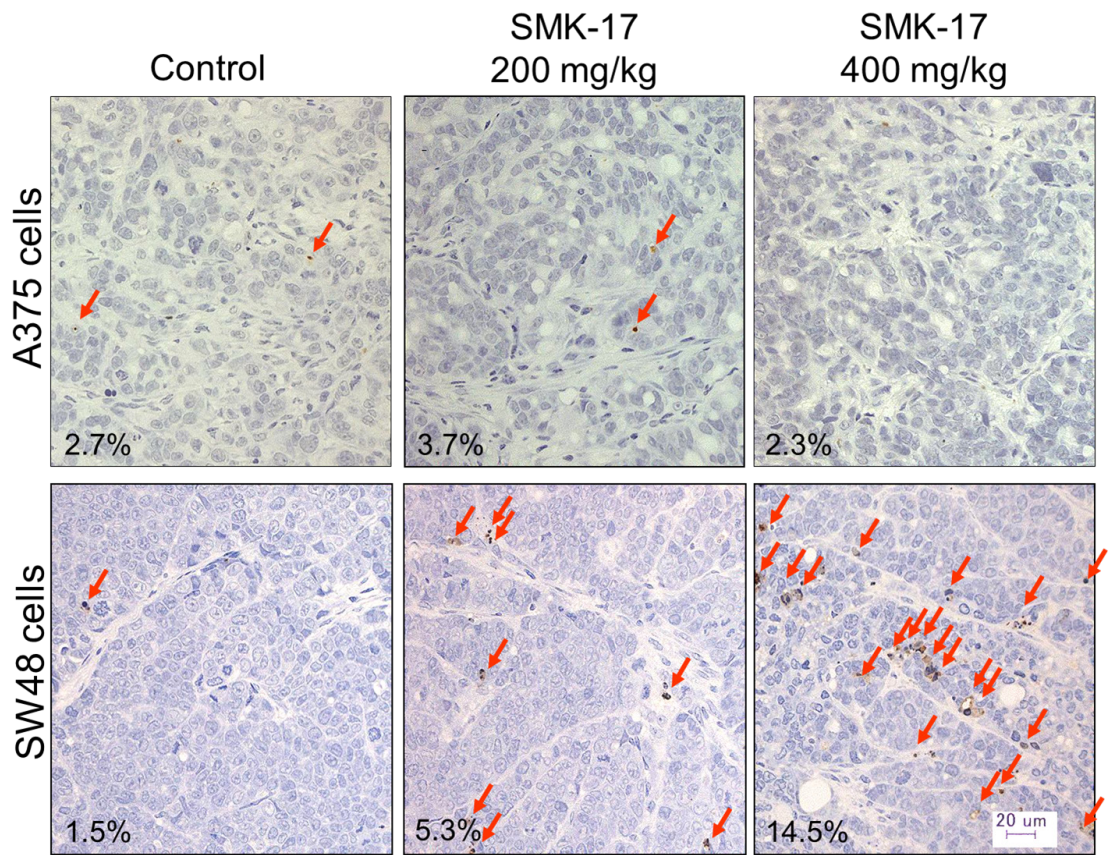


Figure 48 Apoptosis induction by SMK-17 administration in a  $\beta$ -catenin mutated tumor model in vivo

SMK-17 induced apoptosis in tumors in vivo. TUNEL staining results were obtained from tumors from xenograft mice 6 h after final oral administration of SMK-17 (q.d. x 2 days). Each indicated score (%) is the mean ratio of the apoptotic cells in the tissue slices from 4 independent tumor-bearing mice.

### 4.3 Conclusion of Chapter 4

We demonstrated that  $\beta$ -catenin mutation accelerates MEK1/2 inhibitor induced apoptosis. Our selective MEK1/2 inhibitor, SMK-17, induced apoptosis in tumor cell lines harboring  $\beta$ -catenin mutations at the effective concentration. To confirm the possibility of mutation of  $\beta$ -catenin and mutant  $\beta$ -catenin-mediated TCF4 transcriptional activity as a prediction marker of MEK inhibitors, we evaluated the effects of dominant negative TCF4 and active mutated  $\beta$ -catenin on MEK inhibitor induced apoptosis. As a result, dominant negative TCF4 (DN-TCF4) reduced MEK inhibitor induced apoptosis. In contrast, active mutated  $\beta$ -catenin accelerated MEK inhibitor induced apoptosis.

On the other hand, because this study did not clearly identify the key regulator of MEK inhibitor induced apoptosis, which shown as “Gene X” in Figure 49, these results highlight the need for further studies of the signal crosstalk between MAPK pathway and Wnt pathway regarding apoptosis induction.

Our findings provide the  $\beta$ -catenin mutation (i.e. S37A or S45A point mutation) as a novel and important responder biomarker for the treatment of MEK1/2 inhibitors.

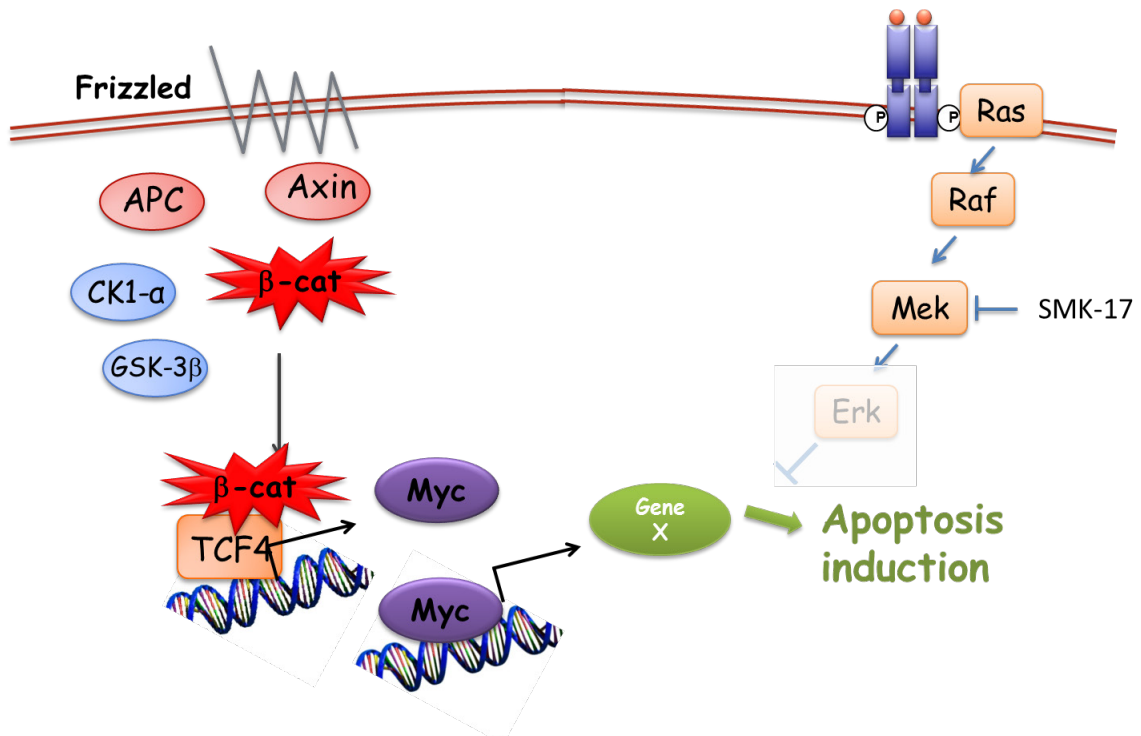


Figure 49 Possible mechanism for SMK-17-induced apoptosis and crosstalk between Wnt/β-catenin and MAPK pathways

## **4.4 Materials and methods in Chapter 4**

### **4.4.1 Cell lines and cell culture**

JIMT-1 cells were provided by Deutsche Sammlung von Mikroorganismen und Zellkulturen GmbH (DSMZ, Braunschweig, Germany). OVCAR-5 cells were obtained from National Cancer Institute (NCI, Bethesda, MD). EC109 were provided from Columbia University (USA). MS-1 cells were obtained from Dr. M. Takada in Rinku General Medical Center (Osaka). The other cell lines used in the experiments were purchased from American Type Culture Collection (ATCC, Rockville, MD) and maintained with the recommended media supplemented with 10% heat-inactivated fetal bovine serum (HyClone Laboratories, Thermo Fisher Scientific, Waltham, MA). Cells were passaged every 2–3 days to maintain exponential growth.

### **4.4.2 Cell growth inhibition assay**

For growth inhibition experiments, cells were plated in black 96-well plates (Corning, Corning NY) at 1,000-2,000 cells/100  $\mu$ L/well. After 24 h culture, the compound was added and incubated for another 72 h. The cell number was measured using CellTiter-Glo Luminescent Cell Viability Assay (Promega, Madison, WI). A nonlinear curve fitting was performed from triplicate sets of data.

#### 4.4.3 Western blot analysis

Anti-phospho-ERK 1/2 (T202/Y204), anti-phospho-MEK (S217/221), anti-ERK1/2, anti-cleaved PARP, anti-c-Myc, anti-BIM, anti-survivin, anti-mouse IgG HRP-linked and anti-rabbit IgG HRP-linked were obtained from Cell Signaling Technology (Danvers, MA). Anti-unphosphorylated  $\beta$ -catenin was purchased from Promega. Anti- $\beta$ -actin was purchased from Sigma-Aldrich. PhosphoSTOP; phosphatase inhibitor cocktail tablets and Complete Mini; protease inhibitor cocktail tablets were purchased from Roche Diagnostics (Indianapolis, IN). The cells were seeded in 6-well plates (Corning) and incubated for 1 day before the compound treatment. Then, the cells were treated with the compound for the indicated time. The cells were harvested and lysed immediately with a RIPA buffer (50 mM Tris HCl pH 7.5, 150 mM NaCl, 1 mM  $\text{Na}_3\text{VO}_4$ , 0.1% SDS, 0.5% deoxycholic acid, 1% IGEPAL CA-630, PhosphoSTOP tablet, and Complete Mini tablet). Tumor tissues were harvested from mice and stored at  $-80^\circ\text{C}$ , and then disrupted by grinding for 30 sec at 2,500 rpm twice with a Multi-Beads Shocker (Yasui Kikai, Shizuoka, Japan) in the RIPA buffer. After incubation on ice for 30 min, the lysates were centrifuged at 14,000 G for 15 min to clear insoluble fragments. The supernatants were used for Western blot analysis. Equal amounts of total protein were resolved on SDS-PAGE gels and blotted with antibodies as indicated. The chemiluminescent signal was generated with Western Lightning Plus (PerkinElmer, Waltham, MA) and detected with LAS-1000 imager (Fujifilm, Tokyo, Japan). The densitometric quantitation of specific bands was determined using Multi Gauge Software (Fujifilm).

#### **4.4.4 Cell cycle and apoptosis measurements**

The percentage of cells in different cell cycle phases including the sub G1 population was measured by flow cytometry using propidium iodide (PI, Wako) staining cells. In brief, cells were treated with each compound for the indicated time, fixed with 70% ethanol at 4°C, and then stained with 50 µg/mL PI and 10 µg/mL RNase A (Wako) at 37°C for 20 min. PI fluorescence was measured with an EPICS ALTRA (Beckman Coulter, Brea, CA).

Detection of early apoptotic cells was determined using an annexin V/APC and 7AAD (BD Biosciences, San Jose, CA) according to the manufacturer's protocol. Briefly,  $1 \times 10^5$  cells were exposed to each compound and washed by PBS twice. Then, they were incubated at room temperature with annexin V/APC and 7AAD for 15 minutes. Annexin V/APC and 7AAD staining cells were enumerated by FACSCanto (BD Biosciences). Annexin V/APC positive or negative cells were regarded as apoptotic or non-apoptotic cells, respectively.

In the vector-transfection experiments, we co-transfected the EGFP expression vector as a transfectant marker with DN-TCF4 (Merck Millipore, Billerica, MA) or active-mutated human  $\beta$ -catenin (S37A and S45A) expression vectors (made in Daiichi Sankyo Co. Ltd.). We gated GFP negative cells on the FCM analysis due to the cut-off results of non-transfectant cells.

#### **4.4.5 TCF4 reporter and expression vectors**

We used commercially available TOP FLASH, Renilla Luciferase reporter (Invitrogen Life Technologies, Carlsbad, CA), and a DN-TCF4 vector. Transfection of plasmid

vectors was performed using Lipofectamine LTX (Invitrogen Life Technologies) according to the manufacturer's protocol. Reporter activity was measured by Dual-Glo Luciferase Assay System (Promega).

#### **4.4.6 RNA interference**

siRNA double-stranded oligonucleotides against *c-myc* (Dharmacon, Lafayette, CO) and non-coding siRNA (Invitrogen Life Technologies) as a negative control were used for RNA interference assays. Reverse transfection was demonstrated using RNAiMAX (Invitrogen Life Technologies) according to the manufacturer's protocol.

#### **4.4.7 In vivo antitumor experiments**

Specific pathogen-free female nude mice (BALB/cA Jcl-nu) were purchased from CLEA Japan. NOD-SCID mice were purchased from Charles River Laboratories International Inc. SMK-17 was suspended in 0.5% methyl cellulose solution (Wako), and given daily to the animals by gavage at the volume of 0.1 mL/10 g body weight. Control animals received 0.5% methyl cellulose solution for vehicle control. For the SW48 xenograft study,  $1 \times 10^7$  cell suspension was injected subcutaneously into the axillar region of the NOD-SCID mice on Day 0. For the other tumor cell line's study,  $2 \times 10^6$  cells were injected subcutaneously into female Balb/c-nu/nu mice on Day 0. Tumor-bearing mice were grouped according to the tumor volume, and drug administration was conducted. The administration volume for each animal was calculated based on its recent body weight. Tumor volumes were calculated according to the



following equations: Tumor volume ( $\text{mm}^3$ ) =  $1/2 \times (\text{tumor length}) \times (\text{tumor width})^2$ . All the animal care and experiments were conducted under the standard operational protocol of the Daiichi Sankyo's Institutional Animal Care and Use Committee.

TUNEL staining for xenograft tumor tissue was based on the protocol of the TdT-Fragel DNA Fragmentation detection kit (Merck Millipore). The tissue sections were viewed at 100 magnification and images were captured with a digital camera (Olympus, Tokyo, Japan). Four fields per section were analyzed, excluding peripheral connective tissue and necrotic regions. The total tissue area analyzed in each section was  $2.0 \text{ mm}^2$ . The areas of TUNEL-positive objects were quantified manually.

**5. Chapter 5; Beyond therapy for  $\beta$ -catenin mutated tumors with MEK1/2 inhibitors**

## 5.1 Background of Chapter 5

In the previous chapters, we suggested the usage of MEK1/2 inhibitors to  $\beta$ -catenin mutated cell lines. However, we were still not certain about a suitable therapy for APC mutated tumors. In this study, we used three APC mutant colorectal tumor cells, SW480, SW620 and DLD-1 cells: SW480 and SW620 cells have a mutant version of the APC tumor suppressor gene, causing a premature termination of the protein at amino acid 133<sup>70,71</sup>), and DLD-1 cells have a mutation at codon 1416 of the APC gene and loss of the other allele, resulting in constitutively active TCF/LEF<sup>72</sup>).  $\beta$ -catenin and APC mutations seem to be mutually exclusive, possibly reflecting the fact that both components act in the same pathway. Nevertheless, SMK-17 induced cell death in SW480 cells as well as  $\beta$ -catenin mutant cells, but not in SW620 and DLD-1 cells. SW480 and SW620 are two colon tumor cell lines established from the same patient with different metastatic potentials<sup>73</sup>) and are well characterized and represent the different features between primary and distinct metastatic sites<sup>74</sup>).

Indeed, we found that the expression levels of survivin, an anti-apoptotic protein, are significantly higher in SW620 than in SW480 cells (data not shown and unpublished data by Y Shikata), and this difference of survivin levels may explain why SW620 cells but not SW480 cells are resistant to SMK-17 induced apoptosis. On the contrary, in DLD-1 cells, SMK-17 induced neither cell growth inhibition nor apoptosis inhibition. DLD-1 expressed a relative higher amount of ERK1/2 protein, but its phosphorylation level was quite low. Therefore, it is possible that proliferation of DLD-1 is independent of MEK/MAPK pathways. Thus, although we do not know at present why the  $\beta$ -catenin mutation, but not the APC mutation, could predict sensitivity to MEK inhibitors, TCF4

transcription activity is found to be relatively higher in APC mutants than in  $\beta$ -catenin mutants. This difference may influence the balance between c-Myc-mediated expressions of pro-apoptotic and anti-apoptotic protein to efficiently affect tumor cell survival, therefore moderately enhanced TCF4 activity regulated by  $\beta$ -catenin mutation might be required for apoptosis induced by MEK inhibitors.

On the contrary, hypothetically, the moderate and suitable TCF4 transcription activity may be important to MEK1/2 induced apoptosis because the APC mutated cell line harbors hyperactive transcription activity by way of contrast in  $\beta$ -catenin mutated cell lines with moderate TCF4 activities (data not shown and unpublished data by A Nakayama).

## **5.2 Results and discussion**

### **5.2.1 Manipulation of TCF4 transcription activity in an APC mutated cell line**

We generated two clones expressing Gene-Switch vectors<sup>75)</sup> encoding dominant negative TCF4 (DN-TCF4) from the DLD-1 tumor cell line harboring mutated APC. The vectors of the Gene-Switch system were induced by mifepristone (MFP). Firstly, I confirmed the expression level of DN TCF4 induced by MFP in a dose-correlation manner from 0.01 nM to 0.1 nM (Figure 50).

Secondly, I monitored TCF4 transcription activity in the two clones using a TOP FLASH assay. MFP treatment from 0.01 nM to 0.1 nM attenuated TCF4 transcription activity in DLD1 (Figure 51). Furthermore, TCF4 transcription activity was not affected by SMK-17 treatment.

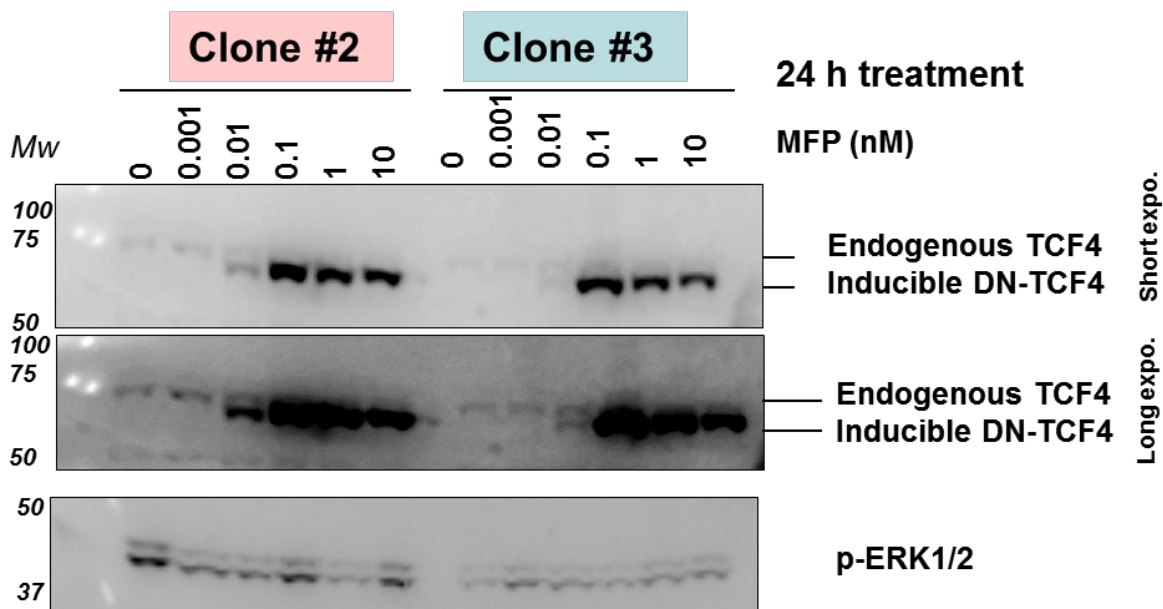


Figure 50 MFP-induced DN-TCF4 expression using a Gene-Switch system in DLD-1 cells

DN-TCF4 encoding in Gene-Switch vectors was induced by MFP treatment in a dose-correlation manner in both clones, Clone #2 and #3 of DLD-1 cells.

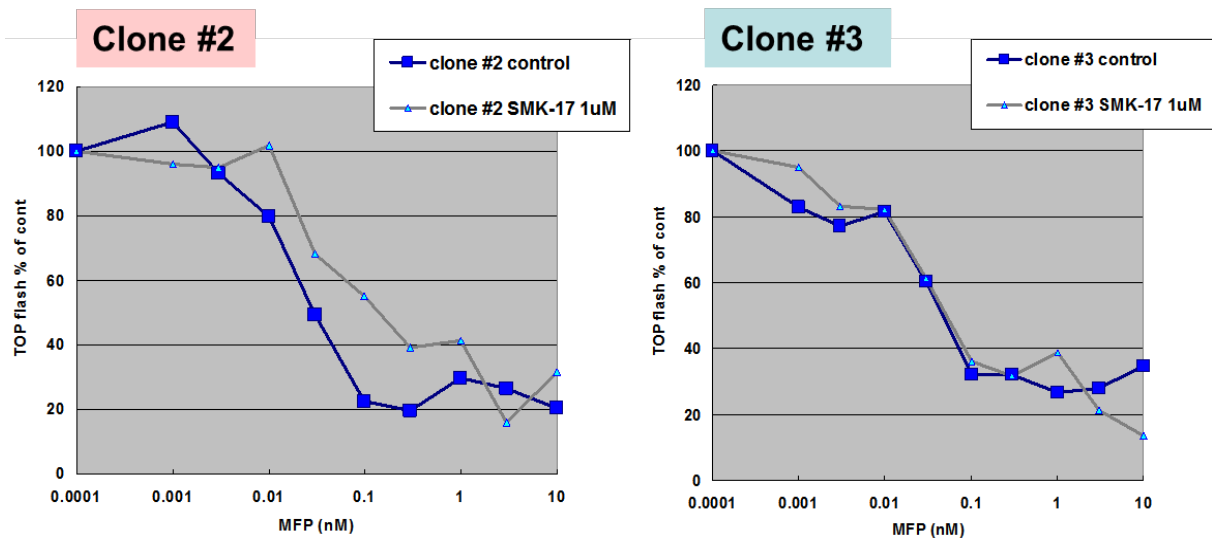


Figure 51 Attenuated TCF4 transcription activity by MFP treatment in DN-TCF4 expressing DLD1 cells

MFP treatment for 24 h induced DN-TCF4 encoding in Gene-Switch vectors and attenuated TCF4 transcription activity in DN-TCF4 expressing clone #2 and #3 of DLD1 cells.

### **5.2.2 Partial inhibition of TCF4 transcription activity in an APC mutated cell line maximized by SMK-17 induced apoptosis**

We monitored SMK-17 induced apoptosis with or without MFP treatment. As a result, SMK-17 induced apoptosis was maximized in 0.3 nM MFP treatment, which showed moderate TCF4 transcription activity (Figure 52). Furthermore, transfection of active  $\beta$ -catenin did not accelerate apoptosis in the DLD1 cell line (Figure 53).



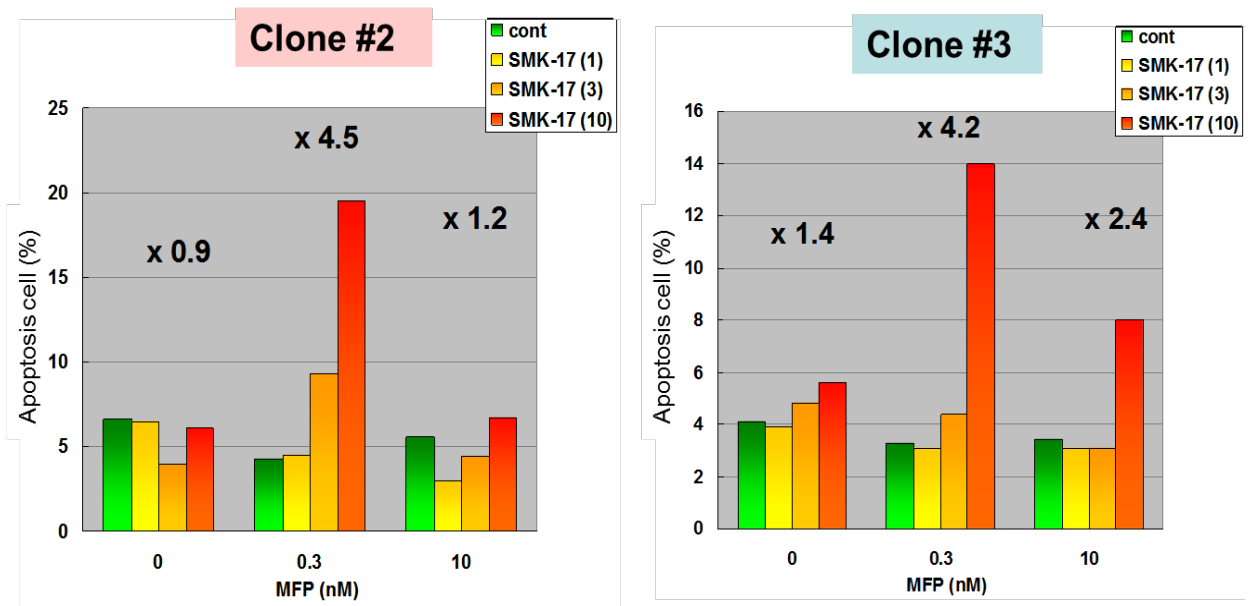


Figure 52 SMK-17 induced apoptosis was maximized by a low concentration treatment of MFP in DN-TCF4 expressing DLD-1 cells

SMK-17 induced apoptosis was maximized in 0.3 nM MFP treatment, which showed moderate TCF4 transcription activity.

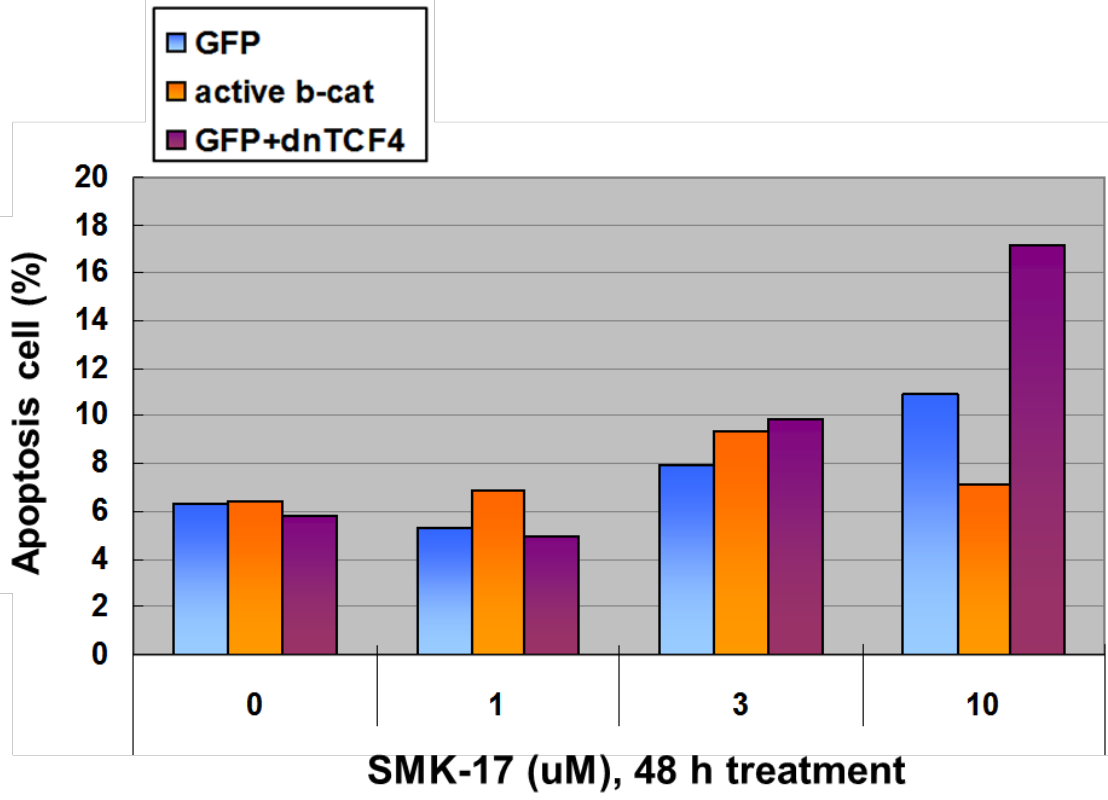


Figure 53 SMK-17 induced apoptosis was not significantly accelerated by overexpression of active  $\beta$ -catenin in DLD-1 cells

SMK-17 induced apoptosis was not accelerated by active  $\beta$ -catenin. On the other hand, DN-TCF4 with 0.3 nM MFP accelerated SMK-17 induced apoptosis.

### **5.3 Conclusion of Chapter 5**

Here, I confirmed that moderate TCF4 transcription activity is important for SMK-17 induced apoptosis. As I previously described in Chapter 4, apoptosis was induced by single treatment of SMK-17 in  $\beta$ -catenin mutated cell lines. Furthermore, moderate TCF4 transcription activity may be suitable for apoptosis also in an APC mutated cell line.

Although we need further investigation about this possibility and MoA analysis, we may use MEK1/2 inhibitors with the inhibitor of a Wnt pathway to maximize the potency of MEK1/2 inhibitors.

## **5.4 Materials and methods in Chapter 5**

### **5.4.1 Gene-Switch system to manipulate TCF4 transcription activity**

We designed a plasmid-based GeneSwitch system (Invitrogen, Thermo Fisher Scientific Inc.) and provided mifepristone (MFP) regulated DN-TCF4 expression plasmid. DLD-1 cells were cotransfected with both plasmids (pSwitch and pGene-DN-TCF4) and then dual-selected with hygromycin B (300  $\mu\text{g}/\text{ml}$ ) and Zeocin (200  $\mu\text{g}/\text{ml}$ ) to isolate single stable cell lines expressing both the regulatory fusion protein and DN-TCF4. We selected highly transfected clones of DLD-1 cells, clone #2 and #3. Regulation of this system was effective at 0.1 to 10 nM of MFP in a dose response manner and provided regulated biological responses (suppression of TCF4 transcription activity) in both clones. This plasmid-based MFP-inducible GeneSwitch system was used for the investigation of suitable intensity of Wnt pathways for MEK inhibitor induced apoptosis.

### **5.4.2 Other protocol except for the Gene-Switch system**

The other experiments including apoptosis detection, vector transfection, and cell culture were performed using the same methods as described in the previous chapters.

**6. Chapter 6; Conclusion of this study**

Here, we found a very potent MEK1/2 inhibitor, SMK-17, from our structure-activity-correlation study of a new derivative series of diphenyl amine sulfonamide. A Kinase profiler and kinetics study revealed that SMK-17 is a completely- non-ATP-competitive and highly selective MEK1/2 inhibitor. Moreover, SMK-17 exhibited potent antitumor activity in animal models by oral administration. SMK-17 selectively blocked the MAPK pathway signaling without affecting other signal pathways both in vitro and in vivo. These findings suggest that SMK-17 is a useful chemical biology tool for characterizing the function of MEK/MAPK signaling both in vitro and in vivo.

MEK1/2 inhibitors have been evaluated in both preclinical and clinical studies as a potential therapeutic option for patients with melanoma carrying the BRAF V600-mutation, however, single-agent efficacy has been limited. Therefore, rational combination strategies of MEK1/2 inhibitors with other molecularly targeted drugs are expected to lead to greater efficacy. For example, because several studies have reported the indirect crosstalk between Wnt/ $\beta$ -catenin and MAPK signaling<sup>76)</sup>, the combination of a MEK1/2 blockade and Wnt pathway modulation has shown synergistic antiproliferative effects in both in vitro and in vivo preclinical colorectal tumor models<sup>77)</sup>.

We clearly demonstrated that  $\beta$ -catenin mutation accelerates MEK1/2 inhibitor induced apoptosis. MEK1/2 inhibitors, not only SMK-17 but also PD184352, induced apoptosis in tumor cell lines harboring  $\beta$ -catenin mutations at effective concentrations. To confirm the possibility of mutations of  $\beta$ -catenin and mutant  $\beta$ -catenin-mediated TCF4

transcriptional activity as a prediction marker of an MEK1/2 inhibitor, we evaluated the effects of dominant negative TCF4 and active mutated  $\beta$ -catenin on MEK inhibitor induced apoptosis. As a result, dominant negative TCF4 (DN-TCF4) reduced MEK inhibitor induced apoptosis. In contrast, active mutated  $\beta$ -catenin accelerated MEK inhibitor induced apoptosis.

Our findings provide a  $\beta$ -catenin mutation (i.e. S37A or S45A point mutation) as an important predictive biomarker to identify the responder tumors for MEK1/2 inhibitors (the digested diagrams are shown in Figure 54).

Moreover, I discovered that moderate TCF4 transcription activity is important for SMK-17 induced apoptosis. Moderate TCF4 transcription activity may be suitable for apoptosis also in the APC mutated cell lines. I proposed the structure of the relationship between Wnt/ $\beta$ -catenin pathway activities and tumor response to MEK1/2 inhibitors described in Figure 55.

Because  $\beta$ -catenin is mutated in up to 10% of all sporadic colon carcinoma by point mutations or in frame deletions of the serine and threonine residues that are phosphorylated by GSK3 $\beta$ <sup>78</sup>, our findings would provide clinical usefulness of the MEK1/2 inhibitor as a single agent for patients with tumors carrying active  $\beta$ -catenin mutations.

This study revealed for the first time in the world that active mutation of  $\beta$ -catenin is one of predictive markers of MEK inhibitors.

Tumor harboring ...

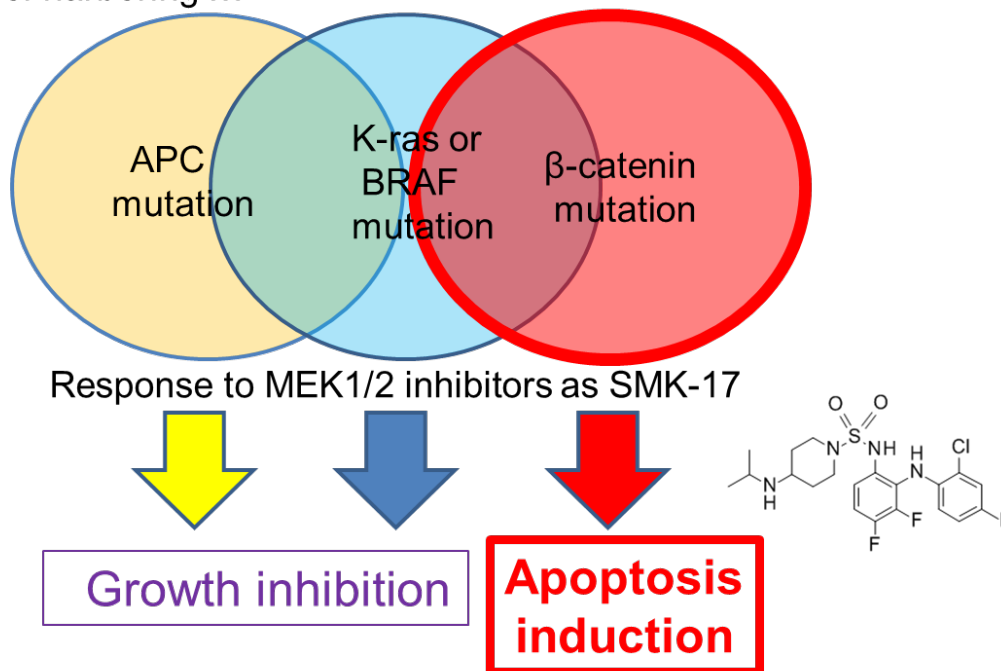


Figure 54 Diagram of this study showing the response of MEK1/2 inhibitors of tumors harboring oncogenic mutations



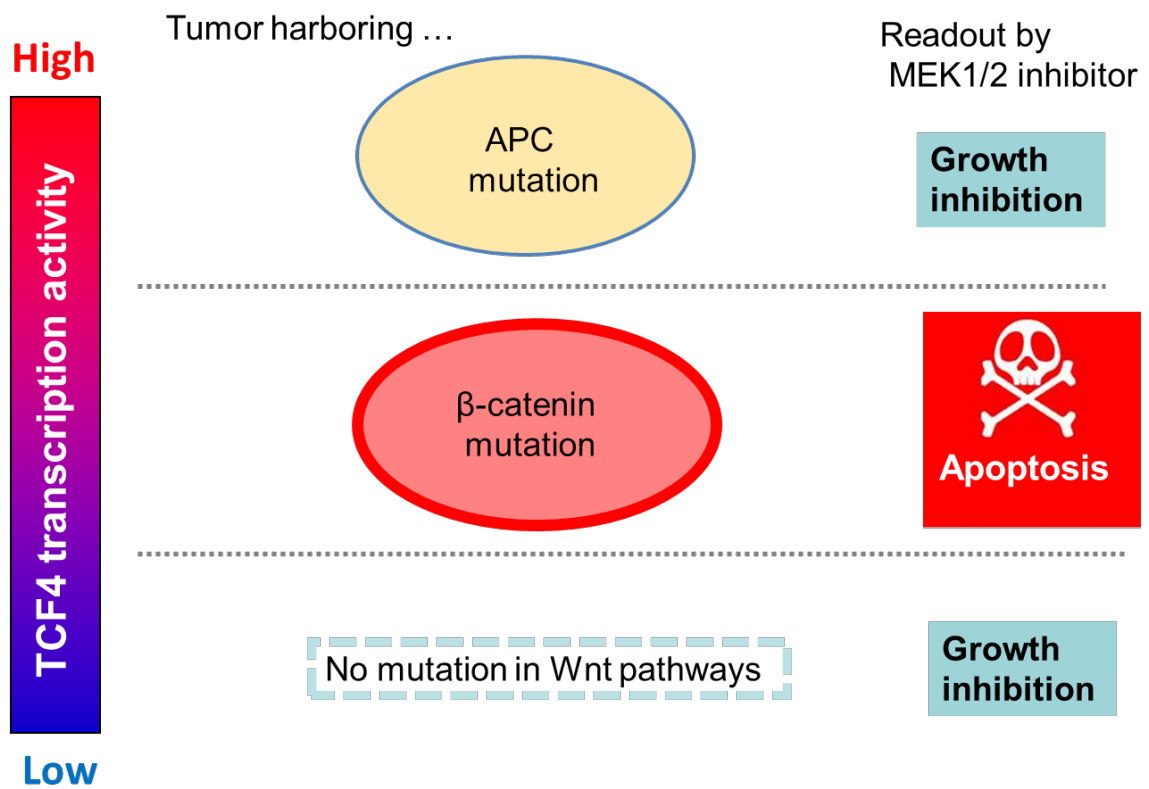


Figure 55 Proposed machinery of the response of tumor cells with various TCF4 activities to MEK1/2 inhibitors

## 7. References

### 7.1 References in Chapter 1

- 1) Jones GB. History of anticancer drugs. eLS. 2014; [Wiley Online Library](#).
- 2) Morange M. History of cancer research. eLS. 2003; [Wiley Online Library](#).
- 3) Wani MC, Taylor HL, Wall ME, Coggon P, McPhail AT. Plant antitumor agents. VI. Isolation and structure of taxol, a novel antileukemic and antitumor agent from *Taxus brevifolia*. *Journal of the American Chemical Society*. 1971; 93(9): 2325-2327. PubMed PMID: [5553076](#).
- 4) Schiff PB, Fant J, Horwitz SB. Promotion of microtubule assembly in vitro by taxol. *Nature*. 1979, 277(5698): 665-667. PubMed PMID: [423966](#).
- 5) Sawyers C. Targeted cancer therapy. *Nature*. 2004, 432(7015): 294-297. PubMed PMID: [15549090](#).
- 6) Sawyers CL. Opportunities and challenges in the development of kinase inhibitor therapy for cancer. *Genes & development*. 2003; 17(24): 2998-3010. PubMed PMID: [14701871](#).
- 7) Paez JG, Jänne PA, Lee JC, Tracy S, Greulich H, Gabriel S, Meyerson M. EGFR mutations in lung cancer: correlation with clinical response to gefitinib therapy. *Science*. 2004; 304(5676): 1497-1500. PubMed PMID: [15118125](#).
- 8) Sordella R, Bell DW, Haber DA, Settleman J. Gefitinib-sensitizing EGFR mutations in lung cancer activate anti-apoptotic pathways. *Science*. 2004; 305(5687): 1163-1167. PubMed PMID: [15284455](#).

- 9) Adams MD, Kelley JM, Gocayne JD, Dubnick M, Polymeropoulos MH, Moreno RF. Complementary DNA sequencing: expressed sequence tags and human genome project. *Science*. 1991; 252(5013): 1651-1656. PubMed PMID: [2047873](#).
- 10) Stephens P, Hunter C, Bignell G, Edkins S, Davies H, Teague J, Cole J. Lung cancer: intragenic ERBB2 kinase mutations in tumours. *Nature*. 2004; 431(7008): 525-526. PubMed PMID: [15457249](#).
- 11) Davies H, Bignell GR, Cox C, Stephens P, Edkins S, Clegg S, Davis N. Mutations of the BRAF gene in human cancer. *Nature*. 2002. 417(6892): 949-954. PubMed PMID: [12068308](#).
- 12) Bardelli A, Parsons, DW, Silliman N, Ptak J, Szabo S, Saha S, Velculescu VE. Mutational analysis of the tyrosine kinome in colorectal cancers. *Science*. 2003. 300(5621): 949-949. PubMed PMID: [12738854](#).
- 13) Samuels Y, Wang Z, Bardelli A, Silliman N, Ptak J, Szabo S, Velculescu VE. High frequency of mutations of the PIK3CA gene in human cancers. *Science*. 2004. 304(5670): 554-554. PubMed PMID: [15016963](#).
- 14) Cools J, DeAngelo DJ, Gotlib J, Stover EH, Legare RD, Cortes J, Gilliland DG. A tyrosine kinase created by fusion of the PDGFRA and FIP1L1 genes as a therapeutic target of imatinib in idiopathic hypereosinophilic syndrome. *New England Journal of Medicine*. 2003. 348(13), 1201-1214. PubMed PMID: [12660384](#).
- 15) Roux PP, Blenis J. ERK and p38 MAPK-activated protein kinases: a family of protein kinases with diverse biological functions. *Microbiol Mol Biol Rev*. 2004; 68(2):320-44. PubMed PMID: [15187187](#).

- 16) Dalby KN, Morrice N, Caudwell FB, Avruch J, Cohen P. Identification of regulatory phosphorylation sites in mitogen-activated protein kinase (MAPK)-activated protein kinase-1a/p90rsk that are inducible by MAPK. *J Biol Chem.* 1998; 273(3):1496-505. PubMed PMID: [9430688](#).
- 17) Marais R, Wynne J, Treisman R. The SRF accessory protein Elk-1 contains a growth factor-regulated transcriptional activation domain. *Cell.* 1993; 73(2):381-93. PubMed PMID: [8386592](#).
- 18) Crews CM, Alessandrini A, Erikson RL. The primary structure of MEK, a protein kinase that phosphorylates the ERK gene product. *Science.* 1992; 258(5081):478-80. PubMed PMID: [1411546](#).
- 19) Sebolt-Leopold JS, Herrera R. Targeting the mitogen-activated protein kinase cascade to treat cancer. *Nat Rev Cancer.* 2004; 4(12):937-47. PubMed PMID: [15573115](#).
- 20) Bos JL. ras oncogenes in human cancer. *Cancer Res.* 1989; 49(17):4682-9. PubMed PMID: [2547513](#).
- 21) Davies H, Bignell GR, Cox C, Stephens P, Futreal PA. Mutations of the BRAF gene in human cancer. *Nature.* 2002; 417(6892):949-54. PubMed PMID: [12068308](#).
- 22) Cohen Y, Xing M, Mambo E, Guo Z, Wu G, Trink B, Beller U, Westra WH, Ladenson PW, Sidransky D. BRAF mutation in papillary thyroid carcinoma. *J Natl Cancer Inst.* 2003; 95(8):625-7. PubMed PMID: [12697856](#).
- 23) Houben R, Becker JC, Kappel A, Terheyden P, Bröcker EB, Goetz R, Rapp UR. Constitutive activation of the Ras-Raf signaling pathway in metastatic melanoma is

- associated with poor prognosis. *J Carcinog.* 2004; 3(1):6. PubMed PMID: [15046639](#).
- 24) Mansour SJ, Matten WT, Hermann AS, Candia JM, Rong S, Fukasawa K, Vande Woude GF, Ahn NG. Transformation of mammalian cells by constitutively active MAP kinase kinase. *Science.* 1994; 265(5174):966-70. PubMed PMID: [8052857](#).
- 25) Hoshino R, Chatani Y, Yamori T, Tsuruo T, Oka H, Yoshida O, Shimada Y, Ari-i S, Wada H, Fujimoto J, Kohno M. Constitutive activation of the 41-/43-kDa mitogen-activated protein kinase signaling pathway in human tumors. *Oncogene.* 1999; 18(3):813-22. PubMed PMID: [9989833](#).
- 26) Sebolt-Leopold JS. MEK inhibitors: a therapeutic approach to targeting the Ras-MAP kinase pathway in tumors. *Curr Pharm Des.* 2004;10(16):1907-14. PubMed PMID: [15180527](#).
- 27) Roberts PJ, Der CJ. Targeting the Raf-MEK-ERK mitogen-activated protein kinase cascade for the treatment of cancer. *Oncogene.* 2007; 26(22):3291-310. PubMed PMID: [17496923](#).
- 28) Rinehart J, Adjei AA, Lorusso PM, Waterhouse D, Hecht JR, Meyer MB. Multicenter phase II study of the oral MEK inhibitor, CI-1040, in patients with advanced non-small-cell lung, breast, colon, and pancreatic cancer. *J Clin Oncol.* 2004; 22(22):4456-62. PubMed PMID: [15483017](#).
- 29) Haura EB, Ricart AD, Larson TG, Stella PJ, Bazhenova L, Gadgeel SM. A phase II study of PD-0325901, an oral MEK inhibitor, in previously treated patients with advanced non-small cell lung cancer. *Clin Cancer Res.* 2010; 16(8):2450-7. PubMed PMID: [20332327](#).

- 30) Borthakur G, Popplewell L, Boyiadzis M, Gautam ,Kantarjian HM. "Phase I/II trial of the MEK1/2 inhibitor trametinib (GSK1120212) in relapsed/refractory myeloid malignancies: evidence of activity in patients with RAS mutation-positive disease." ASH Annual Meeting Abstracts. 2012; Vol. 120. No. 21. Not available in PubMed [Direct Link](#)
- 31) Thomson Pharma's database, CORTELLIS™ HP; [www.thomson-pharma.com](http://www.thomson-pharma.com)
- 32) Adjei AA, Cohen RB, Franklin W, Morris C, Wilson D, Eckhardt SG. Phase I pharmacokinetic and pharmacodynamic study of the oral, small-molecule mitogen-activated protein kinase kinase 1/2 inhibitor AZD6244 (ARRY-142886) in patients with advanced cancers. J Clin Oncol. 2008; 26(13):2139-46. PubMed PMID: [18390968](#).
- 33) Wodarz A, Nusse R. Mechanisms of Wnt signaling in development. Annu Rev Cell Dev Biol. 1998; 14:59-88. PubMed PMID: [9891778](#).
- 34) Hülsken J, Birchmeier W, Behrens J. E-cadherin and APC compete for the interaction with beta-catenin and the cytoskeleton. J Cell Biol. 1994; 127: 2061-9. PubMed PMID: [7806582](#).
- 35) Clevers H. Wnt/beta-catenin signaling in development and disease. Cell. 2006; 127(3):469-80. PubMed PMID: [17081971](#).
- 36) Chien AJ, Moore EC, Lonsdorf AS, Kulikauskas RM, Rothberg BG, Moon RT. Activated Wnt/beta-catenin signaling in melanoma is associated with decreased proliferation in patient tumors and a murine melanoma model. Proc Natl Acad Sci U S A. 2009; 106(4):1193-8. PubMed PMID: [19144919](#).
- 37) Peifer M, Polakis P. Wnt signaling in oncogenesis and embryogenesis- a look outside the nucleus. Science. 2000; 287(5458):1606-9. PubMed PMID:[10733430](#).

- 38) Pegram MD, Pauletti G, Slamon DJ. HER-2/neu as a predictive marker of response to breast cancer therapy. *Breast Cancer Res Treat.* 1998; 52(1-3):65-77. PubMed PMID: [10066073](#).
- 39) Yoo C, Ryu MH, Ryoo BY, Beck MY, Kang YK. Efficacy, safety, and pharmacokinetics of imatinib dose escalation to 800 mg/day in patients with advanced gastrointestinal stromal tumors. *Invest New Drugs.* 2013; 31(5):1367-74. PubMed PMID: [23591629](#).
- 40) Shih JY, Gow CH, Yang PC. EGFR mutation conferring primary resistance to gefitinib in non-small-cell lung cancer. *N Engl J Med.* 2005; 353(2):207-8. PubMed PMID: [16014893](#).

## **7.2 References in Chapter 2**

- 41) Gérard M. HTRF™ Technology. *Journal of biomolecular screening* 1999; 4(6): 309-314. PubMed PMID: [10838427](#).
- 42) Linassier C, Pierre M, Le Pecq JB, Pierre J. Mechanisms of action in NIH-3T3 cells of genistein, an inhibitor of EGF receptor tyrosine kinase activity. *Biochem Pharmacol.* 1990; 39(1):187-93. PubMed PMID: [2153378](#).
- 43) Russell M, Lange-Carter CA, Johnson GL. Regulation of recombinant MEK1 and MEK2b expressed in *Escherichia coli*. *Biochemistry.* 1995; 34(20):6611-5. PubMed PMID: [7756292](#).

### 7.3 References in Chapter 3

- 44) Fischmann TO, Smith CK, Mayhood TW, Myers JE, Reichert P, Madison VS. Crystal structures of MEK1 binary and ternary complexes with nucleotides and inhibitors. *Biochemistry*. 2009; 48(12):2661-74. PubMed PMID: [19161339](#).
- 45) Mody N, Leitch J, Armstrong C, Dixon J, Cohen P. Effects of MAP kinase cascade inhibitors on the MKK5/ERK5 pathway. *FEBS Lett*. 2001; 502(1-2):21-4. PubMed PMID: [11478941](#).
- 46) Daouti S, Wang H, Li WH, Higgins B, Kolinsky K, Niu H. Characterization of a novel mitogen-activated protein kinase kinase 1/2 inhibitor with a unique mechanism of action for cancer therapy. *Cancer Res*. 2009; 69(5):1924-32. PubMed PMID: [19244124](#).
- 47) Roberts PJ, Der CJ. Targeting the Raf-MEK-ERK mitogen-activated protein kinase cascade for the treatment of cancer. *Oncogene*. 2007; 26(22):3291-310. PubMed PMID: [17496923](#).
- 48) Guo Y, Stacey DW, Hitomi M. Post-transcriptional regulation of cyclin D1 expression during G2 phase. *Oncogene*. 2002; 21(49):7545-56. PubMed PMID: [12386817](#).
- 49) Shao J, Sheng H, DuBois RN, Beauchamp RD. Oncogenic Ras-mediated cell growth arrest and apoptosis are associated with increased ubiquitin-dependent cyclin D1 degradation. *J Biol Chem*. 2000; 275(30):22916-24. PubMed PMID: [10781597](#).
- 50) Dougherty MK, Müller J, Ritt DA, Zhou M, Zhou XZ, Copeland TD, Conrads TP, Veenstra TD, Lu KP, Morrison DK. Regulation of Raf-1 by direct feedback phosphorylation. *Mol Cell*. 2005; 17(2):215-24. PubMed PMID: [15664191](#).



- 51) Yao Z, Okabayashi Y, Yutsudo Y, Kitamura T, Ogawa W, Kasuga M. Role of Akt in growth and survival of PANC-1 pancreatic cancer cells. *Pancreas*. 2002; 24(1): 42-6. PubMed PMID: [11741181](#).
- 52) Takeda A, Osaki M, Adachi K, Honjo S, Ito H. Role of the phosphatidylinositol 3'-kinase-Akt signal pathway in the proliferation of human pancreatic ductal carcinoma cell lines. *Pancreas*. 2004; 28(3):353-8. PubMed PMID: [15084985](#).
- 53) Perugini RA, McDade TP, Vittimberga FJ Jr, Callery MP. Pancreatic cancer cell proliferation is phosphatidylinositol 3-kinase dependent. *J Surg Res*. 2000; 90(1): 39-44. PubMed PMID: [10781373](#).

#### **7.4 References in Chapter 4**

- 54) Solit DB, Garraway LA, Pratilas CA, Sawai A, Getz G, Basso A, Ye Q, Lobo JM, She Y, Osman I, Golub TR, Sebolt-Leopold J, Sellers WR, Rosen N. BRAF mutation predicts sensitivity to MEK inhibition. *Nature*. 2006; 19; 439 (7074):358-62. PubMed PMID: [16273091](#).
- 55) Orford K, Crockett C, Jensen JP, Weissman AM, Byers SW. Serine phosphorylation-regulated ubiquitination and degradation of beta-catenin. *J Biol Chem*. 1997; 272(40):24735-8. PubMed PMID: [9312064](#).
- 56) DasGupta R, Kaykas A, Moon RT, Perrimon N. Functional genomic analysis of the Wnt-wingless signaling pathway. *Science*. 2005; 308(5723):826-33. PubMed PMID: [15817814](#).
- 57) Behre G, Smith LT, Tenen DG. Use of a promoterless Renilla luciferase vector as an internal control plasmid for transient co-transfection assays of Ras-mediated

- transcription activation. *Biotechniques*. 1999; 26(1):24-6, 28. PubMed PMID: [9894587](#).
- 58) Biechele TL, Kulikauskas RM, Toroni RA, Lucero OM, Swift RD, Chien AJ. Wnt/ $\beta$ -catenin signaling and AXIN1 regulate apoptosis triggered by inhibition of the mutant kinase BRAFV600E in human melanoma. *Sci Signal*. 2012; 5(206), PubMed PMID: [22234612](#).
- 59) Gordon MD, Nusse R. Wnt signaling: multiple pathways, multiple receptors, and multiple transcription factors. *J Biol Chem*. 2006; 281(32):22429-33. PubMed PMID: [16793760](#).
- 60) Dominguez-Sola D, Ying CY, Grandori C, Ruggiero L, Chen B, Dalla-Favera R. Non-transcriptional control of DNA replication by c-Myc. *Nature*. 2007; 448(7152):445-51. PubMed PMID: [17597761](#).
- 61) Pelengaris S, Khan M, Evan G. c-MYC: more than just a matter of life and death. *Nat Rev Cancer*. 2002; 2(10):764-76. PubMed PMID: [12360279](#).
- 62) Lee SH, Hu LL, Gonzalez-Navajas J, Seo GS, Shen C, Raz E. ERK activation drives intestinal tumorigenesis in Apc(min/+) mice. *Nat Med*. 2010; 16(6):665-70. PubMed PMID: [20473309](#).
- 63) Campone M, Noël B, Couriaud C, Grau M, Guillemin Y, S, Juin P. c-Myc dependent expression of pro-apoptotic Bim renders HER2-overexpressing breast cancer cells dependent on anti-apoptotic Mcl-1. *Mol Cancer*. 2011; 10:110. PubMed PMID: [21899728](#).
- 64) Sun C, Hobor S, Bertotti A, Zecchin D, Huang S, Bardelli A, Trusolino L, Bernards R. Intrinsic resistance to MEK inhibition in KRAS mutant lung and colon cancer

- through transcriptional induction of ERBB3. *Cell Rep.* 2014; 7(1):86-93. PubMed PMID: [24685132](#).
- 65) Wickenden JA, Jin H, Johnson M, Gillings AS, Newson C, Austin M, Cook SJ. Colorectal cancer cells with the BRAF(V600E) mutation are addicted to the ERK1/2 pathway for growth factor-independent survival and repression of BIM. *Oncogene.* 2008; 27(57):7150-61. PubMed PMID: [18806830](#).
- 66) Cragg MS, Jansen ES, Cook M, Harris C, Strasser A, Scott CL. Treatment of B-RAF mutant human tumor cells with a MEK inhibitor requires Bim and is enhanced by a BH3 mimetic. *J Clin Invest.* 2008; 118(11):3651-9 PubMed PMID: [18949058](#).
- 67) Sale MJ, Cook SJ. The BH3 mimetic ABT-263 synergizes with the MEK1/2 inhibitor selumetinib/AZD6244 to promote BIM-dependent tumour cell death and inhibit acquired resistance. *Biochem J.* 2013; 450(2):285-94. PubMed PMID: [23234544](#).
- 68) Hemann MT, Bric A, Teruya-Feldstein J, Herbst A, Nilsson JA, Cordon-Cardo C, Lowe SW. Evasion of the p53 tumour surveillance network by tumour-derived MYC mutants. *Nature.* 2005; 436(7052):807-11. PubMed PMID: [16094360](#).
- 69) Cartlidge RA, Thomas GR, Cagnol S, Jong KA, Molton SA, Finch AJ, McMahon M. Oncogenic BRAF(V600E) inhibits BIM expression to promote melanoma cell survival. *Pigment Cell Melanoma Res.* 2008; 21(5):534-44. PubMed PMID: [18715233](#).

## 7.5 References in Chapter 5

- 70) Hargest R, Williamson R. Expression of the APC gene after transfection into a colonic cancer cell line. *Gut*. 1995; 37(6):826-9. PubMed PMID: [8537055](#).
- 71) Goss KH, Groden J. Biology of the adenomatous polyposis coli tumor suppressor. *J Clin Oncol*. 2000; 18(9):1967-79. PubMed PMID: [10784639](#).
- 72) Morin PJ, Sparks AB, Korinek V, Barker N, Clevers H, Kinzler KW. Activation of beta-catenin-Tcf signaling in colon cancer by mutations in beta-catenin or APC. *Science*. 1997; 275(5307):1787-90. PubMed PMID: [9065402](#).
- 73) Leibovitz A, Stinson JC, McCombs WB 3rd, McCoy CE, Mazur KC, Mabry ND. Classification of human colorectal adenocarcinoma cell lines. *Cancer Res*. 1976; 36(12):4562-9. PubMed PMID: [1000501](#).
- 74) Hewitt RE, McMarlin A, Kleiner D, Wersto R, Martin P, Tsokos M, Stetler-Stevenson WG. Validation of a model of colon cancer progression. *J Pathol*. 2000; 192(4):446-54. PubMed PMID: [11113861](#).
- 75) Wang Y, O'Malley BW Jr, Tsai SY, O'Malley BW. A regulatory system for use in gene transfer. *Proc Natl Acad Sci U S A*. 1994; 91(17):8180-4. PubMed PMID: [8058776](#).

## 7.6 References in Chapter 6

- 76) Bikkavilli RK, Malbon CC. Mitogen-activated protein kinases and Wnt/beta-catenin signaling: Molecular conversations among signaling pathways. *Commun Integr Biol*. 2009;2(1):46-9. PubMed PMID: [19513264](#).

- 77) Spreafico A, Tentler JJ, Pitts TM, Tan AC, Gregory MA, Arcaroli JJ, Eckhardt SG. Rational combination of a MEK inhibitor, selumetinib, and the Wnt/calcium pathway modulator, cyclosporin A, in preclinical models of colorectal cancer. *Clin Cancer Res.* 2013; 19(15):4149-62. PubMed PMID: [23757356](#).
- 78) Polakis P. Wnt signaling and cancer. *Genes Dev.* 2000; 14(15):1837-51. PubMed PMID: [10921899](#).

## **8. Appendix data**

## **8.1 Complete potency data of our MEK inhibitors**

This part is described in an added edition due to limitations of space. More detailed information is described in the patent, WO2004-083167.

## **9. The archive location of specimens and raw data**

All raw data in Chapters 2 and 3 is described in Kiga's experiment notebooks J0694 p177-199, AK0060 p 1-182, AK0229 p1-181, AK0318 p1-195, and AK0555 p1-199.

All raw data in Chapters 4 and 5 is described in Kiga's experiment notebooks AF07-H0023, BD10-H0039-002, and BD10-H0039-008.

All of the above-described records are stored in Daiichi Sankyo R&D Scientific Archives.



## 10. Related our patents and publications

All chemical structures of compounds including SMK-17 in this manuscript are disclosed in the patent, WO2004-083167; Sulfamide derivative and medicinal composition thereof (Echigo T, Fujiwara K, Iwadare H, Kiga M, Shibata T, Shimazaki N, and Tanzawa F).

The discovery described in Chapter 4 is protected by the patent, WO2014-133071; Methods of response prediction for inhibitory agents against MAPK signal (Kiga M).

Our related articles are listed below;

Kiga M, Tanzawa F, Iwasaki S, Inaba F, Fujiwara K, Iwadare H, Echigo T, Nakamura Y, Shibata T, Suzuki K, Yasumatsu I, Nakayama A, Sasazawa Y, Tashiro E, Imoto M, Kurakata S. Antitumor effects of novel highly hydrophilic and non-ATP-competitive MEK1/2 inhibitor, SMK-17 (Anti-Cancer Drugs. 2012. 23(1): 119-130).

PubMed PMID: [22008853](https://pubmed.ncbi.nlm.nih.gov/22008853/).

Kiga M, Nakayama A, Shikata Y, Sasazawa Y, Murakami R, Nakanishi T, Tashiro E, Imoto M. SMK-17, a MEK1/2-specific inhibitor, selectively induces apoptosis in  $\beta$ -catenin-mutated tumors (Scientific Reports. 2015. 5, [doi:10.1038/srep08155](https://doi.org/10.1038/srep08155)).

## 11. COI disclosure information of the author

The financial relationships to be disclosed are as follows.

Leadership position/advisory role for: None

Stockholder in: None

Patents and royalties from:

WO2004-083167, WO2013-183578, and WO2014-133071

Honoraria (lecture fee) from: None

Honoraria (manuscript fee) from: None

Grant/Research funding from: None

Other remuneration from: None

Employee of: Daiichi Sankyo Co. Ltd.

The author: Masaki Kiga

Masaki Kiga

## 12. Acknowledgments

Firstly, I would like to thank and deeply apologize to Prof. Masaya Imoto regarding my slow-paced research throughout this study. This work has been performed with support from his great leadership and perseverance.

I also would like to thank my mentors and collaborators as described below;

For members in Keio university

Dr. Etsu Tashiro for his constant support and care during this study and submission of papers.

Dr. Yukiko Sasazawa for her technical support and care of Nakayama-san and Shikata-san.

Mr. Yuki Shikata for his in-depth background work during this study.

And Ms. Ayako Nakayama for her fruitful collaboration on this innovative study and conclusive efforts with our research.

For members in Daiichi Sankyo Co. Ltd.

Dr. Yuichi Tominaga, Dr. Toshiyuki Nakanishi, Ms Naomi Shimazaki, Dr. Ryo Murakami, and Dr. Kosaku Fujiwara for their continuous support and patience with my research.

Dr. Masashi Aonuma and Dr. Koichi Akahane for their kind support and valuable lessons.

Dr. Hayato Iwadare, Ms. Fumie Tanzawa, Ms. Tomoki Echigo, Ms. Shiho Iwasaki, and Mr. Isao Yasumatsu for their fruitful collaboration on the MEK1/2 inhibitor project in Daiichi Sankyo.

Dr. Kenichi Wakita for his outstanding collaboration about the clinical entry of our mTOR inhibitor, DS-3078, during my doctoral program.

Dr. Martin Hager, Ms. Noriko Togashi, and Ms. Reina Kaneko for their outstanding and smooth collaboration from the compound screening to the clinical entry of our ROS1-NTRK inhibitor, DS-6051, during my doctoral program.

Ms. Akiko Toyota and Dr. Yasuyuki Kaneta for their outstanding collaboration with the ongoing internal project during preparation for this manuscript.

Finally I deeply thank Nobuko, Yuki, Hiroaki, Taro, Shigeo, Yaeko, Akane, Keita, Kazma, Rie, and both Nakajima and Kiga families for all the support you have provided me.

Feb. 3, 2015 Masaki Kiga

Masaki Kiga